

EUROPEAN ORGANISATION FOR NUCLEAR RESEARCH (CERN)



CERN-EP-2018-137
July 18, 2018

Search for lepton-flavor violation in different-flavor, high-mass final states in $p p$ collisions at $\sqrt{s} = 13$ TeV with the ATLAS detector

The ATLAS Collaboration

A search is performed for a heavy particle decaying into different-flavor, dilepton pairs ($e\mu$, $e\tau$ or $\mu\tau$), using 36.1 fb^{-1} of proton–proton collision data at $\sqrt{s} = 13$ TeV collected in 2015–2016 by the ATLAS detector at the Large Hadron Collider. No excesses over the Standard Model predictions are observed. Bayesian lower limits at the 95% credibility level are placed on the mass of a Z' boson, the mass of a supersymmetric τ -sneutrino, and on the threshold mass for quantum black-hole production. For the Z' and sneutrino models, upper cross-section limits are converted to upper limits on couplings, which are compared with similar limits from low-energy experiments and which are more stringent for the $e\tau$ and $\mu\tau$ modes.

1 Introduction

Direct charged-lepton flavor violation (LFV) is forbidden in the Standard Model (SM) of particle physics but is allowed in many extensions of the SM. Many such models predict new particles with LFV decays, such as Z' bosons [1], scalar neutrinos in R -parity-violating (RPV) [2, 3] supersymmetry (SUSY) and quantum black holes (QBH) in low-scale gravity [4]. Processes with flavor-violating dilepton decays are expected to produce pairs of prompt, different-flavor leptons, a final state with a clear experimental signature and a low background from SM processes. The $Z/\gamma^* \rightarrow \ell\ell$ process is an irreducible background for same-flavor lepton searches but in different-flavor searches is limited to the production and decay of a $\tau\tau$ pair. This paper describes a search for new phenomena in final states with two leptons of different flavor using 36.1 fb^{-1} of data from proton–proton (pp) collisions at $\sqrt{s} = 13 \text{ TeV}$ at the Large Hadron Collider (LHC).

A common extension of the SM is the addition of an extra $U(1)$ gauge symmetry resulting in a massive neutral vector boson known as a Z' boson [1]. The search presented in this paper assumes a Z' boson with the same quark couplings and chiral structure as the SM Z boson but only leptonic decays that violate Lepton Flavour Conservation are allowed. The parameter Q_{ij} , where $i, j = 1 \dots 3$ represent the three lepton generations, gives the strength of the LFV couplings relative to the SM $\ell\ell$ couplings. The ATLAS Collaboration placed lower limits of 3.3, 2.9, and 2.7 TeV on the mass of a Z' boson decaying into $e\mu$, $e\tau$, and $\mu\tau$ pairs, respectively, using 3.2 fb^{-1} of the 13 TeV data [5], while the CMS Collaboration has placed limits up to 4.4 TeV on a Z' boson decaying into an $e\mu$ final state using 35.9 fb^{-1} [6]. Following the same methodology as in Ref. [5], this paper assumes only one LFV coupling is different from zero at any time for the purpose of setting limits on the cross-section times branching of each final state considered. Polarization of τ -leptons is not included in the model, but its impact on the τ -lepton acceptance is found to be negligible.

In RPV SUSY, the superpotential terms allowing LFV are expressed as $\frac{1}{2}\lambda_{ijk}L_iL_jE_k^c + \lambda'_{ijk}L_iQ_jD_k^c$, where L and Q are the $SU(2)$ doublet superfields of leptons and quarks, E and D are the $SU(2)$ singlet superfields of charged leptons and down-type quarks, λ and λ' are Yukawa couplings, and the indices i , j , and k denote generations. A τ -sneutrino ($\tilde{\nu}_\tau$) may be produced in pp collisions by $d\bar{d}$ annihilation and subsequently decay into $e\mu$, $e\tau$, or $\mu\tau$. Although only $\tilde{\nu}_\tau$ is considered in this paper, results apply to any sneutrino flavor. For the theoretical prediction of the cross-section times branching ratio, the $\tilde{\nu}_\tau$ coupling to first-generation quarks (λ'_{311}) is assumed to be 0.11 for all channels. As in the Z' model, each lepton-flavor-violating final state is considered separately. It is assumed that $\lambda_{312} = \lambda_{321} = 0.07$ for the $e\mu$ final state, $\lambda_{313} = \lambda_{331} = 0.07$ for the $e\tau$ final state, and $\lambda_{323} = \lambda_{332} = 0.07$ for the $\mu\tau$ final state. These values are consistent with benchmark models used in previous ATLAS and CMS searches [5, 7, 8]. The CMS Collaboration has recently excluded R -parity-violating supersymmetric models below 1.7 TeV for $\lambda_{132} = \lambda_{231} = \lambda'_{311} = 0.01$ [6].

Various models introduce extra spatial dimensions to reduce the value of the Planck mass and resolve the hierarchy problem. The search described in this paper presents interpretations based on the Arkani-Hamed–Dimopoulos–Dvali (ADD) model [9], assuming $n = 6$, where n is the number of extra dimensions, and on the Randall–Sundrum (RS) model [10] with one extra dimension. Due to the increased strength of gravity at short distances in these models, pp collisions at the LHC could produce states exceeding the threshold mass (m_{th}) and form black holes. For the models considered, m_{th} is assumed to be equivalent to the extra-dimensional Planck scale. For masses beyond $3\text{--}5m_{\text{th}}$, it is expected that thermal black holes would be produced [11, 12], characterized by high-multiplicity final states. The search presented in this paper focuses on the mass region below $3\text{--}5 m_{\text{th}}$, known as the quantum gravity regime [13–15], where

production of non-thermal (or quantum) black holes is expected and these black holes could decay into two-particle final states, producing the topology investigated in this paper. Non-thermal quantum black holes would have a continuum mass distribution from m_{th} up to the beginning of the thermal regime. For the models considered in this paper, the thermal regime is assumed to start at $3m_{\text{th}}$. The decay of quantum black holes would be governed by a yet unknown theory of quantum gravity. The two main assumptions of the extra-dimensions models considered [4] in this paper are (a) gravity couples with equal strength to all SM particle degrees of freedom and (b) gravity conserves local symmetries (color and electric charge) but can violate global symmetries such as lepton-flavor and baryon-number conservation. Following these assumptions, the branching ratio to each final state is calculated. QBHs decaying into different-flavor, opposite-charge lepton pairs are created via $q\bar{q}$ or gg annihilation. The branching ratio to $\ell\ell'$ is 0.87% (0.34%) for a $q\bar{q}$ (gg) initial state [4]. These models were used in previous ATLAS and CMS searches for quantum black holes in dijet [16–18], lepton+jet [19], photon+jet [20], $e\mu$ [6], and same-flavor dilepton [21] final states.

2 The ATLAS detector

The ATLAS detector [22] is a general-purpose particle detector with approximately forward–backward symmetric cylindrical geometry.¹ It is composed of four main components, each responsible for identifying and reconstructing different types of particles: the inner detector (ID), the electromagnetic and hadronic calorimeters, and the muon spectrometer (MS). Each of the subdetectors is divided into two components, barrel and endcap, to provide coverage close to 4π in solid angle. In addition, two magnet systems allow charge and momentum measurements: an axial magnetic field of 2.0 T provided by a solenoid surrounding the ID and a toroidal magnetic field for the MS. The ID, the closest component to the interaction point, is used to reconstruct the trajectories of charged particles in the region $|\eta| < 2.5$ and measure their momenta. It is composed of three subsystems: (1) the silicon pixel detector, including an additional inner layer at a radius of 3.2 cm added in 2015 [23, 24], (2) the semiconductor tracker, used in conjunction with the silicon pixel detector to determine primary and secondary vertices with high precision thanks to their high granularity, (3) the transition radiation tracker, providing additional tracking in the region $|\eta| < 2.0$ and electron identification.

The calorimeter system covers the pseudorapidity range $|\eta| < 4.9$. Within the region $|\eta| < 3.2$, electromagnetic calorimetry is provided by barrel and endcap high-granularity lead/liquid-argon (LAr) electromagnetic calorimeters, with an additional thin LAr presampler covering $|\eta| < 1.8$, to correct for energy loss in material upstream of the calorimeters. Hadronic calorimetry is provided by the steel/scintillating-tile calorimeter, segmented into three barrel structures within $|\eta| < 1.7$, and two copper/LAr hadronic endcap calorimeters. The solid angle coverage is completed with forward copper/LAr and tungsten/LAr calorimeter modules optimised for electromagnetic and hadronic measurements respectively.

Surrounding the calorimeter system, the MS is the subdetector furthest from the interaction point. It consists of three layers of precision tracking chambers and fast detectors for triggering on muons. Tracking coverage is provided for $|\eta| < 2.7$ by three layers of precision drift tube chambers, with cathode strip

¹ ATLAS uses a right-handed coordinate system with its origin at the nominal interaction point (IP) in the center of the detector and the z -axis along the beam pipe. The x -axis points from the IP to the center of the LHC ring, and the y -axis points upward. The x – y plane is referred to as the transverse plane, used to define quantities such as the transverse momentum (p_T). Cylindrical coordinates (r, ϕ) are used in the transverse plane, ϕ being the azimuthal angle around the z -axis. The pseudorapidity is defined in terms of the polar angle θ as $\eta = -\ln(\tan(\theta/2))$. Angular distance is measured as $\Delta R = \sqrt{(\Delta\eta)^2 + (\Delta\phi)^2}$.

chambers in the innermost layer for $|\eta| > 2.0$, while trigger coverage is provided by resistive plate and thin gap chambers for $|\eta| < 2.4$.

The trigger and data-acquisition system is based on two levels of online event selection [25]: the level-1 trigger and the high-level trigger. The level-1 trigger is hardware-based and uses a subset of detector information to provide quick trigger decisions and reduce the accepted rate to 100 kHz. The high-level trigger is software-based and exploits the full detector information to further reduce the acceptance rate to about one kHz.

3 Data and simulated samples

The data sample used for this analysis was collected during 2015 and 2016 from pp collisions at a center-of-mass energy of 13 TeV. After selecting periods with stable beams and applying data-quality requirements, the total integrated luminosity is 36.1 fb^{-1} with an uncertainty of 2.1%, derived following a methodology similar to that detailed in Ref. [26] from a calibration of the luminosity scale using x - y beam-separation scans.

The $pp \rightarrow Z' \rightarrow \ell\ell'$ samples were generated at leading order (LO) using the generator PYTHIA 8.186 [27] with the NNPDF23LO [28] parton distribution function (PDF) set and the A14 [29] set of tuned parameters. Signal samples for 25 mass points ranging from 0.5 TeV to 5 TeV were generated in 0.1 TeV steps from 0.5 to 2 TeV, 0.2 TeV steps from 2 to 3 TeV, and 0.5 TeV steps from 3 to 5 TeV. The production cross-section was calculated with the same generator used for simulation. The cross-section and signal shape in the dilepton invariant mass distribution were corrected from LO to next-to-next-to-leading order (NNLO) in the strong coupling constant with a rescaling that depends on the dilepton invariant mass and which was computed with VRAP 0.9 [30] and the CT14NNLO PDF [31] set. This correction is applied as a multiplicative factor of about 0.98 at a dilepton invariant mass $m_{\ell\ell'}$ of 3 TeV. No mixing of the Z' boson with the Z and γ^* bosons is included.

The $d\bar{d} \rightarrow \tilde{\nu}_\tau \rightarrow \ell\ell'$ samples were generated at LO with MADGRAPH5_AMC@NLO v2.3.3 [32] interfaced to the PYTHIA 8.186 parton shower model with the NNPDF23LO PDF set and the A14 tune. The signal samples were generated at the same masses as for the Z' model described above. The cross-section was calculated at LO with the same generator used for simulation and corrected to next-to-leading order (NLO) using LOOPTOOLS v2.2 [33].

The $pp \rightarrow \text{QBH} \rightarrow \ell\ell'$ samples were generated with the program QBH 3.00 [34] using the CTEQ6L1 [35] PDF set and the A14 tune, for which PYTHIA 8.183 provides showering and hadronization. For each extra-dimensional model, eleven m_{th} points in 0.5 TeV steps were produced: from 3 to 8 TeV for the ADD $n = 6$ model and from 1 to 6 TeV for the RS $n = 1$ model. The production cross-section was calculated with the same generator used for simulation. These two models differ in the number and nature of the additional extra dimensions (large extra dimensions for ADD and one highly warped extra dimension for RS). In particular, the ADD model produces black holes with a larger gravitational radius and hence the parton–parton cross-section for this model is larger than for the RS model. Therefore, the m_{th} range of the generated samples differs for the two models.

The SM background in the LFV dilepton search is due to several processes which produce a final state with two different-flavor leptons. For the $e\mu$ mode, the dominant background contributions originate from $t\bar{t}$ and single-top production, with the subsequent decays of the top quark producing leptonically decaying W bosons. Other backgrounds originate from diboson (WW , WZ , and ZZ) production, and τ -lepton

pair production $q\bar{q} \rightarrow Z/\gamma^* \rightarrow \tau\tau$, which both produce different-flavor final states, through the leptonic decays of the W and Z bosons or the τ -leptons. They contribute about 15% and 1% of the background, respectively. Multijet and W +jets processes contribute due to the misidentification of jets as leptons and are the dominant background for the final states with a τ -lepton.

Backgrounds from top-quark production include $t\bar{t}$ and single-top with an associated W boson (tW). Both were generated at NLO using the PowHEG-Box [36–38] generator (v2 for $t\bar{t}$ and v1 for single-top) with the CT10 [39] PDF set used in the matrix-element calculations. PYTHIA 6.4.28 [40] and the corresponding Perugia 2012 tune [41] were used to simulate the parton shower, hadronization, and the underlying event. Top quarks were decayed using MADSPIN [42], preserving all spin correlations. The h_{damp} parameter, which controls the p_T of the first emission beyond the Born configuration in PowHEG-Box, was set to the mass of the top quark. The main effect of this parameter is to regulate the high- p_T emission against which the $t\bar{t}$ system recoils. The mass was set to the top quark mass of 172.5 GeV. The EvtGen 1.2.0 program [43] was used for the properties of b - and c -hadron decays. A value of 831^{+20}_{-29} (scale) $^{+35}_{-35}$ (PDF+ α_S) $^{+23}_{-22}$ (mass uncertainty) pb is used for the $t\bar{t}$ production cross-section, computed with Top++ 2.0 [44], incorporating NNLO QCD corrections, including resummation of next-to-next-to-leading logarithmic (NNLL) soft gluon terms. A Wt production cross-section of 71.7 ± 3.8 pb is used, as computed in Ref. [45] to approximately NNLO (NNLL+NLO) accuracy.

Diboson processes producing at least two charged leptons were simulated using the SHERPA 2.2.2 generator [46]. The matrix elements contain all diagrams with four electroweak vertices. Fully leptonic decays were calculated for up to one parton (four leptons, or two leptons and two neutrinos) or zero partons (three leptons and one neutrino) at NLO and up to three partons at LO using the Comix [47] and OPENLOOPS [48] matrix-element generators and merged with the SHERPA parton shower [49] using the ME+PS@NLO prescription [50]. The CT10 PDF set was used in conjunction with the default parton shower tuning provided by the authors of SHERPA. Inclusive cross-section values of 1.28, 4.51, and 10.64 pb are used for ZZ , WZ , and WW production, respectively.

Events containing W or Z bosons are generated using PowHEG-Box v2 interfaced to the PYTHIA 8.186 parton shower model. The CT10 PDF set is used in the matrix element. The AZNLO set of tuned parameters [51] is used, with PDF set CTEQ6L1, for the modelling of non-perturbative effects. The EvtGen 1.2.0 program is used for the properties of b - and c -hadron decays. Photos++ 3.52 [52] is used for QED emissions from electroweak vertices and charged leptons. The W/Z samples are normalised with the NNLO cross sections. This background contribution is normalized to an inclusive cross-section of 1.9 nb, calculated for $m_{\ell\ell} > 60$ GeV.

Processes such as W +jets and multijet production with jets that are misidentified as leptons were estimated through a combination of data-driven methods and simulation, detailed in Section 5. The W +jets contribution was estimated with the aid of the SHERPA 2.2.2 simulated samples. Matrix elements were calculated for up to two partons at NLO and four partons at LO using Comix and OpenLoops and merged with the SHERPA parton shower [49] according to the ME+PS@NLO prescription [50]. The overall cross-section times branching ratio for the $W^\pm \rightarrow \ell^\pm \nu + \text{jets}$ events is taken to be 59.6 nb.

For all samples used in this analysis, the effects of multiple proton–proton interactions per bunch crossing (pileup) were included by overlaying minimum-bias events simulated with PYTHIA8.186 using the ATLAS A14 set of tuned parameters [53] and reweighting the simulated events to reproduce the distribution of the number of interactions per bunch crossing observed in the data. The generated events were processed with the ATLAS simulation infrastructure [54], based on GEANT4 [55], and passed through the trigger simulation and the same reconstruction software used for the data.

4 Event reconstruction and selection

This search is optimized to look for new phenomena in the high mass range. Events are selected if they satisfy a single-muon or single-electron trigger with a p_T threshold of 50 GeV for muons and 60 or 120 GeV for electrons. The single-electron trigger with higher p_T threshold has a looser identification requirement, resulting in an increased trigger efficiency at high p_T .

Electron candidates are formed by associating the energy in clusters of cells in the electromagnetic calorimeter with a track in the ID [56]. A likelihood discriminant suppresses contributions from hadronic jets, photon conversions, Dalitz decays, and semileptonic heavy-flavor hadron. The likelihood discriminant utilizes lateral and longitudinal calorimeter shower shapes plus tracking and cluster-track matching quantities. The discriminant criterion is a function of the p_T and $|\eta|$ of the electron candidate. Two operating points are used in this analysis, as defined in Ref. [57]: *Medium* and *Tight*. The *Tight* working point (85% efficient at $p_T = 65$ GeV determined with $Z \rightarrow ee$ events) is required for electron candidates. Electron candidates must have $p_T > 65$ GeV and $|\eta| < 2.47$, excluding the region $1.37 < |\eta| < 1.52$, where the energy reconstruction performance is degraded due to the presence of extra inactive material. Further requirements are made on the transverse and longitudinal impact parameters of the track, which is the distance between the z -position of the point of closest approach of the track in the ID to the beamline and the z -coordinate of the primary vertex relative to the primary vertex of the event (d_0 and Δz_0). The requirements are the following: $|d_0/\sigma_{d_0}| < 5$ and $|\Delta z_0 \sin \theta| < 0.5$ mm. Candidates are required to satisfy relative track-based (as defined above for muon candidates) and calorimeter-based isolation requirements with an efficiency of 99% to suppress background from non-prompt electrons originating from heavy-flavor semileptonic decays, charged hadrons, and photon conversions from π^0 decays. The sum of the calorimeter transverse energy deposits (excluding the electron itself) in an isolation cone of size $\Delta R = 0.2$ divided by the electron p_T is the discriminant used in the calorimeter-based isolation criterion. For the reducible background estimation, electron candidates passing the *Medium* working point (95% efficient at $p_T = 65$ GeV determined with $Z/\gamma^* \rightarrow ee$ events) are referred to as “loose electrons”.

Candidate muon tracks are initially reconstructed independently in the ID and the MS. The two tracks are input to a combined fit which takes into account the energy loss in the calorimeter and multiple scattering. Muon identification is based on information from both the ID and MS to ensure that muons are reconstructed with the optimal momentum resolution up to very high p_T using the *High- p_T* operating point [58]. Only tracks with hits in each of the three stations of the muon spectrometer are considered. This provides a muon transverse momentum resolution of about 10% at 1 TeV. Moreover, muon candidates are required to be within the ID acceptance region² of $|\eta| < 2.5$, fulfill $|d_0/\sigma_{d_0}| < 3$ and $|\Delta z_0 \sin \theta| < 0.5$ mm, have a transverse momentum larger than 65 GeV, and fulfill a track-based isolation criterion with an efficiency of 99% over the full range of muon momenta to further reduce contamination from non-prompt muons. The scalar sum of the transverse momenta of tracks (excluding the muon itself) in an isolation cone of size $\Delta R = 0.2$ divided by the muon p_T is the discriminant used in the track-based isolation criterion. For the reducible background estimation, muon candidates fulfilling all selection criteria except the isolation criterion are called “loose muons”.

Jets are reconstructed using the anti- k_t algorithm [59] with a radius parameter of 0.4 using energy clusters [60] of calorimeter cells as input. Jet calibrations [61] derived from $\sqrt{s} = 13$ TeV simulated data and from collision data taken at 13 TeV are used to correct the jet energies and directions to those of the particles from the hard-scatter interaction.

² For the $\mu\tau$ channel, the muon acceptance is limited by the coverage of the muon trigger system ($|\eta| < 2.4$).

Hadronic decays of τ -leptons are composed of a neutrino and a set of visible decay products ($\tau_{\text{had-vis}}$), typically one or three charged pions and up to two neutral pions. The reconstruction of τ -leptons and their visible hadronic decay products starts with jets reconstructed from topological clusters [62]. The $\tau_{\text{had-vis}}$ candidates must have $|\eta| < 2.5$ with the transition region between the barrel and endcap calorimeters ($1.37 < |\eta| < 1.52$) excluded, a transverse momentum greater than 65 GeV, one or three associated tracks with ± 1 total electric charge. Their identification is performed using a multivariate algorithm that employs boosted decision trees (BDT) using shower shape and tracking information to discriminate against jets. All $\tau_{\text{had-vis}}$ candidates are required to fulfill the “loose” identification requirements of Ref. [63]. An additional dedicated likelihood-based veto is used to reduce the number of electrons misidentified as $\tau_{\text{had-vis}}$ candidates. For the purpose of the reducible background estimation, $\tau_{\text{had-vis}}$ candidates failing the “loose” identification requirements are used.

Jets containing b -hadrons (b -jets) are identified with a b -tagging algorithm based on a multivariate technique [64]. Operating points are defined by a single value in the domain of discriminant outputs and are chosen to provide a specific b -jet efficiency in an inclusive $t\bar{t}$ sample. The employed working point has an efficiency of 77% and rejection factors of 6 and 134 for charm and light-quark/gluon jets, respectively [64].

Only events with exactly two different-flavour leptons are chosen. As such, there is no overlap between the three channels considered: $e\mu$, $e\tau$, $\mu\tau$. They must have a reconstructed primary vertex, defined as the vertex whose constituent tracks have the highest sum of p_T^2 , and exactly two reconstructed different-flavor lepton candidates meeting the above-mentioned criteria. Events with an additional electron, muon or $\tau_{\text{had-vis}}$ are vetoed. For the $e\mu$ channel only, events with an extra electron or muon fulfilling the “loose” criteria are also vetoed, including events used for the purpose of the reducible background estimation. For all three channels, the lepton candidates must be back-to-back in the transverse plane with $\Delta\phi(\ell, \ell') > 2.7$. The invariant mass of the dilepton pair is used as the discriminant. No requirement is made on the respective charges of the leptons since it reduces the signal efficiency by as much as 6% for the highest-mass signals considered due to charge misassignment without a significant effect on the background rejection. To account for differences between data and simulation, corrections are applied to the lepton trigger, reconstruction, identification, and isolation efficiencies as well as the lepton energy/momenta resolution and scale [56–58, 63].

Double-counting of leptons and jets is avoided by applying an overlap removal algorithm based on the ΔR distance metric. First, jets within $\Delta R < 0.2$ of any identified muons or electrons are removed. Then, any muons and electrons within $0.2 < \Delta R < 0.4$ from the jet axis are removed.

The missing transverse momentum vector (\vec{E}_T^{miss}) is defined as the negative vector sum of the transverse momenta of all identified physics objects and an additional soft term. The soft term is constructed from all tracks that are associated with the primary vertex, but not with any selected physics object. In this way, the missing transverse momentum incorporates the best calibration of the jets and the other identified physics objects, while maintaining pileup independence in the soft term [65].

The dominant background for the $e\mu$ channel is $t\bar{t}$ production, which can be suppressed by rejecting events that contain one or more b -jets (b -veto).

For a Z' boson with a mass of 1.5 TeV, the fractions of events that pass all of the selection requirements are approximately 45%, 45%, 20%, and 15% for the $e\mu$, $e\mu$ with b -veto, $e\tau$, and $\mu\tau$ final states, respectively.

For the reducible background estimation in the $e\tau$ and $\mu\tau$ channels, the transverse mass m_T of a lepton and the missing transverse momentum is defined as

$$m_T = \sqrt{2p_T E_T^{\text{miss}} [1 - \cos \Delta\phi(\ell, E_T^{\text{miss}})]},$$

where p_T is the transverse momentum of the lepton, E_T^{miss} is the magnitude of the missing transverse momentum vector, and $\Delta\phi(\ell, E_T^{\text{miss}})$ is the azimuthal angle between the lepton and \vec{E}_T^{miss} directions.

For the dilepton mass calculation in the $e\tau$ and $\mu\tau$ channels, the missing momentum from the neutrino in the hadronic decay of a τ -lepton is estimated and added to the four-momentum of the $\tau_{\text{had-vis}}$ candidate. At the considered momenta, the hadronic decay of the τ -lepton results in the neutrino and the resultant jet being nearly collinear. The neutrino four-momentum is reconstructed from the magnitude of the missing transverse momentum and the direction of the $\tau_{\text{had-vis}}$ candidate. This technique significantly improves the dilepton mass resolution and search sensitivity [7]. For a simulated Z' boson with a mass of 2 TeV, the mass resolution improves from 8% (17%) to 4% (12%) in the $e\tau$ ($\mu\tau$) channel.

5 Background estimation

The background processes for this search can be divided into two categories: reducible and irreducible. The latter is composed of processes which produce two different-flavor prompt leptons, including $Z/\gamma^* \rightarrow \tau\tau$, $t\bar{t}$, single-top, and diboson production. These processes are modeled using simulated samples and normalized to their theoretically predicted cross-sections. Reducible backgrounds originate from jets misreconstructed as leptons and require the use of data-driven techniques. The contribution from reducible backgrounds is small in the $e\mu$ channel, about 5%, whereas in the $e\tau$ and $\mu\tau$ channels they are the leading components and make up 50–60% of the total background.

5.1 Top-quark background extrapolation

The simulated samples used to estimate single-top-quark and $t\bar{t}$ production are statistically limited for dilepton invariant masses above 1 TeV. Therefore, for $m_{\ell\ell'} > 700$ GeV, the $t\bar{t}$ plus single-top contributions are evaluated using monotonically decreasing functions fitted to the $m_{\ell\ell'}$ distribution. Two functional forms are chosen for their stability when varying the fit range and for the quality of the fit:

$$a \cdot m_{\ell\ell'}^b \cdot m_{\ell\ell'}^{c \cdot \ln(m_{\ell\ell'})} \quad \text{and} \quad \frac{a}{(m_{\ell\ell'} + b)^c},$$

where a , b and c are free parameters in the fit. To account for fit variations, the lower and upper limits of the fit range were varied in 25 GeV steps between 200–300 GeV and 1000–1200 (800–1000) GeV for $e\mu$ ($e\tau$ and $\mu\tau$). The nominal extrapolation is taken as the average of all the tested fit ranges using both functional forms. The extrapolation is found to agree within statistical uncertainties with the simulated data. For each mass bin, the up and down variations obtained from varying the fit parameters are combined in quadrature with the uncertainty of the fit range variation. This uncertainty is 32% at 2 TeV for the $e\mu$ channel.

5.2 Reducible background

The main reducible backgrounds are W +jets and multi-jet production. The contribution to the reducible background from muons originating from decays of hadrons in jets is found to be negligible compared with the contribution from fake electrons and τ -leptons. Therefore, in the $e\mu$ channel, where reducible backgrounds are a small contribution to the total, non-prompt muons are neglected and only events with one prompt muon and a jet faking an electron are considered. In channels involving taus, however, reducible backgrounds are more significant, and so contributions from both electrons and muons, primarily non-prompt leptons from heavy flavor decays, are taken into account. However, the dominant source of reducible background in these channels remains fake taus from gluon-initiated jets.

5.2.1 $e\mu$ channel: matrix method

For the $e\mu$ channel, the matrix method is employed, as detailed in Ref. [21]. The selection criteria are loosened for electron candidates to create a sample of events with a muon and a “loose” electron as defined in Section 4. These events are referred to as “loose”, while those in which both the electron and muon pass all selections are “tight”. The probability of a “loose” electron matched to a generated electron to pass the full object selection (the “real efficiency”) is evaluated from $Z \rightarrow ee$ simulated events, while the probability that a jet is misidentified as an electron (the “fake rate”) is obtained in a multijet-enriched data sample. To suppress the W +jets contribution to the multijet-enriched sample, its events are required to have $E_T^{\text{miss}} < 25$ GeV and $m_T < 50$ GeV as well as to pass the signal region selection outlined in Section 4. Both the real efficiency and the fake rate are determined as a function of p_T , and they are used to estimate the reducible background contribution by solving a system of linear equations involving the numbers of loose and tight events in the signal region. Residual contaminations from W +jets and other SM background processes (top, diboson, and $Z \rightarrow \ell\ell$) in the multi-jet CR are subtracted using simulation. This background is estimated up to around 1.5 TeV, where there are no data. However, at this stage, the expectation of this background is well below one event, and generally negligible compared to diboson and top quark processes.

The uncertainties associated with the matrix method are evaluated by considering systematic effects on the electron fake rate. Uncertainties of the real electron efficiency have a negligible impact on the estimation and are not considered. The systematic uncertainties in the fake rate include

- the choice of multijet-enriched region,
- uncertainties on the MC subtraction in the multijet-enriched region, and
- the difference in the fake rates obtained using this method and those obtained from simulated W +jets events.

The overall uncertainty of the $e\mu$ reducible background is about 30%. Given that in the $e\mu$ channel this contribution is about 7% of the total background over the invariant mass range considered, the uncertainties in the estimation method have a small impact on the results.

5.2.2 $e\tau$ and $\mu\tau$ channels: $W+\text{jets}$ estimate

The dominant background for the $e\tau$ and $\mu\tau$ channels is the $W+\text{jets}$ process, where a jet is misidentified as a $\tau_{\text{had-vis}}$ candidate. It is estimated using simulated events with each jet weighted by its probability to pass the τ -lepton identification as measured in data. This not only ensures the correct fake rate but also improves the statistical precision of the estimate, since events failing the τ -lepton identification requirements are not discarded. The $\tau_{\text{had-vis}}$ fake rate is measured in a $W \rightarrow e/\mu + \text{jets}$ control region as a function of the p_T , η , and number of tracks of the $\tau_{\text{had-vis}}$ candidates. The $W+\text{jets}$ -enriched control region uses the same selection as the signal region, but reverses the back-to-back criterion to $\Delta\phi(\ell, \ell') < 2.7$, and uses τ -leptons fulfilling all requirements except identification, although a minimum requirement on the BDT discriminant is retained. Only events with exactly one electron or muon fulfilling all selection criteria, as well as $m_T > 80$ GeV to enrich the $W+\text{jets}$ contribution, are used. Events where the invariant mass of the e or μ and the $\tau_{\text{had-vis}}$ candidate is between 80 and 110 GeV are vetoed to reduce contamination from Z boson decays. Contributions from non- $W+\text{jets}$ processes are subtracted using simulation. The $\tau_{\text{had-vis}}$ candidates present in the remaining events are dominated by jets. The contribution of events with non-prompt electrons is estimated from simulation and found to be less than 1%. The $\tau_{\text{had-vis}}$ fake rate is defined as the fraction of $\tau_{\text{had-vis}}$ candidates in the sample that also pass the $\tau_{\text{had-vis}}$ identification. This rate is used to weight simulated $W+\text{jets}$ events. The resulting distribution obtained for the $W+\text{jets}$ is validated in the $W+\text{jets}$ -enriched control region, where good agreement is found between data and the expected SM background processes.

The uncertainties in the $\tau_{\text{had-vis}}$ fake rate are evaluated from

- the modeling of the “loose” $\tau_{\text{had-vis}}$ identification requirement in simulation,
- the statistical uncertainty of the data-driven estimation of the τ -lepton fake rate, and
- the differences in τ -lepton fake rate between signal and control regions.

These errors are detailed in the following paragraphs.

The $\tau_{\text{had-vis}}$ fake rate is re-evaluated when removing the $m_T > 80$ GeV requirement to check the contamination from non- $W+\text{jets}$ processes. The effect on the fake rate and the final estimation of the $W+\text{jets}$ background is about 2%.

The statistical uncertainty of the fake rate in the control regions is propagated through the estimate. The impact is small at low $m_{\ell\tau}$ but is the leading uncertainty of the fake rate in the range $m_{\ell\tau} > 1$ TeV.

The jet composition of the fake $\tau_{\text{had-vis}}$ background is evaluated from simulated $W+\text{jets}$ events. The control region where the $\tau_{\text{had-vis}}$ fake rate is evaluated should have a jet composition similar to that in the signal region. Therefore, $W+\text{jets}$ simulated events are used to investigate the difference between the fake rates measured in the $W+\text{jets}$ control and signal regions. The comparison reveals a slightly lower fake rate in the signal region, consistent with the lower expected gluon contribution. The relative difference between these fake rates is assigned as a systematic uncertainty, which contributes an uncertainty of about 8% to the total background at $m_{\ell\tau} = 1$ TeV.

5.2.3 $e\tau$ and $\mu\tau$ channels: multijet estimate

The multijet background contributions in the $e\tau$ and $\mu\tau$ channels are evaluated using events in three control regions (R_1 , R_2 , R_3). The events must pass the selection for the signal region, except that in R_1 and R_3 the electron/muon must fail isolation and the $\tau_{\text{had-vis}}$ candidate must fail identification, and in R_1 and R_2 the leptons must have the same electric charge and the electron/muon p_T must be less than 200 GeV to avoid signal contamination. For a Z' boson with a mass of 500 GeV, the lowest signal mass considered in this paper, the contamination from the signal processs in R_2 is found to be below 1%. The region definitions are summarized in Table 1. The background contribution is estimated as $N_{\text{MJ}} = N_{R_3} \times N_{R_2}/N_{R_1}$. The transfer factor N_{R_2}/N_{R_1} is calculated as a function of the dilepton mass to encapsulate correlations between $m_{\ell\tau}$ and the isolation and identification requirements, and it is fitted with a polynomial function. In each of the regions defined, the contributions from other SM processes, such as $W+\text{jets}$, $Z+\text{jets}$, $Z/\gamma^* \rightarrow \ell\ell$, diboson, and top-quark production, are subtracted using simulation. The contribution from the multijet background is $\sim 60\%$ ($\sim 20\%$) of the $W+\text{jets}$ background for the $e\tau$ ($\mu\tau$) channel, corresponding to $\sim 25\%$ ($\sim 10\%$) of the total expected background.

Table 1: Definition of the regions used for the multijet background estimation in the $e\tau$ and $\mu\tau$ channels.

	Object selection	Lepton-pair charges
R_1	Non-isolated e/μ & $\tau_{\text{had-vis}}$ failing τ ID requirements ($p_{T_\ell} \& p_{T_\tau} < 200$ GeV)	Same-charge
R_2	Isolated e/μ & pass ID $\tau_{\text{had-vis}}$ ($p_{T_\ell} \& p_{T_\tau} < 200$ GeV)	Same-charge
R_3	Non-isolated e/μ & $\tau_{\text{had-vis}}$ failing τ ID requirements	Same-charge + Opposite-charge

The multijet background is estimated using a transfer factor obtained using same-charge lepton pairs and applied to opposite-charge plus same-charge lepton pairs. To check the validity of this procedure, the multijet background is also estimated using a transfer factor obtained with opposite-charge pairs. The difference between the resulting shape and transfer factors is assigned as a systematic uncertainty. The impact of this uncertainty is about 7% at 1 TeV.

The statistical uncertainties in the $m_{\ell\tau}$ -dependent transfer factor and the subtraction of simulated events are propagated to the final estimate and assigned as a systematic uncertainty. The overall uncertainty is 50% (15%) at 1 TeV for the $e\tau$ ($\mu\tau$) channel. The uncertainty in the $\mu\tau$ channel is smaller because the transfer factor is found to have a negligible effect on the dilepton invariant mass, and the transfer-factor fit uncertainties are reduced.

5.3 Reducible background validation

The validity of the background estimation is checked in the $W+\text{jets}$ control region. Figures 1 and 2 show the electron, muon, and τ -lepton transverse momentum, $\ell\tau$ invariant mass and jet multiplicity distributions for the $e\tau$ and $\mu\tau$ channels, respectively, in the $W+\text{jets}$ control region. Good agreement is observed between the data and the background prediction. The contribution from each SM background for each of the final states in the signal region is given in Section 7.

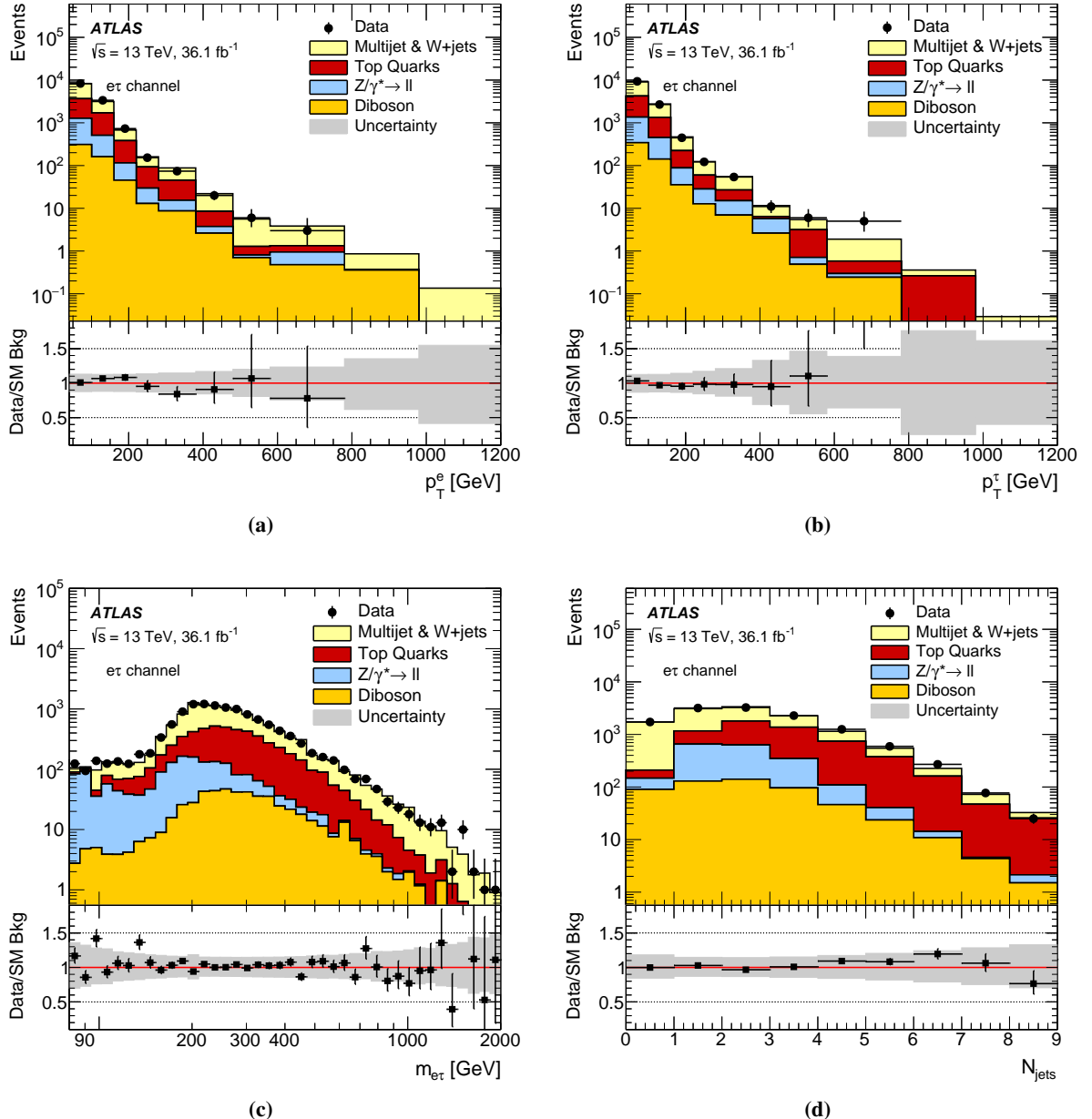


Figure 1: Distributions in the $W + \text{jets}$ -enriched control region for the $e\tau$ channel: (a) the electron and (b) τ -lepton transverse momentum, (c) the $e\tau$ invariant mass, and (d) the jet multiplicity. No further data points are found in overflow bins.

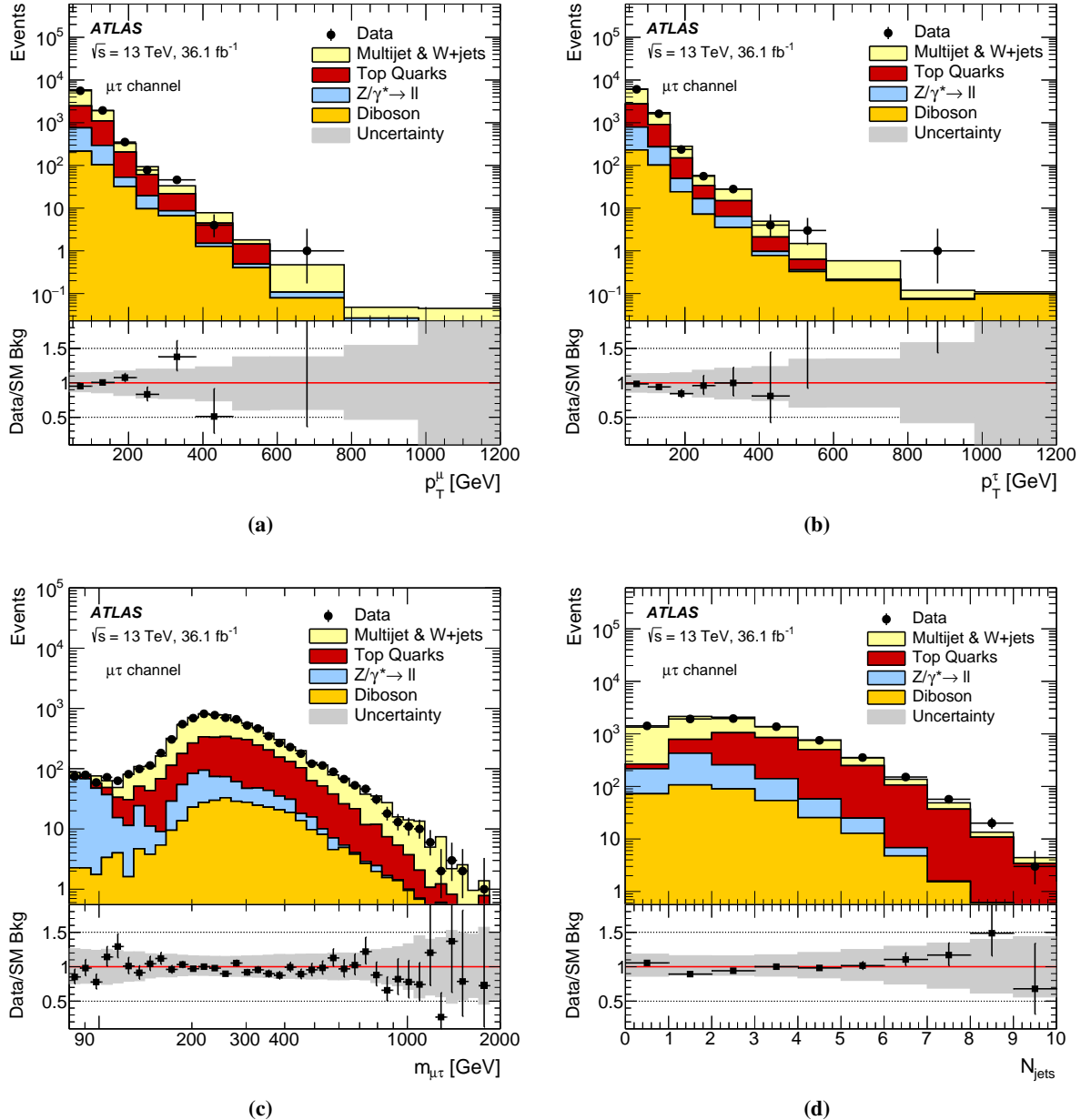


Figure 2: Distributions in the $W+\text{jets}$ -enriched control region for the $\mu\tau$ channel: (a) the muon and (b) τ -lepton transverse momentum, (c) the $\mu\tau$ invariant mass, and (d) the jet multiplicity. No further data points are found in overflow bins.

6 Systematic uncertainties

The sources of experimental uncertainty considered are pileup effects; lepton efficiencies due to triggering, identification, reconstruction, isolation, energy scale, and resolution [56–58, 63, 66]; jet energy scale and resolution [61]; b -tagging [64]; and missing transverse momentum [65]. Sources of uncertainty are considered for both the simulated background and signal processes.

Mismodeling of the muon momentum resolution at the TeV scale from residual misalignment of the muon precision chambers can alter the signal and background shapes. A corresponding uncertainty is obtained from studies performed in dedicated data-taking periods with no magnetic field in the MS. The muon reconstruction efficiency is affected at high p_T by possible large energy losses in the calorimeter. The associated uncertainty is estimated by comparing studies of $Z \rightarrow \mu\mu$ data events extrapolated to high p_T with the results predicted by simulation [67]. The effect on the muon reconstruction efficiency was found to be approximately 3% per TeV as a function of muon p_T .

The uncertainty of the electron identification efficiency extrapolation is determined from the differences in the electron shower shapes in the EM calorimeters between data and simulation in the $Z \rightarrow ee$ peak, which are propagated to the high p_T electron sample. The effect on the electron identification efficiency is 2% and is independent of p_T for electrons with transverse momentum above 150 GeV [67].

The treatment of systematic uncertainties for τ -leptons with p_T up to 100 GeV is detailed in Ref. [62]. An additional uncertainty of 20% per TeV is assigned to the reconstruction efficiency of τ -leptons with $p_T > 100$ GeV to account for the degradation of the modeling and reconstruction efficiency from track merging, derived from studies in simulation and in dijet data events at 8 TeV [68].

The missing transverse momentum uncertainty is derived from the uncertainties of the momenta of physics objects and uncertainties of the soft term determined by comparisons with simulation.

A mis-modeling of the dilepton p_T variable is found in the $t\bar{t}$ simulation. After reweighting to data in a $t\bar{t}$ control region, an uncertainty is assigned to account for the effect on the dilepton invariant mass spectrum.

A pile-up modeling uncertainty is estimated by varying the distribution of pile-up events in the reweighting of the MC, to cover the uncertainty on the ratio between the predicted and measured inelastic cross-section in the fiducial volume defined by $M_X > 13$ GeV where M_X is the mass of the hadronic system [69].

The uncertainty of 2.1% in the luminosity applies to the signal and to backgrounds derived from simulations.

The uncertainties of the reducible background estimation in the $e\mu$ channel, and the τ -lepton fake rate, the multijet transfer factor calculation, and the top-quark extrapolation are presented in Section 5.

The PDF uncertainties are the dominant systematic uncertainties affecting the background estimates, together with the uncertainty on the extrapolation to estimate the top-quark background contribution at high mass. The contribution from PDF uncertainties is estimated using different PDF sets and eigenvector variations within a particular PDF set for the top-quark, diboson, and W +jets backgrounds. The CT10 PDF uncertainty due to eigenvector variations is evaluated through the use of LHAPDF [70] following the prescriptions of Ref. [71]. The uncertainty related to the choice of PDF is evaluated by comparing the results with those from the central value of other PDF sets: MMHT2014 [72], NNPDF3.0 [73], and CT14 [31]. PDF-related uncertainties in the signal shape are not considered. The uncertainties of the $m_{\ell\ell\ell}$ modeling in $t\bar{t}$ events are obtained using separate simulated samples generated with the renormalization

scale and h_{damp} parameter varied by factors of 2 and 1/2, and are referred to as “Top scale” in Table 2. These uncertainties for W+jets are not considered as they are found to be small, given that this background is mainly composed of real lepton (e or mu) and fake tau pairs. For the diboson background prediction, the PDF systematic is the leading uncertainty.

Experimental systematic uncertainties common to signal and background processes are assumed to be correlated. The systematic uncertainties of the estimated SM background and signal yields are summarized in Tables 2 and 3. For signal processes, only experimental systematic uncertainties are considered. The simulated samples contribute a 3% statistical uncertainty to the overall signal acceptance times efficiency.

Table 2: Summary of the systematic uncertainties taken into account for background processes. Values are provided for $m_{\ell\ell'}$ values of 1, 2 and 3 TeV. Uncertainties are quoted as a percentage of the total background. The “-” sign indicates that the systematic uncertainty is not applicable.

Source	1 TeV				2 TeV				3 TeV			
	$e\mu$	$e\mu$	$e\tau$	$\mu\tau$	$e\mu$	$e\mu$	$e\tau$	$\mu\tau$	$e\mu$	$e\mu$	$e\tau$	$\mu\tau$
Luminosity	2	2	2	2	2	2	2	2	2	2	2	2
Top-quark extrapolation	5	3	2	2	32	8	3	4	63	12	3	14
Top scale	7	6	7	8	40	15	1	14	65	15	3	27
PDF	16	15	12	14	32	34	17	20	51	69	16	53
Pile-up	1	1	3	7	9	6	3	13	32	12	2	17
Dilepton p_T modeling	7	4	2	1	11	5	0	1	15	6	0	4
Electron iden. and meas.	4	4	5	-	4	8	6	-	5	11	8	-
Muon iden. and meas.	3	4	-	4	7	7	-	16	17	10	-	18
τ iden. and meas.	-	-	2	2	-	-	1	1	-	-	1	2
τ reconstruction eff.	-	-	2	2	-	-	1	1	-	-	1	3
τ fake rate	-	-	6	9	-	-	5	12	-	-	2	12
Multijet transf. factor	-	-	31	2	-	-	53	0	-	-	64	0
Reducible $e\mu$ estimation	2	-	-	-	2	-	-	-	2	-	-	-
Jet eff. and resol.	1	4	9	8	2	12	17	42	5	17	22	48
b -tagging	-	3	-	-	-	2	-	-	-	2	-	-
E_T^{miss} resol. and scale	-	-	3	4	-	-	5	6	-	-	8	8
Total	19	20	37	25	62	45	61	62	110	79	73	91

7 Results

Tables 4–7 show the expected and observed numbers of events in the low and high mass regions for each channel. The $e\mu$ background is dominated by $t\bar{t}$ and diboson events, while W+jets events are dominant for the $e\tau$ and $\mu\tau$ final states.

Figure 3 shows the dilepton invariant mass distributions for the $e\mu$, $e\mu$ with b -veto, $e\tau$, and $\mu\tau$ channels. The largest deviation found in the data is a deficit in the 1.1–1.4 TeV range of the $e\mu$ channel, with a global significance of 1.8 standard deviations, obtained using the BumpHunter program [74]. Due to the parton luminosity tail in the LFV Z' model, the impact of the deficit in the 1.1–1.4 TeV range is also seen in the observed limit for Z' boson masses up to 4–5 TeV. No significant excess is found in any channel.

Table 3: Summary of the systematic uncertainties taken into account for signal processes. Values are provided for $m_{\ell\ell'}$ values of 1, 2 and 3 TeV. The “-” sign indicates that the systematic uncertainty is not applicable.

Source	1 TeV				2 TeV				3 TeV			
	$e\mu$	$e\mu$	$e\tau$	$\mu\tau$	$e\mu$	$e\mu$	$e\tau$	$\mu\tau$	$e\mu$	$e\mu$	$e\tau$	$\mu\tau$
	b -jet veto		b -jet veto		b -jet veto		b -jet veto		b -jet veto		b -jet veto	
Luminosity	2	2	2	2	2	2	2	2	2	2	2	2
Pile-up	1	1	4	3	3	3	4	3	2	2	3	4
Electron iden. and meas.	6	6	8	-	7	7	13	-	9	9	14	-
Muon iden. and meas.	5	5	-	5	6	6	-	7	7	7	-	8
τ iden. and meas.	-	-	8	6	-	-	10	8	-	-	11	9
τ reconstruction eff.	-	-	2	2	-	-	2	2	-	-	3	3
Jet eff. and resol.	1	1	2	2	1	1	3	4	1	1	3	3
b -tagging	-	1	-	-	-	1	-	-	-	1	-	-
E_T^{miss} resol. and scale	-	2	3	2	-	-	2	2	-	-	3	2
Total	8	8	13	9	10	10	17	12	12	12	19	14

Table 4: Expected and observed numbers of $e\mu$ events in the low (a) and high (b) mass regions after applying all selection criteria. The statistical and systematic uncertainties are quoted.

Process	$m_{e\mu} < 300$ GeV	$300 < m_{e\mu} < 600$ GeV
Top	$8460 \pm 60 \pm 860$	$2770 \pm 30 \pm 380$
Diboson	$1500 \pm 20 \pm 130$	$493 \pm 9 \pm 57$
W +jets	$550 \pm 30 \pm 190$	$214 \pm 14 \pm 75$
$Z/\gamma^* \rightarrow \ell\ell$	$90 \pm 6 \pm 12$	$19.5 \pm 1.6 \pm 3.2$
Total background	$10600 \pm 70 \pm 980$	$3490 \pm 40 \pm 440$
Data	10353	3417

(a) N_{events} with $m_{e\mu} < 600$ GeV

Process	$600 < m_{e\mu} < 1200$ GeV	$1200 < m_{e\mu} < 2000$ GeV
Top	$140 \pm 6 \pm 27$	$4.6 \pm 0.7 \pm 2.7$
Diboson	$47.5 \pm 1.2 \pm 8.0$	$2.96 \pm 0.31 \pm 0.79$
W +jets	$24.1 \pm 3.9 \pm 8.4$	$0.1 \pm 2.3 \pm 0.0$
$Z/\gamma^* \rightarrow \ell\ell$	$1.31 \pm 0.07 \pm 0.27$	$0.07 \pm 0.01 \pm 0.02$
Total background	$213 \pm 7 \pm 37$	$7.7 \pm 2.4 \pm 2.8$
Data	196	1

Process	$2000 < m_{e\mu} < 3000$ GeV	$m_{e\mu} > 3000$ GeV
Top	$0.28 \pm 0.09 \pm 0.32$	$(0.16 \pm 0.08 \pm 0.28) \cdot 10^{-1}$
Diboson	$0.25 \pm 0.10 \pm 0.11$	$(0.44 \pm 0.01 \pm 0.56) \cdot 10^{-2}$
W +jets	< 0.01	< 0.001
$Z/\gamma^* \rightarrow \ell\ell$	$(0.48 \pm 0.03 \pm 0.23) \cdot 10^{-2}$	$(0.16 \pm 0.02 \pm 0.31) \cdot 10^{-3}$
Total background	$0.54 \pm 0.13 \pm 0.41$	$(0.21 \pm 0.08 \pm 0.30) \cdot 10^{-1}$
Data	0	0

(b) N_{events} with $m_{e\mu} > 600$ GeV

Table 5: Expected and observed numbers of $e\mu$ events in the low (a) and high (b) mass regions after applying all selection criteria including the b -jet veto. The statistical and systematic uncertainties are quoted.

Process	$m_{e\mu} < 300$ GeV	$300 < m_{e\mu} < 600$ GeV
Top	$1660 \pm 20 \pm 260$	$570 \pm 10 \pm 100$
Diboson	$1470 \pm 20 \pm 130$	$479 \pm 8 \pm 55$
W +jets	$231 \pm 18 \pm 87$	$87 \pm 8 \pm 33$
$Z/\gamma^* \rightarrow \ell\ell$	$86 \pm 6 \pm 12$	$18.4 \pm 1.3 \pm 3.0$
Total background	$3450 \pm 30 \pm 350$	$1150 \pm 20 \pm 150$
Data	3411	1082

(a) N_{events} with $m_{e\mu} < 600$ GeV

Process	$600 < m_{e\mu} < 1200$ GeV	$1200 < m_{e\mu} < 2000$ GeV
Top	$28.6 \pm 1.7 \pm 8.9$	$0.72 \pm 0.10 \pm 0.85$
Diboson	$45.9 \pm 1.2 \pm 7.7$	$2.85 \pm 0.30 \pm 0.76$
W +jets	$11.0 \pm 2.8 \pm 4.3$	$0.1 \pm 1.9 \pm 0.0$
$Z/\gamma^* \rightarrow \ell\ell$	$1.27 \pm 0.06 \pm 0.25$	$(0.70 \pm 0.05 \pm 0.20) \cdot 10^{-1}$
Total background	$87 \pm 3 \pm 15$	$3.7 \pm 2.0 \pm 1.1$
Data	83	0

Process	$2000 < m_{e\mu} < 3000$ GeV	$m_{e\mu} > 3000$ GeV
Top	$(2.8 \pm 0.8 \pm 5.5) \cdot 10^{-2}$	$(0.8 \pm 0.4 \pm 2.3) \cdot 10^{-3}$
Diboson	$0.25 \pm 0.10 \pm 0.11$	$(0.42 \pm 0.01 \pm 0.51) \cdot 10^{-2}$
W +jets	< 0.001	< 0.001
$Z/\gamma^* \rightarrow \ell\ell$	$(0.46 \pm 0.03 \pm 0.23) \cdot 10^{-2}$	$(0.14 \pm 0.02 \pm 0.30) \cdot 10^{-3}$
Total background	$0.28 \pm 0.10 \pm 0.14$	$(0.52 \pm 0.04 \pm 0.60) \cdot 10^{-2}$
Data	0	0

(b) N_{events} with $m_{e\mu} > 600$ GeV

The electron–muon event with an invariant mass of 2.1 TeV found in the previous version of this analysis [5] no longer satisfies the event selection, since the previously selected muon candidate is found to overlap with a jet using the criteria of this paper and is no longer classified as a prompt muon.

Since no deviations from the SM prediction are observed, model-dependent exclusion limits are extracted using a Bayesian method implemented with the Bayesian analysis toolkit [75]. A binned likelihood function is constructed from the product of the Poisson probabilities of the observed and expected numbers of events in each $m_{\ell\ell'}$ mass bin as in Ref. [5]. A 95% credibility level (CL) Bayesian upper limit is placed on the signal cross-section times branching ratio.

Expected exclusion limits are obtained by generating 1000 pseudo-experiments for each signal mass point. The median value of the pseudo-experiment distribution of the 95% CL Bayesian upper limit is taken as the expected limit. The one- and two-standard deviation intervals of the expected limit are obtained by finding the 68% and 95% intervals of the pseudo-experiment upper limit distribution, respectively.

The invariant mass spectrum for each final state is analyzed in 60 bins from 120 GeV to 10 TeV. The bin width is around 7% of the dilepton mass throughout the whole range. The predicted width of the Z' boson, 3% for $m_{Z'} = 2$ TeV, is smaller than the detector resolutions for the $e\mu$ and the $\mu\tau$ channels, which are approximately 8% and 12%, respectively, at the same Z' boson mass. For the $e\tau$ final state the detector

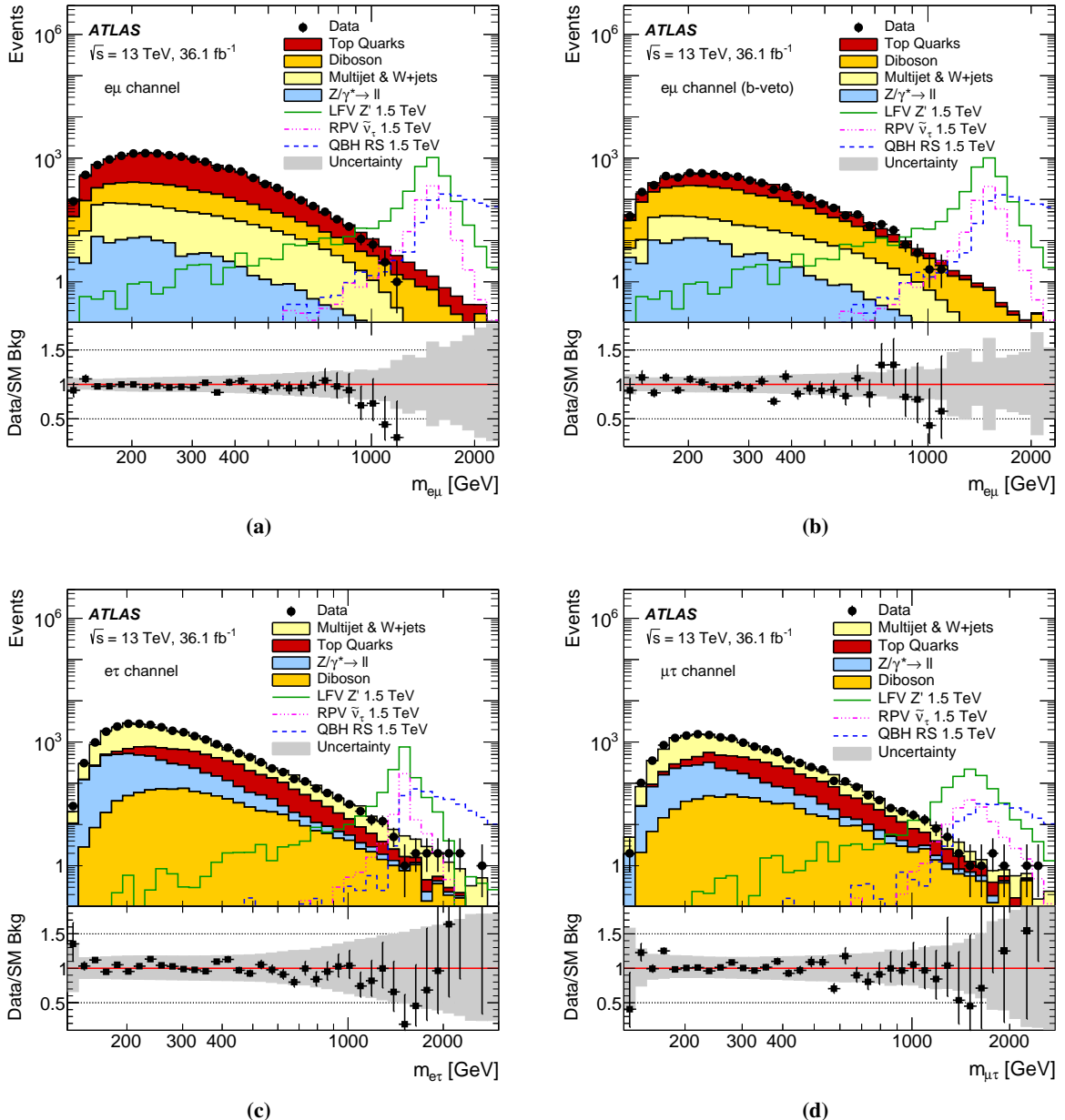


Figure 3: The invariant mass distribution of (a) $e\mu$, (b) $e\mu$ with b -veto, (c) $e\tau$, and (d) $\mu\tau$ pairs for data and the SM predictions. Three signal examples are overlaid: a Z' boson with a mass of 1.5 TeV, a τ -neutrino ($\tilde{\nu}_\tau$) with a mass of 1.5 TeV, and a RS quantum black-hole (QBH) with a threshold mass of 1.5 TeV. The range is chosen such that all data points are visible. The error bars show the Poissonian statistical uncertainty of the observed yields, while the band in the bottom plot includes all systematic uncertainties combined in quadrature. No further data points are found in overflow bins.

Table 6: Expected and observed numbers of $e\tau$ events in the low (a) and high (b) mass regions after applying all selection criteria. The statistical and systematic uncertainties are quoted.

Process	$m_{e\tau} < 300$ GeV	$300 < m_{e\tau} < 600$ GeV
Top	$2020 \pm 30 \pm 390$	$1800 \pm 30 \pm 370$
Diboson	$465 \pm 10 \pm 77$	$330 \pm 8 \pm 58$
Multijet and $W+jets$	$13200 \pm 200 \pm 2900$	$3100 \pm 70 \pm 870$
$Z/\gamma^* \rightarrow \ell\ell$	$3300 \pm 60 \pm 500$	$610 \pm 20 \pm 130$
Total background	$19000 \pm 200 \pm 3300$	$5800 \pm 100 \pm 1100$
Data	19532	5858

(a) N_{events} with $m_{e\tau} < 600$ GeV

Process	$600 < m_{e\tau} < 1200$ GeV	$1200 < m_{e\tau} < 2000$ GeV
Top	$161 \pm 2 \pm 53$	$4.6 \pm 0.4 \pm 2.2$
Diboson	$48 \pm 2 \pm 11$	$4.7 \pm 0.8 \pm 1.7$
Multijet and $W+jets$	$300 \pm 20 \pm 140$	$24 \pm 2 \pm 16$
$Z/\gamma^* \rightarrow \ell\ell$	$25.6 \pm 0.6 \pm 6.0$	$1.30 \pm 0.04 \pm 0.42$
Total background	$540 \pm 20 \pm 160$	$34 \pm 2 \pm 17$
Data	480	24

Process	$2000 < m_{e\tau} < 3000$ GeV	$m_{e\tau} > 3000$ GeV
Top	$0.13 \pm 0.04 \pm 0.10$	$(0.20 \pm 0.10 \pm 0.32) \cdot 10^{-2}$
Diboson	$0.41 \pm 0.16 \pm 0.21$	$(0.35 \pm 0.04 \pm 0.39) \cdot 10^{-2}$
Multijet and $W+jets$	$2.4 \pm 0.3 \pm 2.0$	$0.30 \pm 0.14 \pm 0.19$
$Z/\gamma^* \rightarrow \ell\ell$	$0.09 \pm 0.02 \pm 0.04$	$(0.34 \pm 0.01 \pm 0.39) \cdot 10^{-2}$
Total background	$3.1 \pm 0.4 \pm 2.1$	$0.31 \pm 0.15 \pm 0.23$
Data	5	0

(b) N_{events} with $m_{e\tau} > 600$ GeV

resolution is 4% at $m_{Z'} = 2$ TeV, comparable to the Z' boson width. The width of the $\tilde{\nu}_\tau$ is below 1%, and hence the resolution of the detector is larger than the width for each of the final states investigated.

Figures 4–6 show the observed and expected 95% CL upper limits on the production cross-section times branching ratio of the Z' , RPV SUSY $\tilde{\nu}_\tau$ and QBH models for each of the final states considered. The extracted limits are not as strong for signal masses above about 2.5 TeV due to a decrease in acceptance at very high p_T and, specifically to the LFV Z' model, low-mass signal production due to PDF suppression. The results are summarized in Table 8. The acceptance times efficiency of the ADD and RS QBH models agree within 1%, and the same prediction is used for the limit extraction.

Results expressed in terms of the coupling limits can be directly compared to those obtained from precision low energy experiments [76]. For the Z' model the cross-section times branching ratio is proportional to $Q_{\ell\ell'}^2$, and the same quark couplings as the SM Z boson are used. The limits on $Q_{\ell\ell'}$ are shown in Figure 7 as a function of $m_{Z'}$ for the three channels. The most stringent coupling limits from low-energy experiments are from μ -to- e conversion and $\mu \rightarrow eee$ for the $e\mu$ channel, from $\tau \rightarrow eee$ and $\tau \rightarrow e\mu\mu$ for the $e\tau$ channel, and from $\tau \rightarrow \mu\mu\mu$ and $\tau \rightarrow e\mu\mu$ for the $\mu\tau$ channel. The current experimental limits on these processes are converted to coupling limits using the formulae of Ref. [77] and are shown in Figure 7. For the $e\tau$ and $\mu\tau$ channels, the observed limit is restricted up to the Z' mass point of 4 TeV. This because for the higher mass points, the limit on $Q_{\ell\ell'}$ becomes sufficiently large that the total width of the Z' would be significantly larger than the experimental resolution and violate our assumptions on that. For the $e\mu$

Table 7: Expected and observed numbers of $\mu\tau$ events in the low (a) and high (b) mass regions after applying all selection criteria. The statistical and systematic uncertainties are quoted.

Process	$m_{\mu\tau} < 300$ GeV	$300 < m_{\mu\tau} < 600$ GeV
Top	$1380 \pm 20 \pm 300$	$1160 \pm 20 \pm 250$
Diboson	$318 \pm 8 \pm 55$	$225 \pm 6 \pm 42$
Multijet and $W+jets$	$6900 \pm 200 \pm 1400$	$1650 \pm 50 \pm 380$
$Z/\gamma^* \rightarrow \ell\ell$	$1650 \pm 40 \pm 270$	$339 \pm 14 \pm 71$
Total background	$10300 \pm 200 \pm 1700$	$3380 \pm 60 \pm 550$
Data	10525	3378

(a) N_{events} with $m_{\mu\tau} < 600$ GeV

Process	$600 < m_{\mu\tau} < 1200$ GeV	$1200 < m_{\mu\tau} < 2000$ GeV
Top	$95 \pm 1 \pm 26$	$3.5 \pm 0.2 \pm 2.7$
Diboson	$33.3 \pm 1.7 \pm 9.2$	$2.9 \pm 0.5 \pm 1.5$
Multijet and $W+jets$	$140 \pm 10 \pm 43$	$6.4 \pm 1.0 \pm 2.4$
$Z/\gamma^* \rightarrow \ell\ell$	$14.4 \pm 1.2 \pm 4.3$	$0.88 \pm 0.07 \pm 0.32$
Total background	$282 \pm 10 \pm 61$	$13.7 \pm 1.1 \pm 5.0$
Data	255	12

Process	$2000 < m_{\mu\tau} < 3000$ GeV	$m_{\mu\tau} > 3000$ GeV
Top	$0.17 \pm 0.03 \pm 0.21$	$(0.56 \pm 0.19 \pm 0.94) \cdot 10^{-2}$
Diboson	$0.54 \pm 0.30 \pm 0.38$	$(0.62 \pm 0.09 \pm 0.95) \cdot 10^{-2}$
Multijet and $W+jets$	$0.87 \pm 0.35 \pm 0.89$	$(0.87 \pm 0.70 \pm 0.60) \cdot 10^{-2}$
$Z/\gamma^* \rightarrow \ell\ell$	$(0.78 \pm 0.03 \pm 0.42) \cdot 10^{-1}$	$(0.63 \pm 0.04 \pm 0.84) \cdot 10^{-2}$
Total background	$1.65 \pm 0.46 \pm 1.30$	$(0.27 \pm 0.07 \pm 0.33) \cdot 10^{-1}$
Data	2	0

(b) N_{events} with $m_{\mu\tau} > 600$ GeV

Table 8: Expected and observed 95% credibility-level lower limits on the mass of a Z' boson with lepton-flavor-violating couplings, a supersymmetric τ -sneutrino ($\tilde{\nu}_\tau$) with R -parity-violating couplings, and the threshold mass for quantum black-hole production for the ADD $n = 6$ and RS $n = 1$ models.

Model	Expected limit [TeV]				Observed limit [TeV]			
	$e\mu$	$e\mu$	$e\tau$	$\mu\tau$	$e\mu$	$e\mu$	$e\tau$	$\mu\tau$
	(b-veto)				(b-veto)			
LFV Z'	4.3	4.3	3.7	3.5	4.5	4.4	3.7	3.5
RPV SUSY $\tilde{\nu}_\tau$	3.4	3.4	2.9	2.6	3.4	3.4	2.9	2.6
QBH ADD $n = 6$	5.6	5.5	4.9	4.5	5.6	5.5	4.9	4.5
QBH RS $n = 1$	3.3	3.4	2.8	2.7	3.4	3.4	2.9	2.6

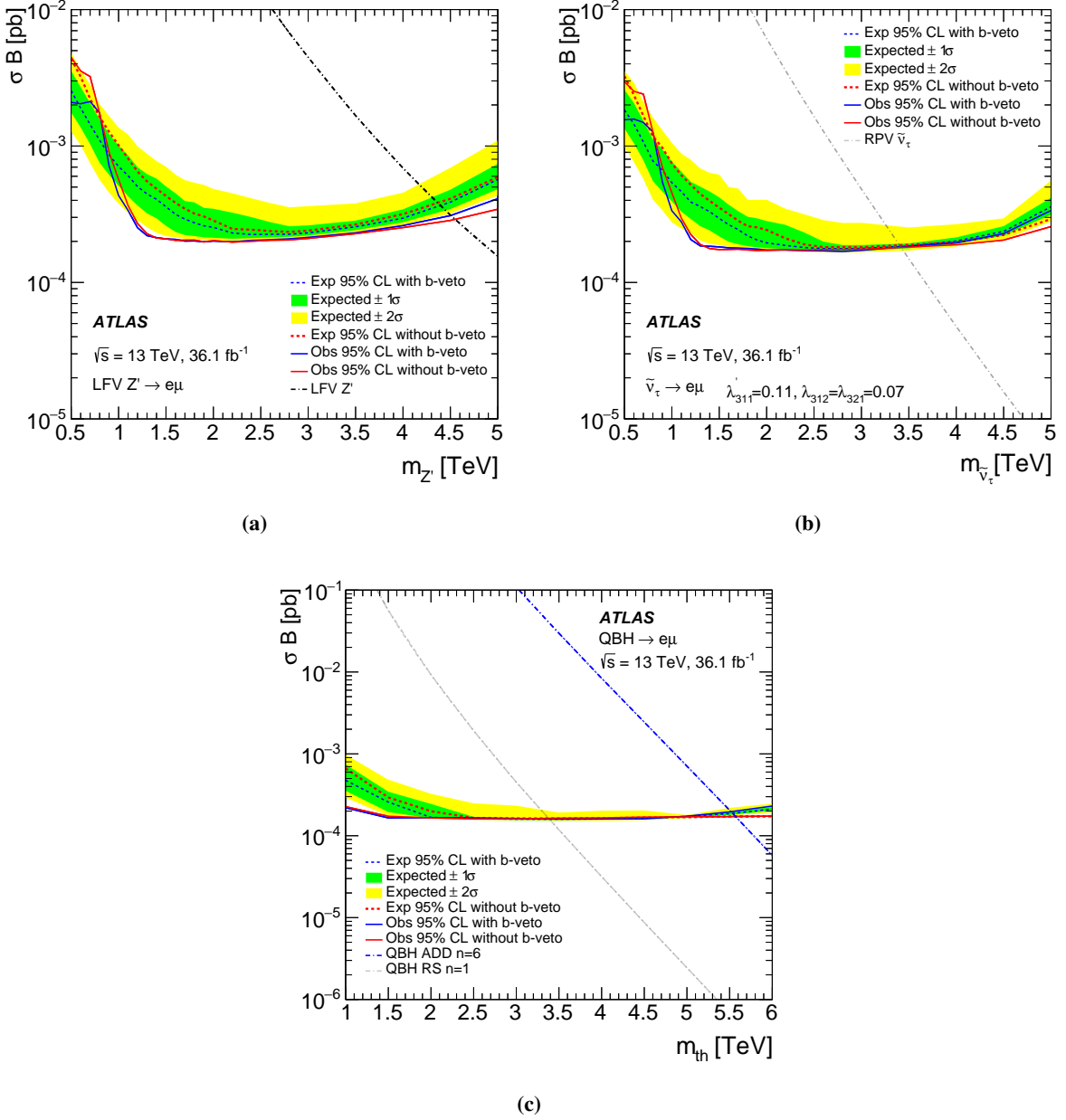


Figure 4: The observed and expected 95% credibility-level upper limits on the (a) Z' boson, (b) τ -sneutrino ($\tilde{\nu}_\tau$), and (c) QBH ADD and RS production cross-section times branching ratio for decays into an $e\mu$ final state with and without the b -veto requirement. The signal theoretical cross-section times branching ratio lines for the Z' model, the QBH ADD model assuming six extra dimensions, and the RS model with one extra dimension are obtained from the simulation of each process, while the RPV SUSY $\tilde{\nu}_\tau$ includes the NLO K -factor calculated using LoopTools [33]. The acceptance times efficiency of the ADD and RS QBH models agree within 1%, and the same curve is used for limit extraction. The expected limits are shown with the ± 1 and ± 2 standard deviation uncertainty bands on the results with the b -veto requirement.

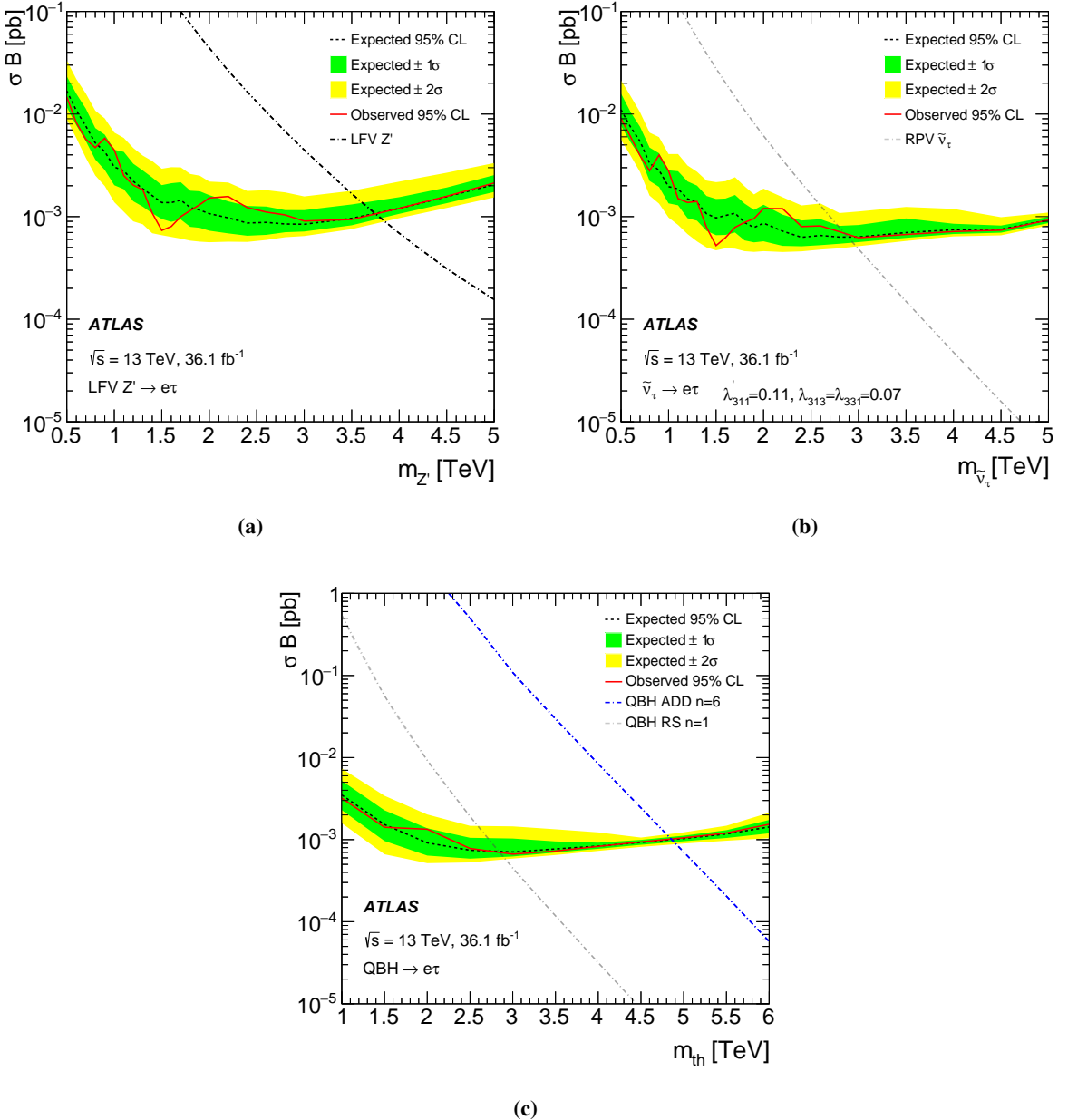


Figure 5: The observed and expected 95% credibility-level upper limits on the (a) Z' boson, (b) τ -sneutrino ($\tilde{\nu}_\tau$), and (c) QBH ADD and RS production cross-section times branching ratio for decays into an $e\tau$ final state. The signal theoretical cross-section times branching ratio lines for the Z' model, the QBH ADD model assuming six extra dimensions, and the RS model with one extra dimension are obtained from the simulation of each process, while the RPV SUSY $\tilde{\nu}_\tau$ includes the NLO K -factor calculated using LoopTools [33]. The acceptance times efficiency of the ADD and RS QBH models agree within 1%, and the same curve is used for limit extraction. The expected limits are shown with the ± 1 and ± 2 standard deviation uncertainty bands.

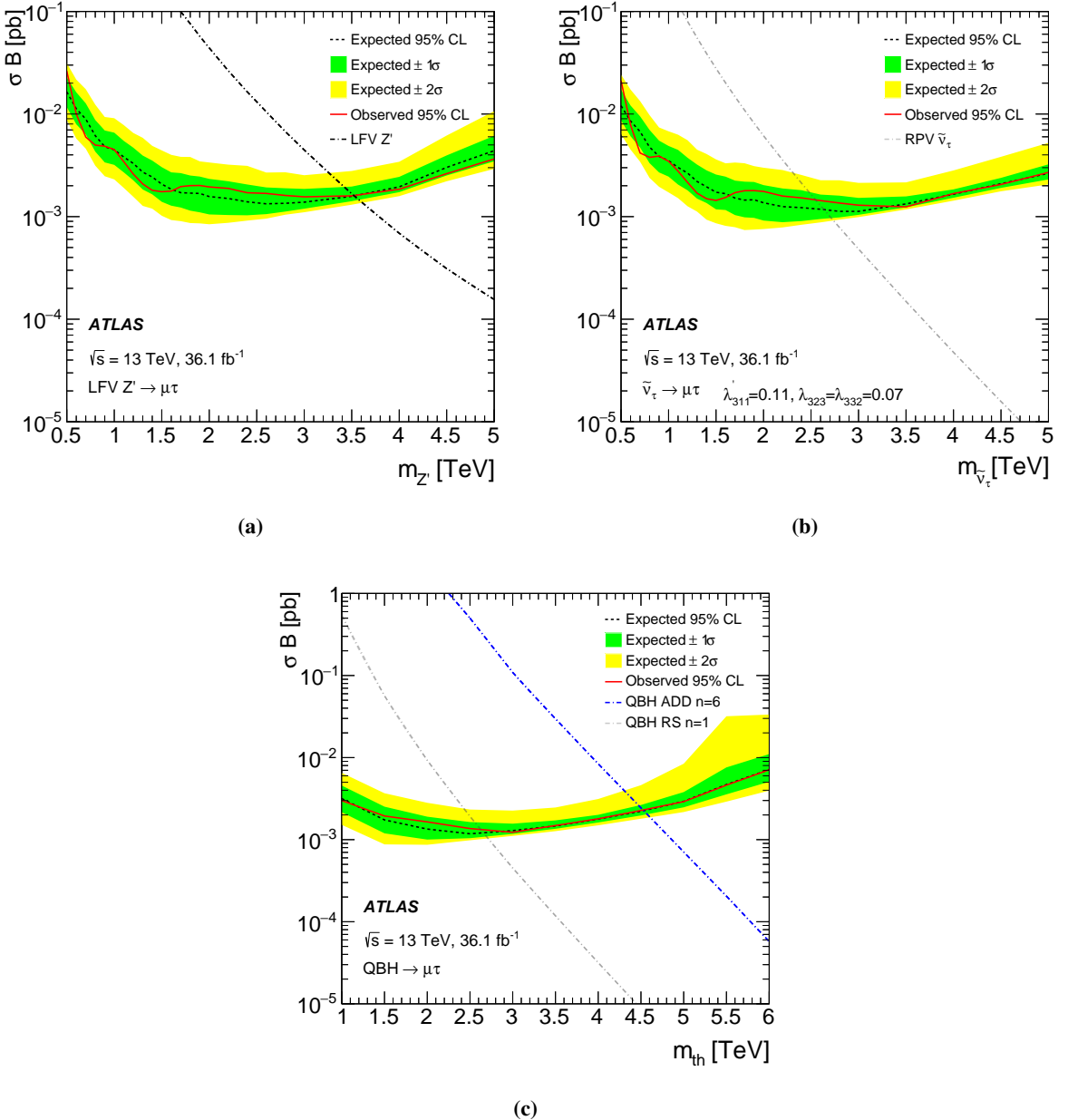


Figure 6: The observed and expected 95% credibility-level upper limits on the (a) Z' boson, (b) τ -sneutrino ($\tilde{\nu}_\tau$), and (c) QBH ADD and RS production cross-section times branching ratio for decays into an $\mu\tau$ final state. The signal theoretical cross-section times branching ratio lines for the Z' model, the QBH ADD model assuming six extra dimensions, and the RS model with one extra dimension are obtained from the simulation of each process, while the RPV SUSY $\tilde{\nu}_\tau$ includes the NLO K -factor calculated using LoopTools [33]. The acceptance times efficiency of the ADD and RS QBH models agree within 1%, and the same curve is used for limit extraction. The expected limits are shown with the ± 1 and ± 2 standard deviation uncertainty bands.

channel, the coupling limits in this paper do not compete with those from low-energy experiments, but for the $e\tau$ and $\mu\tau$ channels, the coupling limits in this paper are more stringent, though they require additional assumptions on the quark couplings.

For the $\tilde{\nu}_\tau$ model, the dependence on the couplings is more complicated because both the production and the decay violate lepton-flavor conservation. Assuming only the $d\bar{d}$ and $\ell\ell'$ couplings, the cross-section times branching ratios are proportional to the Yukawa couplings $|\lambda'_{311}\lambda_{3ij}|^2/(3|\lambda'_{311}|^2 + 2|\lambda_{3ij}|^2)$, where $ij = 12, 13$, and 23 for the $e\mu$, $e\tau$, and $\mu\tau$ channels, respectively. The factor 3 in the denominator accounts for color and the factor 2 is because both final-state charge combinations are allowed ($\ell^\pm\ell'^\mp$). The limits on $|\lambda'_{3ij}|$ versus $|\lambda_{311}|$ are shown in Figure 8 for $\tilde{\nu}_\tau$ masses of 1 TeV, 2 TeV, and 3 TeV. The most stringent coupling limits set by low-energy experiments derive from μ -to- e conversion for the $e\mu$ channel, from $\tau \rightarrow e\eta$ for the $e\tau$ channel, and from $\tau \rightarrow \mu\eta$ for the $\mu\tau$ channel. The coupling limits in Ref. [3] are scaled to current experimental limits on these processes [78] and are shown in Figure 8. For the $e\mu$ channel, the coupling limits in this paper do not compete with those from low-energy experiments, but for $e\tau$ and $\mu\tau$ channels, the coupling limits in this paper are more stringent.

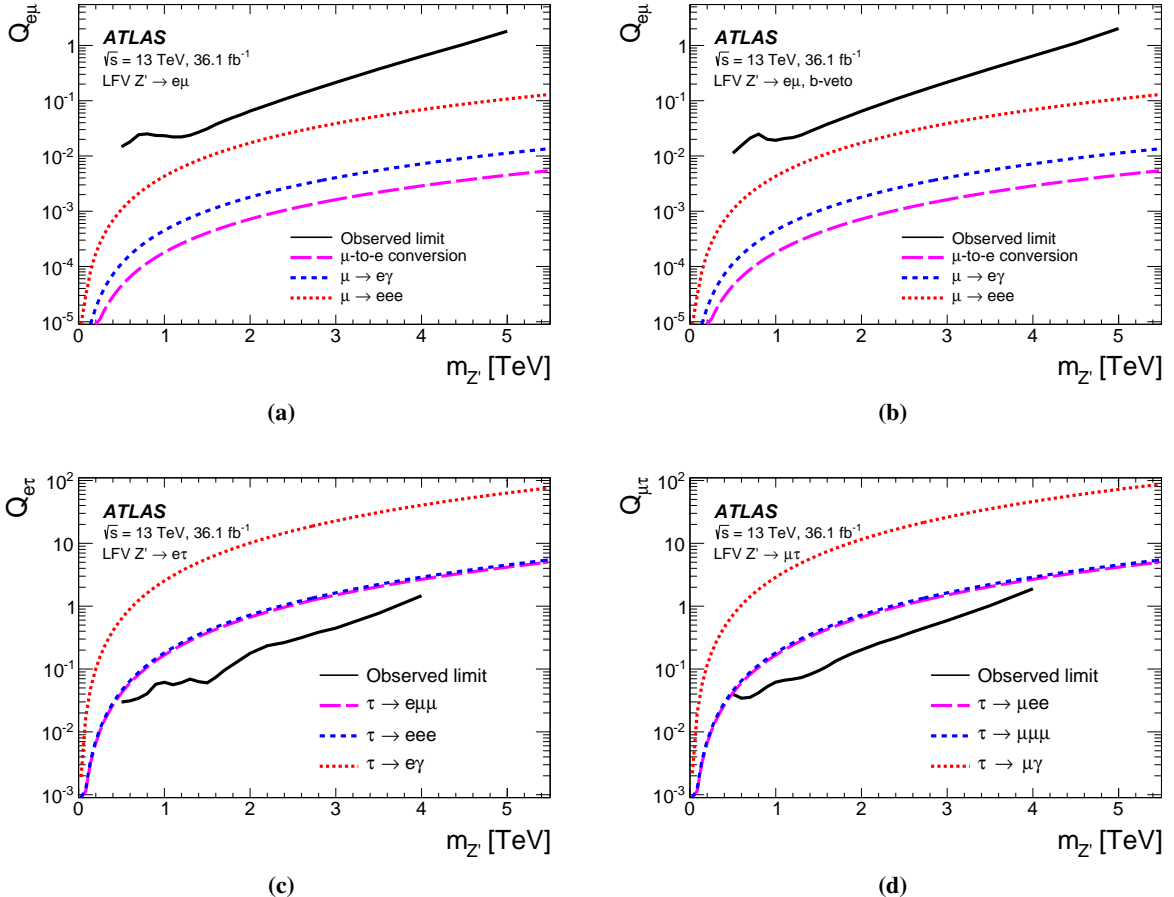


Figure 7: The 95% credibility-level upper limits on the couplings (a) $Q_{e\mu}$, (b) $Q_{e\mu}$ with a b -veto, (c) $Q_{e\tau}$, and (d) $Q_{\mu\tau}$ as a function of $m_{Z'}$ from the cross-section times branching ratio limits in this paper (solid lines) and from low-energy experiments (dashed lines).

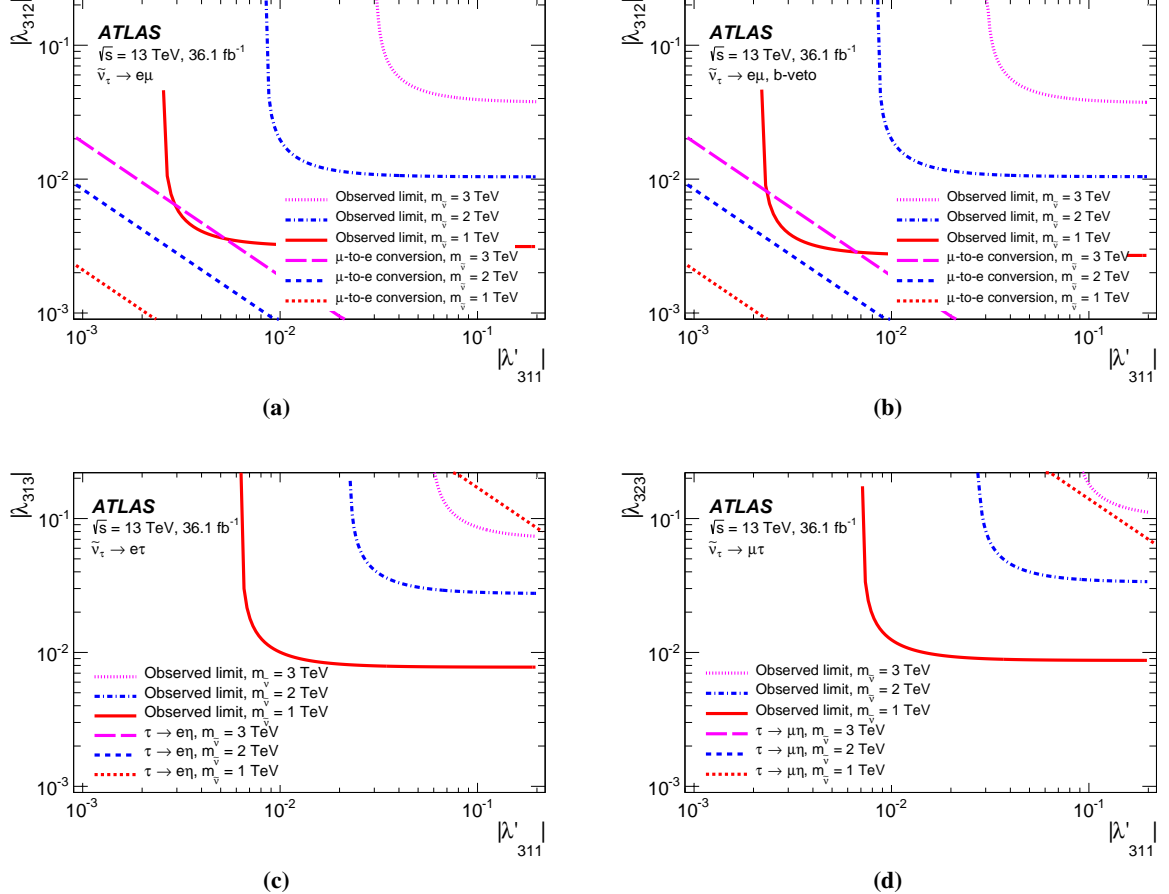


Figure 8: The 95% credibility-level upper limits on the RPV couplings (a) $|\lambda_{312}|$, (b) $|\lambda_{312}|$ with a b -veto, (c) $|\lambda_{313}|$, and (d) $|\lambda_{323}|$ versus $|\lambda'_{311}|$ for a few values of $m_{\tilde{\nu}}$ from the cross-section times branching ratio limits in this paper (solid, dot-dashed, and dotted lines) and from low-energy experiments (short-dashed, medium-dashed, and long-dashed lines). For the $e\tau$ and $\mu\tau$ channels, the low energy limits for the 2 TeV and 3 TeV mass points are outside the frame, beyond the upper-right corner.

8 Conclusions

A search for a heavy particle decaying into an $e\mu$, $e\tau$, or $\mu\tau$ final state is conducted using 36.1 fb^{-1} of proton–proton collision data at $\sqrt{s} = 13\text{ TeV}$ recorded by the ATLAS detector at the Large Hadron Collider. The Standard Model predictions are consistent with the data. From the $e\mu$, $e\tau$, and $\mu\tau$ final states, Bayesian lower limits at 95% credibility level are set on the mass of a Z' vector boson with lepton-flavor-violating couplings at 4.5, 3.7, and 3.5 TeV, respectively; on the mass of a supersymmetric τ -sneutrino with R-parity-violating couplings at 3.4, 2.9, and 2.6 TeV; and on the threshold mass for quantum black-hole production in the context of the Arkani-Hamed–Dimopoulos–Dvali (Randall–Sundrum) model at 5.6 (3.4), 4.9 (2.9), and 4.5 (2.6) TeV. The quantum black hole limits extracted are below those extracted in dijet searches, since the branching ratio to dijet is expected to be much larger than to dilepton. Coupling limits for the lepton-flavor-violating Z' boson and $\tilde{\nu}$ models are more stringent than those from low-energy experiments for the $e\tau$ and $\mu\tau$ modes.

Acknowledgements

We thank CERN for the very successful operation of the LHC, as well as the support staff from our institutions without whom ATLAS could not be operated efficiently.

We acknowledge the support of ANPCyT, Argentina; YerPhI, Armenia; ARC, Australia; BMWFW and FWF, Austria; ANAS, Azerbaijan; SSTC, Belarus; CNPq and FAPESP, Brazil; NSERC, NRC and CFI, Canada; CERN; CONICYT, Chile; CAS, MOST and NSFC, China; COLCIENCIAS, Colombia; MSMT CR, MPO CR and VSC CR, Czech Republic; DNRF and DNSRC, Denmark; IN2P3-CNRS, CEA-DRF/IRFU, France; SRNSFG, Georgia; BMBF, HGF, and MPG, Germany; GSRT, Greece; RGC, Hong Kong SAR, China; ISF, I-CORE and Benoziyo Center, Israel; INFN, Italy; MEXT and JSPS, Japan; CNRST, Morocco; NWO, Netherlands; RCN, Norway; MNiSW and NCN, Poland; FCT, Portugal; MNE/IFA, Romania; MES of Russia and NRC KI, Russian Federation; JINR; MESTD, Serbia; MSSR, Slovakia; ARRS and MIZŠ, Slovenia; DST/NRF, South Africa; MINECO, Spain; SRC and Wallenberg Foundation, Sweden; SERI, SNSF and Cantons of Bern and Geneva, Switzerland; MOST, Taiwan; TAEK, Turkey; STFC, United Kingdom; DOE and NSF, United States of America. In addition, individual groups and members have received support from BCKDF, the Canada Council, CANARIE, CRC, Compute Canada, FQRNT, and the Ontario Innovation Trust, Canada; EPLANET, ERC, ERDF, FP7, Horizon 2020 and Marie Skłodowska-Curie Actions, European Union; Investissements d’Avenir Labex and Idex, ANR, Région Auvergne and Fondation Partager le Savoir, France; DFG and AvH Foundation, Germany; Herakleitos, Thales and Aristeia programmes co-financed by EU-ESF and the Greek NSRF; BSF, GIF and Minerva, Israel; BRF, Norway; CERCA Programme Generalitat de Catalunya, Generalitat Valenciana, Spain; the Royal Society and Leverhulme Trust, United Kingdom.

The crucial computing support from all WLCG partners is acknowledged gratefully, in particular from CERN, the ATLAS Tier-1 facilities at TRIUMF (Canada), NDGF (Denmark, Norway, Sweden), CC-IN2P3 (France), KIT/GridKA (Germany), INFN-CNAF (Italy), NL-T1 (Netherlands), PIC (Spain), ASGC (Taiwan), RAL (UK) and BNL (USA), the Tier-2 facilities worldwide and large non-WLCG resource providers. Major contributors of computing resources are listed in Ref. [79].

References

- [1] P. Langacker, *The physics of heavy Z' gauge bosons*, Rev. Mod. Phys. **81** (2009) 1199, arXiv: [0801.1345 \[hep-ph\]](#).
- [2] G. R. Farrar and P. Fayet, *Phenomenology of the Production, Decay, and Detection of New Hadronic States Associated with Supersymmetry*, Phys. Lett. B **76** (1978) 575.
- [3] R. Barbier et al., *R-Parity-violating supersymmetry*, Phys. Rept. **420** (2005) 1, arXiv: [hep-ph/0406039](#).
- [4] D. M. Gingrich, *Quantum black holes with charge, colour and spin at the LHC*, J. Phys. G **37** (2010) 105008, arXiv: [0912.0826 \[hep-ph\]](#).
- [5] ATLAS Collaboration, *Search for new phenomena in different-flavour high-mass dilepton final states in pp collisions at $\sqrt{s} = 13$ TeV with the ATLAS detector*, Eur. Phys. J. C **76** (2016) 541, arXiv: [1607.08079 \[hep-ex\]](#).
- [6] CMS Collaboration, *Search for lepton-flavor violating decays of heavy resonances and quantum black holes to $e\mu$ final states in proton-proton collisions at $\sqrt{s} = 13$ TeV*, JHEP **04** (2018) 073, arXiv: [1802.01122 \[hep-ex\]](#).
- [7] ATLAS Collaboration, *Search for a Heavy Neutral Particle Decaying to $e\mu$, $e\tau$, or $\mu\tau$ in pp Collisions at $\sqrt{s} = 8$ TeV with the ATLAS Detector*, Phys. Rev. Lett. **115** (2015) 031801, arXiv: [1503.04430 \[hep-ex\]](#).
- [8] CMS Collaboration, *Search for lepton flavour violating decays of heavy resonances and quantum black holes to an $e\mu$ pair in proton–proton collisions at $\sqrt{s} = 8$ TeV*, Eur. Phys. J. C **76** (2016) 317, arXiv: [1604.05239 \[hep-ex\]](#).
- [9] N. Arkani-Hamed, S. Dimopoulos, and G. Dvali, *The hierarchy problem and new dimensions at a millimeter*, Phys. Lett. B **429** (1998) 263, arXiv: [hep-ph/9803315](#).
- [10] L. Randall and R. Sundrum, *A Large Mass Hierarchy from a Small Extra Dimension*, Phys. Rev. Lett. **83** (1999) 3370, arXiv: [hep-ph/9905221](#).
- [11] S. Dimopoulos and G. L. Landsberg, *Black Holes at the Large Hadron Collider*, Phys. Rev. Lett. **87** (2001) 161602, arXiv: [hep-ph/0106295](#).
- [12] S. B. Giddings and S. Thomas, *High energy colliders as black hole factories: The end of short distance physics*, Phys. Rev. D **65** (2002) 056010, arXiv: [hep-ph/0106219](#).
- [13] P. Meade and L. Randall, *Black holes and quantum gravity at the LHC*, JHEP **05** (2008) 003, arXiv: [0708.3017 \[hep-ph\]](#).
- [14] D. M. Gingrich and K. Martell, *Study of highly excited string states at the Large Hadron Collider*, Phys. Rev. D **78** (2008) 115009, arXiv: [0808.2512 \[hep-ph\]](#).
- [15] X. Calmet, W. Gong, and S. D. H. Hsu, *Colorful quantum black holes at the LHC*, Phys. Lett. B **668** (2008) 20, arXiv: [0806.4605 \[hep-ph\]](#).
- [16] ATLAS Collaboration, *Search for new phenomena in the dijet mass distribution using pp collision data at $\sqrt{s} = 8$ TeV with the ATLAS detector*, Phys. Rev. D **91** (2015) 052007, arXiv: [1407.1376 \[hep-ex\]](#).

- [17] ATLAS Collaboration, *Search for New Phenomena in Dijet Mass and Angular Distributions from pp Collisions at $\sqrt{s} = 13$ TeV with the ATLAS Detector*, *Phys. Lett. B* **754** (2016) 302, arXiv: [1512.01530 \[hep-ex\]](#).
- [18] CMS Collaboration, *Search for resonances and quantum black holes using dijet mass spectra in proton–proton collisions at $\sqrt{s} = 8$ TeV*, *Phys. Rev. D* **91** (2015) 052009, arXiv: [1501.04198 \[hep-ex\]](#).
- [19] ATLAS Collaboration, *Search for Quantum Black Hole Production in High-Invariant-Mass Lepton+Jet Final States Using pp Collisions at $\sqrt{s} = 8$ TeV and the ATLAS Detector*, *Phys. Rev. Lett.* **112** (2014) 091804, arXiv: [1311.2006 \[hep-ex\]](#).
- [20] ATLAS Collaboration, *Search for new phenomena in photon+jet events collected in proton–proton collisions at $\sqrt{s} = 8$ TeV with the ATLAS detector*, *Phys. Lett. B* **728** (2014) 562, arXiv: [1309.3230 \[hep-ex\]](#).
- [21] ATLAS Collaboration, *Search for high-mass dilepton resonances in pp collisions at $\sqrt{s} = 8$ TeV with the ATLAS detector*, *Phys. Rev. D* **90** (2014) 052005, arXiv: [1405.4123 \[hep-ex\]](#).
- [22] ATLAS Collaboration, *The ATLAS Experiment at the CERN Large Hadron Collider*, *JINST* **3** (2008) S08003.
- [23] ATLAS Collaboration, *ATLAS Insertable B-Layer Technical Design Report*, CERN-LHCC-2010-013. ATLAS-TDR-19, CERN (2010), URL: <https://cds.cern.ch/record/1291633>.
- [24] ATLAS Collaboration, *ATLAS Insertable B-Layer Technical Design Report Addendum*, CERN-LHCC-2012-009. ATLAS-TDR-19-ADD-1, Addendum to CERN-LHCC-2010-013, ATLAS-TDR-019, CERN (2012), URL: <https://cds.cern.ch/record/1451888>.
- [25] ATLAS Collaboration, *Performance of the ATLAS trigger system in 2015*, *Eur. Phys. J. C* **77** (2017) 317, arXiv: [1611.09661 \[hep-ex\]](#).
- [26] ATLAS Collaboration, *Luminosity determination in pp collisions at $\sqrt{s} = 8$ TeV using the ATLAS detector at the LHC*, *Eur. Phys. J. C* **76** (2016) 653, arXiv: [1608.03953 \[hep-ex\]](#).
- [27] T. Sjöstrand, S. Mrenna, and P. Z. Skands, *A brief introduction to PYTHIA 8.1*, *Comput. Phys. Commun.* **178** (2008) 852, arXiv: [0710.3820 \[hep-ph\]](#).
- [28] R. D. Ball et al., *Parton distributions with LHC data*, *Nucl. Phys. B* **867** (2013) 244, arXiv: [1207.1303 \[hep-ph\]](#).
- [29] ATLAS Collaboration, *ATLAS Pythia 8 tunes to 7 TeV data*, ATL-PHYS-PUB-2014-021, 2014, URL: <https://cds.cern.ch/record/1966419>.
- [30] C. Anastasiou, L. J. Dixon, K. Melnikov, and F. Petriello, *High precision QCD at hadron colliders: Electroweak gauge boson rapidity distributions at next-to-next-to leading order*, *Phys. Rev. D* **69** (2004) 094008, arXiv: [hep-ph/0312266](#).
- [31] S. Dulat et al., *New parton distribution functions from a global analysis of quantum chromodynamics*, *Phys. Rev. D* **93** (2016) 033006, arXiv: [1506.07443 \[hep-ph\]](#).
- [32] J. Alwall et al., *The automated computation of tree-level and next-to-leading order differential cross sections, and their matching to parton shower simulations*, *JHEP* **07** (2014) 079, arXiv: [1405.0301 \[hep-ph\]](#).

- [33] T. Hahn and M. Perez-Victoria, *Automatized one-loop calculations in four and D dimensions*, *Comput. Phys. Commun.* **118** (1999) 153, arXiv: [hep-ph/9807565](#).
- [34] D. Gingrich, *Monte Carlo event generator for black hole production and decay in proton-proton collisions – QBH version 1.02*, *Comput. Phys. Commun.* **181** (2010) 1917, arXiv: [0911.5370 \[hep-ph\]](#).
- [35] J. Pumplin et al.,
New Generation of Parton Distributions with Uncertainties from Global QCD Analysis, *JHEP* **07** (2002) 012, arXiv: [hep-ph/0201195](#).
- [36] P. Nason, *A new method for combining NLO QCD with shower Monte Carlo algorithms*, *JHEP* **11** (2004) 040, arXiv: [hep-ph/0409146](#).
- [37] S. Frixione, P. Nason, and C. Oleari,
Matching NLO QCD computations with parton shower simulations: the POWHEG method, *JHEP* **11** (2007) 070, arXiv: [0709.2092 \[hep-ph\]](#).
- [38] S. Alioli, P. Nason, C. Oleari, and E. Re, *A general framework for implementing NLO calculations in shower Monte Carlo programs: the POWHEG BOX*, *JHEP* **06** (2010) 043, arXiv: [1002.2581 \[hep-ph\]](#).
- [39] H.-L. Lai et al., *New parton distributions for collider physics*, *Phys. Rev. D* **82** (2010) 074024, arXiv: [1007.2241 \[hep-ph\]](#).
- [40] T. Sjöstrand, S. Mrenna, and P. Z. Skands, *PYTHIA 6.4 physics and manual*, *JHEP* **05** (2006) 026, arXiv: [hep-ph/0603175](#).
- [41] P. Z. Skands, *Tuning Monte Carlo generators: The Perugia tunes*, *Phys. Rev. D* **82** (2010) 074018, arXiv: [1005.3457 \[hep-ph\]](#).
- [42] P. Artoisenet, R. Frederix, O. Mattelaer, and R. Rietkerk,
Automatic spin-entangled decays of heavy resonances in Monte Carlo simulations, *JHEP* **03** (2013) 015, arXiv: [1212.3460 \[hep-ph\]](#).
- [43] D. J. Lange, *The EvtGen particle decay simulation package*, *Nucl. Instrum. Meth. A* **462** (2001) 152.
- [44] M. Czakon and A. Mitov,
Top++: A program for the calculation of the top-pair cross-section at hadron colliders, *Comput. Phys. Commun.* **185** (2014) 2930, arXiv: [1112.5675 \[hep-ph\]](#).
- [45] N. Kidonakis,
Two-loop soft anomalous dimensions for single top quark associated production with a W^- or H^- , *Phys. Rev. D* **82** (2010) 054018, arXiv: [1005.4451 \[hep-ph\]](#).
- [46] T. Gleisberg et al., *Event generation with SHERPA 1.1*, *JHEP* **02** (2009) 007, arXiv: [0811.4622 \[hep-ph\]](#).
- [47] T. Gleisberg and S. Höche, *Comix, a new matrix element generator*, *JHEP* **12** (2008) 039, arXiv: [0808.3674 \[hep-ph\]](#).
- [48] F. Cascioli, P. Maierhofer, and S. Pozzorini, *Scattering Amplitudes with Open Loops*, *Phys. Rev. Lett.* **108** (2012) 111601, arXiv: [1111.5206 \[hep-ph\]](#).
- [49] S. Schumann and F. Krauss,
A Parton shower algorithm based on Catani-Seymour dipole factorisation, *JHEP* **03** (2008) 038, arXiv: [0709.1027 \[hep-ph\]](#).

- [50] S. Höche, F. Krauss, M. Schönherr, and F. Siegert, *QCD matrix elements + parton showers. The NLO case*, JHEP **04** (2013) 027, arXiv: [1207.5030 \[hep-ph\]](#).
- [51] ATLAS Collaboration, *Measurement of the Z/γ^* boson transverse momentum distribution in pp collisions at $\sqrt{s} = 7$ TeV with the ATLAS detector*, JHEP **09** (2014) 145, arXiv: [1406.3660 \[hep-ex\]](#).
- [52] N. Davidson, T. Przedzinski, and Z. Was, *PHOTOS Interface in C++: Technical and Physics Documentation*, (2010), arXiv: [1011.0937 \[hep-ph\]](#).
- [53] ATLAS Collaboration, *ATLAS Pythia 8 tunes to 7 TeV data*, (2014), URL: <http://cds.cern.ch/record/1966419>.
- [54] ATLAS Collaboration, *The ATLAS Simulation Infrastructure*, Eur. Phys. J. C **70** (2010) 823, arXiv: [1005.4568 \[physics.ins-det\]](#).
- [55] S. Agostinelli et al., *GEANT4 – a simulation toolkit*, Nucl. Instrum. Meth. A **506** (2003) 250.
- [56] ATLAS Collaboration, *Electron efficiency measurements with the ATLAS detector using 2012 LHC proton–proton collision data*, Eur. Phys. J. C **77** (2017) 195, arXiv: [1612.01456 \[hep-ex\]](#).
- [57] ATLAS Collaboration, *Electron efficiency measurements with the ATLAS detector using the 2015 LHC proton–proton collision data*, ATLAS-CONF-2016-024, 2016, URL: <https://cds.cern.ch/record/2157687>.
- [58] ATLAS Collaboration, *Muon reconstruction performance of the ATLAS detector in proton–proton collision data at $\sqrt{s} = 13$ TeV*, Eur. Phys. J. C **76** (2016) 292, arXiv: [1603.05598 \[hep-ex\]](#).
- [59] M. Cacciari, G. P. Salam, and G. Soyez, *The anti- k_t jet clustering algorithm*, JHEP **04** (2008) 063, arXiv: [0802.1189 \[hep-ph\]](#).
- [60] ATLAS Collaboration, *Topological cell clustering in the ATLAS calorimeters and its performance in LHC Run 1*, Eur. Phys. J. C **77** (2017) 490, arXiv: [1603.02934 \[hep-ex\]](#).
- [61] ATLAS Collaboration, *Jet energy scale measurements and their systematic uncertainties in proton–proton collisions at $\sqrt{s} = 13$ TeV with the ATLAS detector*, Phys. Rev. D **96** (2017) 072002, arXiv: [1703.09665 \[hep-ex\]](#).
- [62] ATLAS Collaboration, *Reconstruction, Energy Calibration, and Identification of Hadronically Decaying Tau Leptons in the ATLAS Experiment for Run-2 of the LHC*, ATL-PHYS-PUB-2015-045 (2015), URL: <https://cds.cern.ch/record/2064383>.
- [63] ATLAS Collaboration, *Measurement of the tau lepton reconstruction and identification performance in the ATLAS experiment using pp collisions at $\sqrt{s} = 13$ TeV*, ATLAS-CONF-2017-029, 2017, URL: <https://cds.cern.ch/record/2261772>.
- [64] ATLAS Collaboration, *Expected performance of the ATLAS b-tagging algorithms in Run-2*, ATL-PHYS-PUB-2015-022, 2015, URL: <https://cds.cern.ch/record/2037697>.
- [65] ATLAS Collaboration, *Performance of missing transverse momentum reconstruction with the ATLAS detector using proton-proton collisions at $\sqrt{s} = 13$ TeV*, (2018), arXiv: [1802.08168 \[hep-ex\]](#).

- [66] ATLAS Collaboration, *Electron and photon energy calibration with the ATLAS detector using data collected in 2015 at $\sqrt{s} = 13$ TeV*, ATL-PHYS-PUB-2016-015, 2016,
URL: <https://cds.cern.ch/record/2203514>.
- [67] ATLAS Collaboration, *Search for high-mass new phenomena in the dilepton final state using proton–proton collisions at $\sqrt{s} = 13$ TeV with the ATLAS detector*, *Phys. Lett. B* **761** (2016) 372,
arXiv: [1607.03669 \[hep-ex\]](https://arxiv.org/abs/1607.03669).
- [68] ATLAS Collaboration, *Identification and energy calibration of hadronically decaying tau leptons with the ATLAS experiment in pp collisions at $\sqrt{s} = 8$ TeV*, *Eur. Phys. J. C* **75** (2015) 303,
arXiv: [1412.7086 \[hep-ex\]](https://arxiv.org/abs/1412.7086).
- [69] ATLAS Collaboration, *Measurement of the Inelastic Proton–Proton Cross Section at $\sqrt{s} = 13$ TeV with the ATLAS Detector at the LHC*, *Phys. Rev. Lett.* **117** (2016) 182002,
arXiv: [1606.02625 \[hep-ex\]](https://arxiv.org/abs/1606.02625).
- [70] A. Buckley et al., *LHAPDF6: parton density access in the LHC precision era*,
Eur. Phys. J. C **75** (2015) 132, arXiv: [1412.7420 \[hep-ph\]](https://arxiv.org/abs/1412.7420).
- [71] J. Butterworth et al., *PDF4LHC recommendations for LHC Run II*,
J. Phys. G Nucl. Phys. **43** (2016) 023001, arXiv: [1510.03865 \[hep-ph\]](https://arxiv.org/abs/1510.03865).
- [72] P. Motylinski, L. Harland-Lang, A. D. Martin, and R. S. Thorne,
Updates of PDFs for the 2nd LHC run, *Nucl. Part. Phys. Proc.* **273-275** (2016) 2136,
arXiv: [1411.2560 \[hep-ph\]](https://arxiv.org/abs/1411.2560).
- [73] R. D. Ball et al., *Parton distributions for the LHC Run II*, *JHEP* **04** (2015) 040,
arXiv: [1410.8849 \[hep-ph\]](https://arxiv.org/abs/1410.8849).
- [74] G. Choudalakis, *On hypothesis testing, trials factor, hypertests and the BumpHunter*, (2011),
arXiv: [1101.0390 \[physics.data-an\]](https://arxiv.org/abs/1101.0390).
- [75] A. Caldwell, D. Kollar and K. Kroeninger, *BAT – The Bayesian analysis toolkit*,
Comput. Phys. Commun. **180** (2009) 2197, arXiv: [0808.2552 \[physics.data-an\]](https://arxiv.org/abs/0808.2552).
- [76] Patrignani, C. et al., *(Particle Data Group) Review of Particle Physics*,
Chin. Phys. C **40** (2016) 100001, URL: <https://pdg.lbl.gov>.
- [77] P. Langacker and M. Plümacher,
Flavor changing effects in theories with a heavy Z' boson with family nonuniversal couplings,
Phys. Rev. D **62** (2000) 013006.
- [78] Belle Collaboration, *Search for lepton flavor violating τ^- decays into $\ell^-\eta$, $\ell^-\eta'$, and $\ell^-\pi^0$* ,
Phys. Lett. B **648** (2007) 341, arXiv: [hep-ex/0703009](https://arxiv.org/abs/hep-ex/0703009).
- [79] ATLAS Collaboration, *ATLAS Computing Acknowledgements*, ATL-GEN-PUB-2016-002,
URL: <https://cds.cern.ch/record/2202407>.

The ATLAS Collaboration

M. Aaboud^{34d}, G. Aad⁹⁹, B. Abbott¹²⁴, O. Abdinov^{13,*}, B. Abeloos¹²⁸, D.K. Abhayasinghe⁹¹, S.H. Abidi¹⁶⁴, O.S. AbouZeid¹⁴³, N.L. Abraham¹⁵³, H. Abramowicz¹⁵⁸, H. Abreu¹⁵⁷, Y. Abulaiti⁶, B.S. Acharya^{64a,64b,o}, S. Adachi¹⁶⁰, L. Adamczyk^{81a}, J. Adelman¹¹⁹, M. Adersberger¹¹², A. Adiguzel^{12c}, T. Adye¹⁴¹, A.A. Affolder¹⁴³, Y. Afik¹⁵⁷, C. Agheorghiesei^{27c}, J.A. Aguilar-Saavedra^{136f,136a}, F. Ahmadov^{77,af}, G. Aielli^{71a,71b}, S. Akatsuka⁸³, T.P.A. Åkesson⁹⁴, E. Akilli⁵², A.V. Akimov¹⁰⁸, G.L. Alberghi^{23b,23a}, J. Albert¹⁷³, P. Albicocco⁴⁹, M.J. Alconada Verzini⁸⁶, S. Alderweireldt¹¹⁷, M. Aleksa³⁵, I.N. Aleksandrov⁷⁷, C. Alexa^{27b}, T. Alexopoulos¹⁰, M. Alhroob¹²⁴, B. Ali¹³⁸, G. Alimonti^{66a}, J. Alison³⁶, S.P. Alkire¹⁴⁵, C. Allaire¹²⁸, B.M.M. Allbrooke¹⁵³, B.W. Allen¹²⁷, P.P. Allport²¹, A. Aloisio^{67a,67b}, A. Alonso³⁹, F. Alonso⁸⁶, C. Alpigiani¹⁴⁵, A.A. Alshehri⁵⁵, M.I. Alstaty⁹⁹, B. Alvarez Gonzalez³⁵, D. Álvarez Piqueras¹⁷¹, M.G. Alvaggi^{67a,67b}, B.T. Amadio¹⁸, Y. Amaral Coutinho^{78b}, L. Ambroz¹³¹, C. Amelung²⁶, D. Amidei¹⁰³, S.P. Amor Dos Santos^{136a,136c}, S. Amoroso³⁵, C.S. Amrouche⁵², C. Anastopoulos¹⁴⁶, L.S. Ancu⁵², N. Andari²¹, T. Andeen¹¹, C.F. Anders^{59b}, J.K. Anders²⁰, K.J. Anderson³⁶, A. Andreazza^{66a,66b}, V. Andrei^{59a}, C.R. Anelli¹⁷³, S. Angelidakis³⁷, I. Angelozzi¹¹⁸, A. Angerami³⁸, A.V. Anisenkov^{120b,120a}, A. Annovi^{69a}, C. Antel^{59a}, M.T. Anthony¹⁴⁶, M. Antonelli⁴⁹, D.J.A. Antrim¹⁶⁸, F. Anulli^{70a}, M. Aoki⁷⁹, L. Aperio Bella³⁵, G. Arabidze¹⁰⁴, Y. Arai⁷⁹, J.P. Araque^{136a}, V. Araujo Ferraz^{78b}, R. Araujo Pereira^{78b}, A.T.H. Arce⁴⁷, R.E. Ardell⁹¹, F.A. Arduh⁸⁶, J.-F. Arguin¹⁰⁷, S. Argyropoulos⁷⁵, A.J. Armbruster³⁵, L.J. Armitage⁹⁰, A Armstrong¹⁶⁸, O. Arnaez¹⁶⁴, H. Arnold¹¹⁸, M. Arratia³¹, O. Arslan²⁴, A. Artamonov^{109,*}, G. Artoni¹³¹, S. Artz⁹⁷, S. Asai¹⁶⁰, N. Asbah⁴⁴, A. Ashkenazi¹⁵⁸, E.M. Asimakopoulou¹⁶⁹, L. Asquith¹⁵³, K. Assamagan²⁹, R. Astalos^{28a}, R.J. Atkin^{32a}, M. Atkinson¹⁷⁰, N.B. Atlay¹⁴⁸, K. Augsten¹³⁸, G. Avolio³⁵, R. Avramidou^{58a}, B. Axen¹⁸, M.K. Ayoub^{15a}, G. Azuelos^{107,as}, A.E. Baas^{59a}, M.J. Baca²¹, H. Bachacou¹⁴², K. Bachas^{65a,65b}, M. Backes¹³¹, P. Bagnaia^{70a,70b}, M. Bahmani⁸², H. Bahrasemani¹⁴⁹, A.J. Bailey¹⁷¹, J.T. Baines¹⁴¹, M. Bajic³⁹, C. Bakalis¹⁰, O.K. Baker¹⁸⁰, P.J. Bakker¹¹⁸, D. Bakshi Gupta⁹³, E.M. Baldin^{120b,120a}, P. Balek¹⁷⁷, F. Balli¹⁴², W.K. Balunas¹³³, J. Balz⁹⁷, E. Banas⁸², A. Bandyopadhyay²⁴, S. Banerjee^{178,k}, A.A.E. Bannoura¹⁷⁹, L. Barak¹⁵⁸, W.M. Barbe³⁷, E.L. Barberio¹⁰², D. Barberis^{53b,53a}, M. Barbero⁹⁹, T. Barillari¹¹³, M.-S. Barisits³⁵, J. Barkeloo¹²⁷, T. Barklow¹⁵⁰, N. Barlow³¹, R. Barnea¹⁵⁷, S.L. Barnes^{58c}, B.M. Barnett¹⁴¹, R.M. Barnett¹⁸, Z. Barnovska-Blenessy^{58a}, A. Baroncelli^{72a}, G. Barone²⁶, A.J. Barr¹³¹, L. Barranco Navarro¹⁷¹, F. Barreiro⁹⁶, J. Barreiro Guimaraes da Costa^{15a}, R. Bartoldus¹⁵⁰, A.E. Barton⁸⁷, P. Bartos^{28a}, A. Basalaev¹³⁴, A. Bassalat¹²⁸, R.L. Bates⁵⁵, S.J. Batista¹⁶⁴, S. Batlamous^{34e}, J.R. Batley³¹, M. Battaglia¹⁴³, M. Bauce^{70a,70b}, F. Bauer¹⁴², K.T. Bauer¹⁶⁸, H.S. Bawa^{150,m}, J.B. Beacham¹²², M.D. Beattie⁸⁷, T. Beau¹³², P.H. Beauchemin¹⁶⁷, P. Bechtle²⁴, H.C. Beck⁵¹, H.P. Beck^{20,r}, K. Becker⁵⁰, M. Becker⁹⁷, C. Becot⁴⁴, A. Beddall^{12d}, A.J. Beddall^{12a}, V.A. Bednyakov⁷⁷, M. Bedognetti¹¹⁸, C.P. Bee¹⁵², T.A. Beermann³⁵, M. Begalli^{78b}, M. Begel²⁹, A. Behera¹⁵², J.K. Behr⁴⁴, A.S. Bell⁹², G. Bella¹⁵⁸, L. Bellagamba^{23b}, A. Bellerive³³, M. Bellomo¹⁵⁷, P. Bellos⁹, K. Belotskiy¹¹⁰, N.L. Belyaev¹¹⁰, O. Benary^{158,*}, D. Benchekroun^{34a}, M. Bender¹¹², N. Benekos¹⁰, Y. Benhammou¹⁵⁸, E. Benhar Noccioli¹⁸⁰, J. Benitez⁷⁵, D.P. Benjamin⁴⁷, M. Benoit⁵², J.R. Bensinger²⁶, S. Bentvelsen¹¹⁸, L. Beresford¹³¹, M. Beretta⁴⁹, D. Berge⁴⁴, E. Bergeaas Kuutmann¹⁶⁹, N. Berger⁵, L.J. Bergsten²⁶, J. Beringer¹⁸, S. Berlendis⁷, N.R. Bernard¹⁰⁰, G. Bernardi¹³², C. Bernius¹⁵⁰, F.U. Bernlochner²⁴, T. Berry⁹¹, P. Berta⁹⁷, C. Bertella^{15a}, G. Bertoli^{43a,43b}, I.A. Bertram⁸⁷, G.J. Besjes³⁹, O. Bessidskaia Bylund^{43a,43b}, M. Bessner⁴⁴, N. Besson¹⁴², A. Bethani⁹⁸, S. Bethke¹¹³, A. Betti²⁴, A.J. Bevan⁹⁰, J. Beyer¹¹³, R.M.B. Bianchi¹³⁵, O. Biebel¹¹², D. Biedermann¹⁹, R. Bielski⁹⁸, K. Bierwagen⁹⁷, N.V. Biesuz^{69a,69b}, M. Biglietti^{72a}, T.R.V. Billoud¹⁰⁷, M. Bindi⁵¹, A. Bingul^{12d}, C. Bini^{70a,70b}, S. Biondi^{23b,23a}, T. Bisanz⁵¹, J.P. Biswal¹⁵⁸, C. Bittrich⁴⁶, D.M. Bjergaard⁴⁷, J.E. Black¹⁵⁰,

K.M. Black²⁵, R.E. Blair⁶, T. Blazek^{28a}, I. Bloch⁴⁴, C. Blocker²⁶, A. Blue⁵⁵, U. Blumenschein⁹⁰,
 Dr. Blunier^{144a}, G.J. Bobbink¹¹⁸, V.S. Bobrovnikov^{120b,120a}, S.S. Bocchetta⁹⁴, A. Bocci⁴⁷, D. Boerner¹⁷⁹,
 D. Bogavac¹¹², A.G. Bogdanchikov^{120b,120a}, C. Bohm^{43a}, V. Boisvert⁹¹, P. Bokan^{169,y}, T. Bold^{81a},
 A.S. Boldyrev¹¹¹, A.E. Bolz^{59b}, M. Bomben¹³², M. Bona⁹⁰, J.S. Bonilla¹²⁷, M. Boonekamp¹⁴²,
 A. Borisov¹⁴⁰, G. Borissov⁸⁷, J. Bortfeldt³⁵, D. Bortoletto¹³¹, V. Bortolotto^{71a,61b,61c,71b},
 D. Boscherini^{23b}, M. Bosman¹⁴, J.D. Bossio Sola³⁰, K. Bouaouda^{34a}, J. Boudreau¹³⁵,
 E.V. Bouhova-Thacker⁸⁷, D. Boumediene³⁷, C. Bourdarios¹²⁸, S.K. Boutle⁵⁵, A. Boveia¹²², J. Boyd³⁵,
 I.R. Boyko⁷⁷, A.J. Bozson⁹¹, J. Bracinik²¹, N. Brahimi⁹⁹, A. Brandt⁸, G. Brandt¹⁷⁹, O. Brandt^{59a},
 F. Braren⁴⁴, U. Bratzler¹⁶¹, B. Brau¹⁰⁰, J.E. Brau¹²⁷, W.D. Breaden Madden⁵⁵, K. Brendlinger⁴⁴,
 A.J. Brennan¹⁰², L. Brenner⁴⁴, R. Brenner¹⁶⁹, S. Bressler¹⁷⁷, B. Brickwedde⁹⁷, D.L. Briglin²¹,
 D. Britton⁵⁵, D. Britzger^{59b}, I. Brock²⁴, R. Brock¹⁰⁴, G. Brooijmans³⁸, T. Brooks⁹¹, W.K. Brooks^{144b},
 E. Brost¹¹⁹, J.H. Broughton²¹, P.A. Bruckman de Renstrom⁸², D. Bruncko^{28b}, A. Bruni^{23b}, G. Bruni^{23b},
 L.S. Bruni¹¹⁸, S. Bruno^{71a,71b}, B.H. Brunt³¹, M. Bruschi^{23b}, N. Bruscino¹³⁵, P. Bryant³⁶,
 L. Bryngemark⁴⁴, T. Buanes¹⁷, Q. Buat³⁵, P. Buchholz¹⁴⁸, A.G. Buckley⁵⁵, I.A. Budagov⁷⁷,
 F. Buehrer⁵⁰, M.K. Bugge¹³⁰, O. Bulekov¹¹⁰, D. Bullock⁸, T.J. Burch¹¹⁹, S. Burdin⁸⁸, C.D. Burgard¹¹⁸,
 A.M. Burger⁵, B. Burghgrave¹¹⁹, K. Burka⁸², S. Burke¹⁴¹, I. Burmeister⁴⁵, J.T.P. Burr¹³¹, D. Büscher⁵⁰,
 V. Büscher⁹⁷, E. Buschmann⁵¹, P. Bussey⁵⁵, J.M. Butler²⁵, C.M. Buttar⁵⁵, J.M. Butterworth⁹², P. Butti³⁵,
 W. Buttinger³⁵, A. Buzatu¹⁵⁵, A.R. Buzykaev^{120b,120a}, G. Cabras^{23b,23a}, S. Cabrera Urbán¹⁷¹,
 D. Caforio¹³⁸, H. Cai¹⁷⁰, V.M.M. Cairo², O. Cakir^{4a}, N. Calace⁵², P. Calafiura¹⁸, A. Calandri⁹⁹,
 G. Calderini¹³², P. Calfayan⁶³, G. Callea^{40b,40a}, L.P. Caloba^{78b}, S. Calvente Lopez⁹⁶, D. Calvet³⁷,
 S. Calvet³⁷, T.P. Calvet¹⁵², M. Calvetti^{69a,69b}, R. Camacho Toro¹³², S. Camarda³⁵, P. Camarri^{71a,71b},
 D. Cameron¹³⁰, R. Caminal Armadans¹⁰⁰, C. Camincher³⁵, S. Campana³⁵, M. Campanelli⁹²,
 A. Camplani³⁹, A. Campoverde¹⁴⁸, V. Canale^{67a,67b}, M. Cano Bret^{58c}, J. Cantero¹²⁵, T. Cao¹⁵⁸,
 Y. Cao¹⁷⁰, M.D.M. Capeans Garrido³⁵, I. Caprini^{27b}, M. Caprini^{27b}, M. Capua^{40b,40a}, R.M. Carbone³⁸,
 R. Cardarelli^{71a}, F.C. Cardillo⁵⁰, I. Carli¹³⁹, T. Carli³⁵, G. Carlino^{67a}, B.T. Carlson¹³⁵,
 L. Carminati^{66a,66b}, R.M.D. Carney^{43a,43b}, S. Caron¹¹⁷, E. Carquin^{144b}, S. Carrá^{66a,66b},
 G.D. Carrillo-Montoya³⁵, D. Casadei^{32b}, M.P. Casado^{14,g}, A.F. Casha¹⁶⁴, M. Casolino¹⁴,
 D.W. Casper¹⁶⁸, R. Castelijn¹¹⁸, F.L. Castillo¹⁷¹, V. Castillo Gimenez¹⁷¹, N.F. Castro^{136a,136e},
 A. Catinaccio³⁵, J.R. Catmore¹³⁰, A. Cattai³⁵, J. Caudron²⁴, V. Cavaliere²⁹, E. Cavallaro¹⁴, D. Cavalli^{66a},
 M. Cavalli-Sforza¹⁴, V. Cavasinni^{69a,69b}, E. Celebi^{12b}, F. Ceradini^{72a,72b}, L. Cerdà Alberich¹⁷¹,
 A.S. Cerqueira^{78a}, A. Cerri¹⁵³, L. Cerrito^{71a,71b}, F. Cerutti¹⁸, A. Cervelli^{23b,23a}, S.A. Cetin^{12b},
 A. Chafaq^{34a}, D. Chakraborty¹¹⁹, S.K. Chan⁵⁷, W.S. Chan¹¹⁸, Y.L. Chan^{61a}, J.D. Chapman³¹,
 D.G. Charlton²¹, C.C. Chau³³, C.A. Chavez Barajas¹⁵³, S. Che¹²², A. Chegwidden¹⁰⁴, S. Chekanov⁶,
 S.V. Chekulaev^{165a}, G.A. Chelkov^{77,ar}, M.A. Chelstowska³⁵, C. Chen^{58a}, C.H. Chen⁷⁶, H. Chen²⁹,
 J. Chen^{58a}, J. Chen³⁸, S. Chen¹³³, S.J. Chen^{15c}, X. Chen^{15b,aq}, Y. Chen⁸⁰, Y-H. Chen⁴⁴, H.C. Cheng¹⁰³,
 H.J. Cheng^{15d}, A. Cheplakov⁷⁷, E. Cheremushkina¹⁴⁰, R. Cherkaoui El Moursli^{34e}, E. Cheu⁷,
 K. Cheung⁶², L. Chevalier¹⁴², V. Chiarella⁴⁹, G. Chiarelli^{69a}, G. Chiodini^{65a}, A.S. Chisholm³⁵,
 A. Chitan^{27b}, I. Chiu¹⁶⁰, Y.H. Chiu¹⁷³, M.V. Chizhov⁷⁷, K. Choi⁶³, A.R. Chomont¹²⁸, S. Chouridou¹⁵⁹,
 Y.S. Chow¹¹⁸, V. Christodoulou⁹², M.C. Chu^{61a}, J. Chudoba¹³⁷, A.J. Chuinard¹⁰¹, J.J. Chwastowski⁸²,
 L. Chytka¹²⁶, D. Cinca⁴⁵, V. Cindro⁸⁹, I.A. Cioara²⁴, A. Ciocio¹⁸, F. Cirotto^{67a,67b}, Z.H. Citron¹⁷⁷,
 M. Citterio^{66a}, A. Clark⁵², M.R. Clark³⁸, P.J. Clark⁴⁸, C. Clement^{43a,43b}, Y. Coadou⁹⁹, M. Cobal^{64a,64c},
 A. Coccaro^{53b,53a}, J. Cochran⁷⁶, A.E.C. Coimbra¹⁷⁷, L. Colasurdo¹¹⁷, B. Cole³⁸, A.P. Colijn¹¹⁸,
 J. Collot⁵⁶, P. Conde Muñoz^{136a,136b}, E. Coniavitis⁵⁰, S.H. Connell^{32b}, I.A. Connolly⁹⁸,
 S. Constantinescu^{27b}, F. Conventi^{67a,at}, A.M. Cooper-Sarkar¹³¹, F. Cormier¹⁷², K.J.R. Cormier¹⁶⁴,
 M. Corradi^{70a,70b}, E.E. Corrigan⁹⁴, F. Corriveau^{101,ad}, A. Cortes-Gonzalez³⁵, M.J. Costa¹⁷¹,
 D. Costanzo¹⁴⁶, G. Cottin³¹, G. Cowan⁹¹, B.E. Cox⁹⁸, J. Crane⁹⁸, K. Cranmer¹²¹, S.J. Crawley⁵⁵,
 R.A. Creager¹³³, G. Cree³³, S. Crépé-Renaudin⁵⁶, F. Crescioli¹³², M. Cristinziani²⁴, V. Croft¹²¹,

G. Crosetti^{40b,40a}, A. Cueto⁹⁶, T. Cuhadar Donszelmann¹⁴⁶, A.R. Cukierman¹⁵⁰, M. Curatolo⁴⁹,
 J. Cúth⁹⁷, S. Czekiera⁸², P. Czodrowski³⁵, M.J. Da Cunha Sargedas De Sousa^{58b,136b}, C. Da Via⁹⁸,
 W. Dabrowski^{81a}, T. Dado^{28a,y}, S. Dahbi^{34e}, T. Dai¹⁰³, F. Dallaire¹⁰⁷, C. Dallapiccola¹⁰⁰, M. Dam³⁹,
 G. D'amen^{23b,23a}, J. Damp⁹⁷, J.R. Dandoy¹³³, M.F. Daneri³⁰, N.P. Dang^{178,k}, N.D Dann⁹⁸,
 M. Dannerger¹⁷², V. Dao³⁵, G. Darbo^{53b}, S. Darmora⁸, O. Dartsi⁵, A. Dattagupta¹²⁷, T. Daubney⁴⁴,
 S. D'Auria⁵⁵, W. Davey²⁴, C. David⁴⁴, T. Davidek¹³⁹, D.R. Davis⁴⁷, E. Dawe¹⁰², I. Dawson¹⁴⁶, K. De⁸,
 R. De Asmundis^{67a}, A. De Benedetti¹²⁴, S. De Castro^{23b,23a}, S. De Cecco^{70a,70b}, N. De Groot¹¹⁷,
 P. de Jong¹¹⁸, H. De la Torre¹⁰⁴, F. De Lorenzi⁷⁶, A. De Maria^{51,t}, D. De Pedis^{70a}, A. De Salvo^{70a},
 U. De Sanctis^{71a,71b}, A. De Santo¹⁵³, K. De Vasconcelos Corga⁹⁹, J.B. De Vivie De Regie¹²⁸,
 C. Debenedetti¹⁴³, D.V. Dedovich⁷⁷, N. Dehghanian³, M. Del Gaudio^{40b,40a}, J. Del Peso⁹⁶,
 D. Delgove¹²⁸, F. Deliot¹⁴², C.M. Delitzsch⁷, M. Della Pietra^{67a,67b}, D. Della Volpe⁵², A. Dell'Acqua³⁵,
 L. Dell'Asta²⁵, M. Delmastro⁵, C. Delporte¹²⁸, P.A. Delsart⁵⁶, D.A. DeMarco¹⁶⁴, S. Demers¹⁸⁰,
 M. Demichev⁷⁷, S.P. Denisov¹⁴⁰, D. Denysiuk¹¹⁸, L. D'Eramo¹³², D. Derendarz⁸², J.E. Derkaoui^{34d},
 F. Derue¹³², P. Dervan⁸⁸, K. Desch²⁴, C. Deterre⁴⁴, K. Dette¹⁶⁴, M.R. Devesa³⁰, P.O. Deviveiros³⁵,
 A. Dewhurst¹⁴¹, S. Dhaliwal²⁶, F.A. Di Bello⁵², A. Di Ciaccio^{71a,71b}, L. Di Ciaccio⁵,
 W.K. Di Clemente¹³³, C. Di Donato^{67a,67b}, A. Di Girolamo³⁵, B. Di Micco^{72a,72b}, R. Di Nardo³⁵,
 K.F. Di Petrillo⁵⁷, A. Di Simone⁵⁰, R. Di Sipio¹⁶⁴, D. Di Valentino³³, C. Diaconu⁹⁹, M. Diamond¹⁶⁴,
 F.A. Dias³⁹, T. Dias Do Vale^{136a}, M.A. Diaz^{144a}, J. Dickinson¹⁸, E.B. Diehl¹⁰³, J. Dietrich¹⁹,
 S. Díez Cornell⁴⁴, A. Dimitrievska¹⁸, J. Dingfelder²⁴, F. Dittus³⁵, F. Djama⁹⁹, T. Djobava^{156b},
 J.I. Djuvsland^{59a}, M.A.B. Do Vale^{78c}, M. Dobre^{27b}, D. Dodsworth²⁶, C. Doglioni⁹⁴, J. Dolejsi¹³⁹,
 Z. Dolezal¹³⁹, M. Donadelli^{78d}, J. Donini³⁷, A. D'onofrio⁹⁰, M. D'Onofrio⁸⁸, J. Dopke¹⁴¹, A. Doria^{67a},
 M.T. Dova⁸⁶, A.T. Doyle⁵⁵, E. Drechsler⁵¹, E. Dreyer¹⁴⁹, T. Dreyer⁵¹, M. Dris¹⁰, Y. Du^{58b},
 J. Duarte-Campderros¹⁵⁸, F. Dubinin¹⁰⁸, M. Dubovsky^{28a}, A. Dubreuil⁵², E. Duchovni¹⁷⁷,
 G. Duckeck¹¹², A. Ducourthial¹³², O.A. Ducu^{107,x}, D. Duda¹¹³, A. Dudarev³⁵, A.C. Dudder⁹⁷,
 E.M. Duffield¹⁸, L. Duflot¹²⁸, M. Dührssen³⁵, C. Dülzen¹⁷⁹, M. Dumancic¹⁷⁷, A.E. Dumitriu^{27b,e},
 A.K. Duncan⁵⁵, M. Dunford^{59a}, A. Duperrin⁹⁹, H. Duran Yildiz^{4a}, M. Düren⁵⁴, A. Durglishvili^{156b},
 D. Duschinger⁴⁶, B. Dutta⁴⁴, D. Duvnjak¹, M. Dyndal⁴⁴, S. Dysch⁹⁸, B.S. Dziedzic⁸², C. Eckardt⁴⁴,
 K.M. Ecker¹¹³, R.C. Edgar¹⁰³, T. Eifert³⁵, G. Eigen¹⁷, K. Einsweiler¹⁸, T. Ekelof¹⁶⁹, M. El Kacimi^{34c},
 R. El Kosseifi⁹⁹, V. Ellajosyula⁹⁹, M. Ellert¹⁶⁹, F. Ellinghaus¹⁷⁹, A.A. Elliot⁹⁰, N. Ellis³⁵,
 J. Elmsheuser²⁹, M. Elsing³⁵, D. Emeliyanov¹⁴¹, Y. Enari¹⁶⁰, J.S. Ennis¹⁷⁵, M.B. Epland⁴⁷,
 J. Erdmann⁴⁵, A. Ereditato²⁰, S. Errede¹⁷⁰, M. Escalier¹²⁸, C. Escobar¹⁷¹, B. Esposito⁴⁹,
 O. Estrada Pastor¹⁷¹, A.I. Etienne¹⁴², E. Etzion¹⁵⁸, H. Evans⁶³, A. Ezhilov¹³⁴, M. Ezzi^{34e}, F. Fabbri⁵⁵,
 L. Fabbri^{23b,23a}, V. Fabiani¹¹⁷, G. Facini⁹², R.M. Faisca Rodrigues Pereira^{136a}, R.M. Fakhrutdinov¹⁴⁰,
 S. Falciano^{70a}, P.J. Falke⁵, S. Falke⁵, J. Faltova¹³⁹, Y. Fang^{15a}, M. Fanti^{66a,66b}, A. Farbin⁸, A. Farilla^{72a},
 E.M. Farina^{68a,68b}, T. Farooque¹⁰⁴, S. Farrell¹⁸, S.M. Farrington¹⁷⁵, P. Farthouat³⁵, F. Fassi^{34e},
 P. Fassnacht³⁵, D. Fassouliotis⁹, M. Fucci Giannelli⁴⁸, A. Favareto^{53b,53a}, W.J. Fawcett⁵², L. Fayard¹²⁸,
 O.L. Fedin^{134,q}, W. Fedorko¹⁷², M. Feickert⁴¹, S. Feigl¹³⁰, L. Feligioni⁹⁹, C. Feng^{58b}, E.J. Feng³⁵,
 M. Feng⁴⁷, M.J. Fenton⁵⁵, A.B. Fenyuk¹⁴⁰, L. Feremenga⁸, J. Ferrando⁴⁴, A. Ferrari¹⁶⁹, P. Ferrari¹¹⁸,
 R. Ferrari^{68a}, D.E. Ferreira de Lima^{59b}, A. Ferrer¹⁷¹, D. Ferrere⁵², C. Ferretti¹⁰³, F. Fiedler⁹⁷,
 A. Filipčić⁸⁹, F. Filthaut¹¹⁷, K.D. Finelli²⁵, M.C.N. Fiolhais^{136a,136c,b}, L. Fiorini¹⁷¹, C. Fischer¹⁴,
 W.C. Fisher¹⁰⁴, N. Flaschel⁴⁴, I. Fleck¹⁴⁸, P. Fleischmann¹⁰³, R.R.M. Fletcher¹³³, T. Flick¹⁷⁹,
 B.M. Flierl¹¹², L.M. Flores¹³³, L.R. Flores Castillo^{61a}, N. Fomin¹⁷, G.T. Forcolin⁹⁸, A. Formica¹⁴²,
 F.A. Förster¹⁴, A.C. Forti⁹⁸, A.G. Foster²¹, D. Fournier¹²⁸, H. Fox⁸⁷, S. Fracchia¹⁴⁶, P. Francavilla^{69a,69b},
 M. Franchini^{23b,23a}, S. Franchino^{59a}, D. Francis³⁵, L. Franconi¹³⁰, M. Franklin⁵⁷, M. Frate¹⁶⁸,
 M. Fraternali^{68a,68b}, D. Freeborn⁹², S.M. Fressard-Batraneanu³⁵, B. Freund¹⁰⁷, W.S. Freund^{78b},
 D. Froidevaux³⁵, J.A. Frost¹³¹, C. Fukunaga¹⁶¹, T. Fusayasu¹¹⁴, J. Fuster¹⁷¹, O. Gabizon¹⁵⁷,
 A. Gabrielli^{23b,23a}, A. Gabrielli¹⁸, G.P. Gach^{81a}, S. Gadatsch⁵², P. Gadow¹¹³, G. Gagliardi^{53b,53a},

L.G. Gagnon¹⁰⁷, C. Galea^{27b}, B. Galhardo^{136a,136c}, E.J. Gallas¹³¹, B.J. Gallop¹⁴¹, P. Gallus¹³⁸,
 G. Galster³⁹, R. Gamboa Goni⁹⁰, K.K. Gan¹²², S. Ganguly¹⁷⁷, Y. Gao⁸⁸, Y.S. Gao^{150,m}, C. García¹⁷¹,
 J.E. García Navarro¹⁷¹, J.A. García Pascual^{15a}, M. Garcia-Sciveres¹⁸, R.W. Gardner³⁶, N. Garelli¹⁵⁰,
 V. Garonne¹³⁰, K. Gasnikova⁴⁴, A. Gaudiello^{53b,53a}, G. Gaudio^{68a}, I.L. Gavrilenko¹⁰⁸, A. Gavrilyuk¹⁰⁹,
 C. Gay¹⁷², G. Gaycken²⁴, E.N. Gazis¹⁰, C.N.P. Gee¹⁴¹, J. Geisen⁵¹, M. Geisen⁹⁷, M.P. Geisler^{59a},
 K. Gellerstedt^{43a,43b}, C. Gemme^{53b}, M.H. Genest⁵⁶, C. Geng¹⁰³, S. Gentile^{70a,70b}, C. Gentsos¹⁵⁹,
 S. George⁹¹, D. Gerbaudo¹⁴, G. Gessner⁴⁵, S. Ghasemi¹⁴⁸, M. Ghasemi Bostanabad¹⁷³, M. Ghneimat²⁴,
 B. Giacobbe^{23b}, S. Giagu^{70a,70b}, N. Giangiacomi^{23b,23a}, P. Giannetti^{69a}, S.M. Gibson⁹¹, M. Gignac¹⁴³,
 D. Gillberg³³, G. Gilles¹⁷⁹, D.M. Gingrich^{3,as}, M.P. Giordani^{64a,64c}, F.M. Giorgi^{23b}, P.F. Giraud¹⁴²,
 P. Giromini⁵⁷, G. Giugliarelli^{64a,64c}, D. Giugni^{66a}, F. Giulini¹³¹, M. Giulini^{59b}, S. Gkaitatzis¹⁵⁹,
 I. Gkialas^{9,j}, E.L. Gkougkousis¹⁴, P. Gkountoumis¹⁰, L.K. Gladilin¹¹¹, C. Glasman⁹⁶, J. Glatzer¹⁴,
 P.C.F. Glaysher⁴⁴, A. Glazov⁴⁴, M. Goblirsch-Kolb²⁶, J. Godlewski⁸², S. Goldfarb¹⁰², T. Golling⁵²,
 D. Golubkov¹⁴⁰, A. Gomes^{136a,136b,136d}, R. Goncalves Gama^{78a}, R. Gonçalo^{136a}, G. Gonella⁵⁰,
 L. Gonella²¹, A. Gongadze⁷⁷, F. Gonnella²¹, J.L. Gonski⁵⁷, S. González de la Hoz¹⁷¹,
 S. Gonzalez-Sevilla⁵², L. Goossens³⁵, P.A. Gorbounov¹⁰⁹, H.A. Gordon²⁹, B. Gorini³⁵, E. Gorini^{65a,65b},
 A. Gorišek⁸⁹, A.T. Goshaw⁴⁷, C. Gössling⁴⁵, M.I. Gostkin⁷⁷, C.A. Gottardo²⁴, C.R. Goudet¹²⁸,
 D. Goujdami^{34c}, A.G. Goussiou¹⁴⁵, N. Govender^{32b,c}, C. Goy⁵, E. Gozani¹⁵⁷, I. Grabowska-Bold^{81a},
 P.O.J. Gradin¹⁶⁹, E.C. Graham⁸⁸, J. Gramling¹⁶⁸, E. Gramstad¹³⁰, S. Grancagnolo¹⁹, V. Gratchev¹³⁴,
 P.M. Gravila^{27f}, C. Gray⁵⁵, H.M. Gray¹⁸, Z.D. Greenwood^{93,ai}, C. Grefe²⁴, K. Gregersen⁹²,
 I.M. Gregor⁴⁴, P. Grenier¹⁵⁰, K. Grevtsov⁴⁴, J. Griffiths⁸, A.A. Grillo¹⁴³, K. Grimm¹⁵⁰, S. Grinstein^{14,z},
 Ph. Gris³⁷, J.-F. Grivaz¹²⁸, S. Groh⁹⁷, E. Gross¹⁷⁷, J. Grosse-Knetter⁵¹, G.C. Grossi⁹³, Z.J. Grout⁹²,
 C. Grud¹⁰³, A. Grummer¹¹⁶, L. Guan¹⁰³, W. Guan¹⁷⁸, J. Guenther³⁵, A. Guerguichon¹²⁸, F. Guescini^{165a},
 D. Guest¹⁶⁸, R. Gugel⁵⁰, B. Gui¹²², T. Guillemin⁵, S. Guindon³⁵, U. Gul⁵⁵, C. Gumpert³⁵, J. Guo^{58c},
 W. Guo¹⁰³, Y. Guo^{58a,s}, Z. Guo⁹⁹, R. Gupta⁴¹, S. Gurbuz^{12c}, G. Gustavino¹²⁴, B.J. Gutelman¹⁵⁷,
 P. Gutierrez¹²⁴, C. Gutschow⁹², C. Guyot¹⁴², M.P. Guzik^{81a}, C. Gwenlan¹³¹, C.B. Gwilliam⁸⁸,
 A. Haas¹²¹, C. Haber¹⁸, H.K. Hadavand⁸, N. Haddad^{34e}, A. Hadef^{58a}, S. Hageböck²⁴, M. Hagihara¹⁶⁶,
 H. Hakobyan^{181,*}, M. Haleem¹⁷⁴, J. Haley¹²⁵, G. Halladjian¹⁰⁴, G.D. Hallewell⁹⁹, K. Hamacher¹⁷⁹,
 P. Hamal¹²⁶, K. Hamano¹⁷³, A. Hamilton^{32a}, G.N. Hamity¹⁴⁶, K. Han^{58a,ah}, L. Han^{58a}, S. Han^{15d},
 K. Hanagaki^{79,v}, M. Hance¹⁴³, D.M. Handl¹¹², B. Haney¹³³, R. Hankache¹³², P. Hanke^{59a}, E. Hansen⁹⁴,
 J.B. Hansen³⁹, J.D. Hansen³⁹, M.C. Hansen²⁴, P.H. Hansen³⁹, K. Hara¹⁶⁶, A.S. Hard¹⁷⁸,
 T. Harenberg¹⁷⁹, S. Harkusha¹⁰⁵, P.F. Harrison¹⁷⁵, N.M. Hartmann¹¹², Y. Hasegawa¹⁴⁷, A. Hasib⁴⁸,
 S. Hassani¹⁴², S. Haug²⁰, R. Hauser¹⁰⁴, L. Hauswald⁴⁶, L.B. Havener³⁸, M. Havranek¹³⁸,
 C.M. Hawkes²¹, R.J. Hawkings³⁵, D. Hayden¹⁰⁴, C. Hayes¹⁵², C.P. Hays¹³¹, J.M. Hays⁹⁰,
 H.S. Hayward⁸⁸, S.J. Haywood¹⁴¹, M.P. Heath⁴⁸, V. Hedberg⁹⁴, L. Heelan⁸, S. Heer²⁴,
 K.K. Heidegger⁵⁰, J. Heilman³³, S. Heim⁴⁴, T. Heim¹⁸, B. Heinemann^{44,an}, J.J. Heinrich¹¹²,
 L. Heinrich¹²¹, C. Heinz⁵⁴, J. Hejbal¹³⁷, L. Helary³⁵, A. Held¹⁷², S. Hellesund¹³⁰, S. Hellman^{43a,43b},
 C. Helsens³⁵, R.C.W. Henderson⁸⁷, Y. Heng¹⁷⁸, S. Henkelmann¹⁷², A.M. Henriques Correia³⁵,
 G.H. Herbert¹⁹, H. Herde²⁶, V. Herget¹⁷⁴, Y. Hernández Jiménez^{32c}, H. Herr⁹⁷, G. Herten⁵⁰,
 R. Hertenberger¹¹², L. Hervas³⁵, T.C. Herwig¹³³, G.G. Hesketh⁹², N.P. Hessey^{165a}, J.W. Hetherly⁴¹,
 S. Higashino⁷⁹, E. Higón-Rodríguez¹⁷¹, K. Hildebrand³⁶, E. Hill¹⁷³, J.C. Hill³¹, K.K. Hill²⁹,
 K.H. Hiller⁴⁴, S.J. Hillier²¹, M. Hils⁴⁶, I. Hincliffe¹⁸, M. Hirose¹²⁹, D. Hirschbuehl¹⁷⁹, B. Hiti⁸⁹,
 O. Hladík¹³⁷, D.R. Hlálučku^{32c}, X. Hoad⁴⁸, J. Hobbs¹⁵², N. Hod^{165a}, M.C. Hodgkinson¹⁴⁶, A. Hoecker³⁵,
 M.R. Hoeferkamp¹¹⁶, F. Hoenig¹¹², D. Hohn²⁴, D. Hohov¹²⁸, T.R. Holmes³⁶, M. Holzbock¹¹²,
 M. Homann⁴⁵, S. Honda¹⁶⁶, T. Honda⁷⁹, T.M. Hong¹³⁵, A. Hönlle¹¹³, B.H. Hooberman¹⁷⁰,
 W.H. Hopkins¹²⁷, Y. Horii¹¹⁵, P. Horn⁴⁶, A.J. Horton¹⁴⁹, L.A. Horyn³⁶, J.-Y. Hostachy⁵⁶, A. Hostiuc¹⁴⁵,
 S. Hou¹⁵⁵, A. Hoummada^{34a}, J. Howarth⁹⁸, J. Hoy⁸⁶, M. Hrabovsky¹²⁶, J. Hrdinka³⁵, I. Hristova¹⁹,
 J. Hrvnac¹²⁸, A. Hrynevich¹⁰⁶, T. Hrynev'ova⁵, P.J. Hsu⁶², S.-C. Hsu¹⁴⁵, Q. Hu²⁹, S. Hu^{58c}, Y. Huang^{15a},

Z. Hubacek¹³⁸, F. Hubaut⁹⁹, M. Huebner²⁴, F. Huegging²⁴, T.B. Huffman¹³¹, E.W. Hughes³⁸,
 M. Huhtinen³⁵, R.F.H. Hunter³³, P. Huo¹⁵², A.M. Hupe³³, N. Huseynov^{77,af}, J. Huston¹⁰⁴, J. Huth⁵⁷,
 R. Hyneman¹⁰³, G. Iacobucci⁵², G. Iakovidis²⁹, I. Ibragimov¹⁴⁸, L. Iconomidou-Fayard¹²⁸, Z. Idrissi^{34e},
 P. Iengo³⁵, R. Ignazzi³⁹, O. Igonkina^{118,ab}, R. Iguchi¹⁶⁰, T. Iizawa⁵², Y. Ikegami⁷⁹, M. Ikeno⁷⁹,
 D. Iliadis¹⁵⁹, N. Ilic¹⁵⁰, F. Iltzsche⁴⁶, G. Introzzi^{68a,68b}, M. Iodice^{72a}, K. Iordanidou³⁸, V. Ippolito^{70a,70b},
 M.F. Isacson¹⁶⁹, N. Ishijima¹²⁹, M. Ishino¹⁶⁰, M. Ishitsuka¹⁶², W. Islam¹²⁵, C. Issever¹³¹, S. Istin^{12c,am},
 F. Ito¹⁶⁶, J.M. Iturbe Ponce^{61a}, R. Iuppa^{73a,73b}, A. Ivina¹⁷⁷, H. Iwasaki⁷⁹, J.M. Izen⁴², V. Izzo^{67a},
 S. Jabbar³, P. Jacka¹³⁷, P. Jackson¹, R.M. Jacobs²⁴, V. Jain², G. Jäkel¹⁷⁹, K.B. Jakobi⁹⁷, K. Jakobs⁵⁰,
 S. Jakobsen⁷⁴, T. Jakoubek¹³⁷, D.O. Jamin¹²⁵, D.K. Jana⁹³, R. Jansky⁵², J. Janssen²⁴, M. Janus⁵¹,
 P.A. Janus^{81a}, G. Jarlskog⁹⁴, N. Javadov^{77,af}, T. Javůrek⁵⁰, M. Javurkova⁵⁰, F. Jeanneau¹⁴², L. Jeanty¹⁸,
 J. Jejelava^{156a,ag}, A. Jelinskas¹⁷⁵, P. Jenni^{50,d}, J. Jeong⁴⁴, C. Jeske¹⁷⁵, S. Jézéquel⁵, H. Ji¹⁷⁸, J. Jia¹⁵²,
 H. Jiang⁷⁶, Y. Jiang^{58a}, Z. Jiang¹⁵⁰, S. Jiggins⁵⁰, F.A. Jimenez Morales³⁷, J. Jimenez Pena¹⁷¹, S. Jin^{15c},
 A. Jinaru^{27b}, O. Jinnouchi¹⁶², H. Jivan^{32c}, P. Johansson¹⁴⁶, K.A. Johns⁷, C.A. Johnson⁶³,
 W.J. Johnson¹⁴⁵, K. Jon-And^{43a,43b}, R.W.L. Jones⁸⁷, S.D. Jones¹⁵³, S. Jones⁷, T.J. Jones⁸⁸,
 J. Jongmanns^{59a}, P.M. Jorge^{136a,136b}, J. Jovicevic^{165a}, X. Ju¹⁷⁸, J.J. Junggeburth¹¹³, A. Juste Rozas^{14,z},
 A. Kaczmarcka⁸², M. Kado¹²⁸, H. Kagan¹²², M. Kagan¹⁵⁰, T. Kaji¹⁷⁶, E. Kajomovitz¹⁵⁷,
 C.W. Kalderon⁹⁴, A. Kaluza⁹⁷, S. Kama⁴¹, A. Kamenshchikov¹⁴⁰, L. Kanjir⁸⁹, Y. Kano¹⁶⁰,
 V.A. Kantserov¹¹⁰, J. Kanzaki⁷⁹, B. Kaplan¹²¹, L.S. Kaplan¹⁷⁸, D. Kar^{32c}, M.J. Kareem^{165b},
 E. Karentzos¹⁰, S.N. Karpov⁷⁷, Z.M. Karpova⁷⁷, V. Kartvelishvili⁸⁷, A.N. Karyukhin¹⁴⁰, K. Kasahara¹⁶⁶,
 L. Kashif¹⁷⁸, R.D. Kass¹²², A. Kastanas¹⁵¹, Y. Kataoka¹⁶⁰, C. Kato¹⁶⁰, J. Katzy⁴⁴, K. Kawade⁸⁰,
 K. Kawagoe⁸⁵, T. Kawamoto¹⁶⁰, G. Kawamura⁵¹, E.F. Kay⁸⁸, V.F. Kazanin^{120b,120a}, R. Keeler¹⁷³,
 R. Kehoe⁴¹, J.S. Keller³³, E. Kellermann⁹⁴, J.J. Kempster²¹, J. Kendrick²¹, O. Kepka¹³⁷, S. Kersten¹⁷⁹,
 B.P. Kerševan⁸⁹, R.A. Keyes¹⁰¹, M. Khader¹⁷⁰, F. Khalil-Zada¹³, A. Khanov¹²⁵,
 A.G. Kharlamov^{120b,120a}, T. Kharlamova^{120b,120a}, A. Khodinov¹⁶³, T.J. Khoo⁵², E. Khramov⁷⁷,
 J. Khubua^{156b}, S. Kido⁸⁰, M. Kiehn⁵², C.R. Kilby⁹¹, S.H. Kim¹⁶⁶, Y.K. Kim³⁶, N. Kimura^{64a,64c},
 O.M. Kind¹⁹, B.T. King⁸⁸, D. Kirchmeier⁴⁶, J. Kirk¹⁴¹, A.E. Kiryunin¹¹³, T. Kishimoto¹⁶⁰,
 D. Kisielewska^{81a}, V. Kitali⁴⁴, O. Kivernyk⁵, E. Kladiva^{28b}, T. Klapdor-Kleingrothaus⁵⁰, M.H. Klein¹⁰³,
 M. Klein⁸⁸, U. Klein⁸⁸, K. Kleinknecht⁹⁷, P. Klimek¹¹⁹, A. Klimentov²⁹, R. Klingenberg^{45,*}, T. Klingl²⁴,
 T. Klioutchnikova³⁵, F.F. Klitzner¹¹², P. Kluit¹¹⁸, S. Kluth¹¹³, E. Kneringer⁷⁴, E.B.F.G. Knoops⁹⁹,
 A. Knue⁵⁰, A. Kobayashi¹⁶⁰, D. Kobayashi⁸⁵, T. Kobayashi¹⁶⁰, M. Kobel⁴⁶, M. Kocian¹⁵⁰, P. Kodys¹³⁹,
 T. Koffas³³, E. Koffeman¹¹⁸, N.M. Köhler¹¹³, T. Koi¹⁵⁰, M. Kolb^{59b}, I. Koletsou⁵, T. Kondo⁷⁹,
 N. Kondrashova^{58c}, K. Köneke⁵⁰, A.C. König¹¹⁷, T. Kono⁷⁹, R. Konoplich^{121,aj}, V. Konstantinides⁹²,
 N. Konstantinidis⁹², B. Konya⁹⁴, R. Kopeliansky⁶³, S. Koperny^{81a}, K. Korcyl⁸², K. Kordas¹⁵⁹, A. Korn⁹²,
 I. Korolkov¹⁴, E.V. Korolkova¹⁴⁶, O. Kortner¹¹³, S. Kortner¹¹³, T. Kosek¹³⁹, V.V. Kostyukhin²⁴,
 A. Kotwal⁴⁷, A. Koulouris¹⁰, A. Kourkoumeli-Charalampidi^{68a,68b}, C. Kourkoumelis⁹, E. Kourlitis¹⁴⁶,
 V. Kouskoura²⁹, A.B. Kowalewska⁸², R. Kowalewski¹⁷³, T.Z. Kowalski^{81a}, C. Kozakai¹⁶⁰,
 W. Kozanecki¹⁴², A.S. Kozhin¹⁴⁰, V.A. Kramarenko¹¹¹, G. Kramberger⁸⁹, D. Krasnopevtsev¹¹⁰,
 M.W. Krasny¹³², A. Krasznahorkay³⁵, D. Krauss¹¹³, J.A. Kremer^{81a}, J. Kretzschmar⁸⁸, P. Krieger¹⁶⁴,
 K. Krizka¹⁸, K. Kroeninger⁴⁵, H. Kroha¹¹³, J. Kroll¹³⁷, J. Kroll¹³³, J. Krstic¹⁶, U. Kruchonak⁷⁷,
 H. Krüger²⁴, N. Krumnack⁷⁶, M.C. Kruse⁴⁷, T. Kubota¹⁰², S. Kuday^{4b}, J.T. Kuechler¹⁷⁹, S. Kuehn³⁵,
 A. Kugel^{59a}, F. Kuger¹⁷⁴, T. Kuhl⁴⁴, V. Kukhtin⁷⁷, R. Kukla⁹⁹, Y. Kulchitsky¹⁰⁵, S. Kuleshov^{144b},
 Y.P. Kulinich¹⁷⁰, M. Kuna⁵⁶, T. Kunigo⁸³, A. Kupco¹³⁷, T. Kupfer⁴⁵, O. Kuprash¹⁵⁸, H. Kurashige⁸⁰,
 L.L. Kurchaninov^{165a}, Y.A. Kurochkin¹⁰⁵, M.G. Kurth^{15d}, E.S. Kuwertz¹⁷³, M. Kuze¹⁶², J. Kvita¹²⁶,
 T. Kwan¹⁰¹, A. La Rosa¹¹³, J.L. La Rosa Navarro^{78d}, L. La Rotonda^{40b,40a}, F. La Ruffa^{40b,40a},
 C. Lacasta¹⁷¹, F. Lacava^{70a,70b}, J. Lacey⁴⁴, D.P.J. Lack⁹⁸, H. Lacker¹⁹, D. Lacour¹³², E. Ladygin⁷⁷,
 R. Lafaye⁵, B. Laforgue¹³², T. Lagouri^{32c}, S. Lai⁵¹, S. Lammers⁶³, W. Lampl⁷, E. Lançon²⁹,
 U. Landgraf⁵⁰, M.P.J. Landon⁹⁰, M.C. Lanfermann⁵², V.S. Lang⁴⁴, J.C. Lange¹⁴, R.J. Langenberg³⁵,

A.J. Lankford¹⁶⁸, F. Lanni²⁹, K. Lantzsch²⁴, A. Lanza^{68a}, A. Lapertosa^{53b,53a}, S. Laplace¹³²,
 J.F. Laporte¹⁴², T. Lari^{66a}, F. Lasagni Manghi^{23b,23a}, M. Lassnig³⁵, T.S. Lau^{61a}, A. Laudrain¹²⁸,
 A.T. Law¹⁴³, P. Laycock⁸⁸, M. Lazzaroni^{66a,66b}, B. Le¹⁰², O. Le Dertz¹³², E. Le Guirriec⁹⁹,
 E.P. Le Quilleuc¹⁴², M. LeBlanc⁷, T. LeCompte⁶, F. Ledroit-Guillon⁵⁶, C.A. Lee²⁹, G.R. Lee^{144a},
 L. Lee⁵⁷, S.C. Lee¹⁵⁵, B. Lefebvre¹⁰¹, M. Lefebvre¹⁷³, F. Legger¹¹², C. Leggett¹⁸, N. Lehmann¹⁷⁹,
 G. Lehmann Miotto³⁵, W.A. Leight⁴⁴, A. Leisos^{159,w}, M.A.L. Leite^{78d}, R. Leitner¹³⁹, D. Lellouch¹⁷⁷,
 B. Lemmer⁵¹, K.J.C. Leney⁹², T. Lenz²⁴, B. Lenzi³⁵, R. Leone⁷, S. Leone^{69a}, C. Leonidopoulos⁴⁸,
 G. Lerner¹⁵³, C. Leroy¹⁰⁷, R. Les¹⁶⁴, A.A.J. Lesage¹⁴², C.G. Lester³¹, M. Levchenko¹³⁴, J. Levêque⁵,
 D. Levin¹⁰³, L.J. Levinson¹⁷⁷, D. Lewis⁹⁰, B. Li¹⁰³, C-Q. Li^{58a}, H. Li^{58b}, L. Li^{58c}, Q. Li^{15d}, Q.Y. Li^{58a},
 S. Li^{58d,58c}, X. Li^{58c}, Y. Li¹⁴⁸, Z. Liang^{15a}, B. Liberti^{71a}, A. Liblong¹⁶⁴, K. Lie^{61c}, S. Liem¹¹⁸,
 A. Limosani¹⁵⁴, C.Y. Lin³¹, K. Lin¹⁰⁴, T.H. Lin⁹⁷, R.A. Linck⁶³, B.E. Lindquist¹⁵², A.L. Lionti⁵²,
 E. Lipeles¹³³, A. Lipniacka¹⁷, M. Lisovyi^{59b}, T.M. Liss^{170,ap}, A. Lister¹⁷², A.M. Litke¹⁴³, J.D. Little⁸,
 B. Liu⁷⁶, B.L. Liu⁶, H.B. Liu²⁹, H. Liu¹⁰³, J.B. Liu^{58a}, J.K.K. Liu¹³¹, K. Liu¹³², M. Liu^{58a}, P. Liu¹⁸,
 Y. Liu^{15a}, Y.L. Liu^{58a}, Y.W. Liu^{58a}, M. Livan^{68a,68b}, A. Lleres⁵⁶, J. Llorente Merino^{15a}, S.L. Lloyd⁹⁰,
 C.Y. Lo^{61b}, F. Lo Sterzo⁴¹, E.M. Lobodzinska⁴⁴, P. Loch⁷, F.K. Loebinger⁹⁸, A. Loesle⁵⁰, K.M. Loew²⁶,
 T. Lohse¹⁹, K. Lohwasser¹⁴⁶, M. Lokajicek¹³⁷, B.A. Long²⁵, J.D. Long¹⁷⁰, R.E. Long⁸⁷, L. Longo^{65a,65b},
 K.A.Looper¹²², J.A. Lopez^{144b}, I. Lopez Paz¹⁴, A. Lopez Solis¹⁴⁶, J. Lorenz¹¹², N. Lorenzo Martinez⁵,
 M. Losada²², P.J. Lösel¹¹², X. Lou⁴⁴, X. Lou^{15a}, A. Lounis¹²⁸, J. Love⁶, P.A. Love⁸⁷,
 J.J. Lozano Bahilo¹⁷¹, H. Lu^{61a}, M. Lu^{58a}, N. Lu¹⁰³, Y.J. Lu⁶², H.J. Lubatti¹⁴⁵, C. Luci^{70a,70b},
 A. Lucotte⁵⁶, C. Luedtke⁵⁰, F. Luehring⁶³, I. Luise¹³², W. Lukas⁷⁴, L. Luminari^{70a}, B. Lund-Jensen¹⁵¹,
 M.S. Lutz¹⁰⁰, P.M. Luzi¹³², D. Lynn²⁹, R. Lysak¹³⁷, E. Lytken⁹⁴, F. Lyu^{15a}, V. Lyubushkin⁷⁷, H. Ma²⁹,
 L.L. Ma^{58b}, Y. Ma^{58b}, G. Maccarrone⁴⁹, A. Macchiolo¹¹³, C.M. Macdonald¹⁴⁶,
 J. Machado Miguens^{133,136b}, D. Madaffari¹⁷¹, R. Madar³⁷, W.F. Mader⁴⁶, A. Madsen⁴⁴, N. Madysa⁴⁶,
 J. Maeda⁸⁰, K. Maekawa¹⁶⁰, S. Maeland¹⁷, T. Maeno²⁹, A.S. Maevskiy¹¹¹, V. Magerl⁵⁰,
 C. Maidantchik^{78b}, T. Maier¹¹², A. Maio^{136a,136b,136d}, O. Majersky^{28a}, S. Majewski¹²⁷, Y. Makida⁷⁹,
 N. Makovec¹²⁸, B. Malaescu¹³², Pa. Malecki⁸², V.P. Maleev¹³⁴, F. Malek⁵⁶, U. Mallik⁷⁵, D. Malon⁶,
 C. Malone³¹, S. Maltezos¹⁰, S. Malyukov³⁵, J. Mamuzic¹⁷¹, G. Mancini⁴⁹, I. Mandic⁸⁹, J. Maneira^{136a},
 L. Manhaes de Andrade Filho^{78a}, J. Manjarres Ramos⁴⁶, K.H. Mankinen⁹⁴, A. Mann¹¹², A. Manousos⁷⁴,
 B. Mansoulie¹⁴², J.D. Mansour^{15a}, M. Mantoani⁵¹, S. Manzoni^{66a,66b}, G. Marceca³⁰, L. March⁵²,
 L. Marchese¹³¹, G. Marchiori¹³², M. Marcisovsky¹³⁷, C.A. Marin Tobon³⁵, M. Marjanovic³⁷,
 D.E. Marley¹⁰³, F. Marroquim^{78b}, Z. Marshall¹⁸, M.U.F Martensson¹⁶⁹, S. Marti-Garcia¹⁷¹,
 C.B. Martin¹²², T.A. Martin¹⁷⁵, V.J. Martin⁴⁸, B. Martin dit Latour¹⁷, M. Martinez^{14,z},
 V.I. Martinez Outschoorn¹⁰⁰, S. Martin-Haugh¹⁴¹, V.S. Martoiu^{27b}, A.C. Martyniuk⁹², A. Marzin³⁵,
 L. Masetti⁹⁷, T. Mashimo¹⁶⁰, R. Mashinistov¹⁰⁸, J. Masik⁹⁸, A.L. Maslennikov^{120b,120a}, L.H. Mason¹⁰²,
 L. Massa^{71a,71b}, P. Mastrandrea⁵, A. Mastroberardino^{40b,40a}, T. Masubuchi¹⁶⁰, P. Mättig¹⁷⁹, J. Maurer^{27b},
 B. Maček⁸⁹, S.J. Maxfield⁸⁸, D.A. Maximov^{120b,120a}, R. Mazini¹⁵⁵, I. Maznas¹⁵⁹, S.M. Mazza¹⁴³,
 N.C. Mc Fadden¹¹⁶, G. Mc Goldrick¹⁶⁴, S.P. Mc Kee¹⁰³, A. McCarn¹⁰³, T.G. McCarthy¹¹³,
 L.I. McClymont⁹², E.F. McDonald¹⁰², J.A. McFayden³⁵, G. Mchedlidze⁵¹, M.A. McKay⁴¹,
 K.D. McLean¹⁷³, S.J. McMahon¹⁴¹, P.C. McNamara¹⁰², C.J. McNicol¹⁷⁵, R.A. McPherson^{173,ad},
 J.E. Mdhluliz^{32c}, Z.A. Meadows¹⁰⁰, S. Meehan¹⁴⁵, T. Megy⁵⁰, S. Mehlhase¹¹², A. Mehta⁸⁸, T. Meideck⁵⁶,
 B. Meirose⁴², D. Melini^{171,h}, B.R. Mellado Garcia^{32c}, J.D. Mellenthin⁵¹, M. Melo^{28a}, F. Meloni²⁰,
 A. Melzer²⁴, S.B. Menary⁹⁸, E.D. Mendes Gouveia^{136a}, L. Meng⁸⁸, X.T. Meng¹⁰³, A. Mengarelli^{23b,23a},
 S. Menke¹¹³, E. Meoni^{40b,40a}, S. Mergelmeyer¹⁹, C. Merlassino²⁰, P. Mermod⁵², L. Merola^{67a,67b},
 C. Meroni^{66a}, F.S. Merritt³⁶, A. Messina^{70a,70b}, J. Metcalfe⁶, A.S. Mete¹⁶⁸, C. Meyer¹³³, J. Meyer¹⁵⁷,
 J-P. Meyer¹⁴², H. Meyer Zu Theenhausen^{59a}, F. Miano¹⁵³, R.P. Middleton¹⁴¹, L. Mijović⁴⁸,
 G. Mikenberg¹⁷⁷, M. Mikestikova¹³⁷, M. Mikuž⁸⁹, M. Milesi¹⁰², A. Milic¹⁶⁴, D.A. Millar⁹⁰,
 D.W. Miller³⁶, A. Milov¹⁷⁷, D.A. Milstead^{43a,43b}, A.A. Minaenko¹⁴⁰, M. Miñano Moya¹⁷¹,

I.A. Minashvili^{156b}, A.I. Mincer¹²¹, B. Mindur^{81a}, M. Mineev⁷⁷, Y. Minegishi¹⁶⁰, Y. Ming¹⁷⁸,
 L.M. Mir¹⁴, A. Mirto^{65a,65b}, K.P. Mistry¹³³, T. Mitani¹⁷⁶, J. Mitrevski¹¹², V.A. Mitsou¹⁷¹, A. Miucci²⁰,
 P.S. Miyagawa¹⁴⁶, A. Mizukami⁷⁹, J.U. Mjörnmark⁹⁴, T. Mkrtchyan¹⁸¹, M. Mlynarikova¹³⁹,
 T. Moa^{43a,43b}, K. Mochizuki¹⁰⁷, P. Mogg⁵⁰, S. Mohapatra³⁸, S. Molander^{43a,43b}, R. Moles-Valls²⁴,
 M.C. Mondragon¹⁰⁴, K. Mönig⁴⁴, J. Monk³⁹, E. Monnier⁹⁹, A. Montalbano¹⁴⁹, J. Montejo Berlingen³⁵,
 F. Monticelli⁸⁶, S. Monzani^{66a}, R.W. Moore³, N. Morange¹²⁸, D. Moreno²², M. Moreno Llácer³⁵,
 P. Morettini^{53b}, M. Morgenstern¹¹⁸, S. Morgenstern³⁵, D. Mori¹⁴⁹, T. Mori¹⁶⁰, M. Morii⁵⁷,
 M. Morinaga¹⁷⁶, V. Morisbak¹³⁰, A.K. Morley³⁵, G. Mornacchi³⁵, A.P. Morris⁹², J.D. Morris⁹⁰,
 L. Morvaj¹⁵², P. Moschovakos¹⁰, M. Mosidze^{156b}, H.J. Moss¹⁴⁶, J. Moss^{150,n}, K. Motohashi¹⁶²,
 R. Mount¹⁵⁰, E. Mountricha³⁵, E.J.W. Moyse¹⁰⁰, S. Muanza⁹⁹, F. Mueller¹¹³, J. Mueller¹³⁵,
 R.S.P. Mueller¹¹², D. Muenstermann⁸⁷, P. Mullen⁵⁵, G.A. Mullier²⁰, F.J. Munoz Sanchez⁹⁸, P. Murin^{28b},
 W.J. Murray^{175,141}, A. Murrone^{66a,66b}, M. Muškinja⁸⁹, C. Mwewa^{32a}, A.G. Myagkov^{140,ak}, J. Myers¹²⁷,
 M. Myska¹³⁸, B.P. Nachman¹⁸, O. Nackenhorst⁴⁵, K. Nagai¹³¹, K. Nagano⁷⁹, Y. Nagasaka⁶⁰,
 K. Nagata¹⁶⁶, M. Nagel⁵⁰, E. Nagy⁹⁹, A.M. Nairz³⁵, Y. Nakahama¹¹⁵, K. Nakamura⁷⁹, T. Nakamura¹⁶⁰,
 I. Nakano¹²³, H. Nanjo¹²⁹, F. Napolitano^{59a}, R.F. Naranjo Garcia⁴⁴, R. Narayan¹¹, D.I. Narrias Villar^{59a},
 I. Naryshkin¹³⁴, T. Naumann⁴⁴, G. Navarro²², R. Nayyar⁷, H.A. Neal¹⁰³, P.Y. Nechaeva¹⁰⁸, T.J. Neep¹⁴²,
 A. Negri^{68a,68b}, M. Negrini^{23b}, S. Nektarijevic¹¹⁷, C. Nellist⁵¹, M.E. Nelson¹³¹, S. Nemecek¹³⁷,
 P. Nemethy¹²¹, M. Nesi^{35,f}, M.S. Neubauer¹⁷⁰, M. Neumann¹⁷⁹, P.R. Newman²¹, T.Y. Ng^{61c}, Y.S. Ng¹⁹,
 H.D.N. Nguyen⁹⁹, T. Nguyen Manh¹⁰⁷, E. Nibigira³⁷, R.B. Nickerson¹³¹, R. Nicolaïdou¹⁴²,
 J. Nielsen¹⁴³, N. Nikiforou¹¹, V. Nikolaenko^{140,ak}, I. Nikolic-Audit¹³², K. Nikolopoulos²¹, P. Nilsson²⁹,
 Y. Ninomiya⁷⁹, A. Nisati^{70a}, N. Nishu^{58c}, R. Nisius¹¹³, I. Nitsche⁴⁵, T. Nitta¹⁷⁶, T. Nobe¹⁶⁰,
 Y. Noguchi⁸³, M. Nomachi¹²⁹, I. Nomidis¹³², M.A. Nomura²⁹, T. Nooney⁹⁰, M. Nordberg³⁵,
 N. Norjoharuddeen¹³¹, T. Novak⁸⁹, O. Novgorodova⁴⁶, R. Novotny¹³⁸, M. Nozaki⁷⁹, L. Nozka¹²⁶,
 K. Ntekas¹⁶⁸, E. Nurse⁹², F. Nuti¹⁰², F.G. Oakham^{33,as}, H. Oberlack¹¹³, T. Obermann²⁴, J. Ocariz¹³²,
 A. Ochi⁸⁰, I. Ochoa³⁸, J.P. Ochoa-Ricoux^{144a}, K. O'Connor²⁶, S. Oda⁸⁵, S. Odaka⁷⁹, A. Oh⁹⁸, S.H. Oh⁴⁷,
 C.C. Ohm¹⁵¹, H. Oide^{53b,53a}, H. Okawa¹⁶⁶, Y. Okazaki⁸³, Y. Okumura¹⁶⁰, T. Okuyama⁷⁹, A. Olariu^{27b},
 L.F. Oleiro Seabra^{136a}, S.A. Olivares Pino^{144a}, D. Oliveira Damazio²⁹, J.L. Oliver¹, M.J.R. Olsson³⁶,
 A. Olszewski⁸², J. Olszowska⁸², D.C. O'Neil¹⁴⁹, A. Onofre^{136a,136e}, K. Onogi¹¹⁵, P.U.E. Onyisi¹¹,
 H. Oppen¹³⁰, M.J. Oreglia³⁶, Y. Oren¹⁵⁸, D. Orestano^{72a,72b}, E.C. Orgill⁹⁸, N. Orlando^{61b},
 A.A. O'Rourke⁴⁴, R.S. Orr¹⁶⁴, B. Osculati^{53b,53a,*}, V. O'Shea⁵⁵, R. Ospanov^{58a}, G. Otero y Garzon³⁰,
 H. Otomo⁸⁵, M. Ouchrif^{34d}, F. Ould-Saada¹³⁰, A. Ouraou¹⁴², Q. Ouyang^{15a}, M. Owen⁵⁵, R.E. Owen²¹,
 V.E. Ozcan^{12c}, N. Ozturk⁸, J. Pacalt¹²⁶, H.A. Pacey³¹, K. Pachal¹⁴⁹, A. Pacheco Pages¹⁴,
 L. Pacheco Rodriguez¹⁴², C. Padilla Aranda¹⁴, S. Pagan Griso¹⁸, M. Paganini¹⁸⁰, G. Palacino⁶³,
 S. Palazzo^{40b,40a}, S. Palestini³⁵, M. Palka^{81b}, D. Pallin³⁷, I. Panagoulias¹⁰, C.E. Pandini³⁵,
 J.G. Panduro Vazquez⁹¹, P. Pani³⁵, G. Panizzo^{64a,64c}, L. Paolozzi⁵², T.D. Papadopoulou¹⁰,
 K. Papageorgiou^{9,j}, A. Paramonov⁶, D. Paredes Hernandez^{61b}, S.R. Paredes Saenz¹³¹, B. Parida^{58c},
 A.J. Parker⁸⁷, K.A. Parker⁴⁴, M.A. Parker³¹, F. Parodi^{53b,53a}, J.A. Parsons³⁸, U. Parzefal⁵⁰,
 V.R. Pascuzzi¹⁶⁴, J.M.P. Pasner¹⁴³, E. Pasqualucci^{70a}, S. Passaggio^{53b}, F. Pastore⁹¹, P. Pasuwani^{43a,43b},
 S. Pataria⁹⁷, J.R. Pater⁹⁸, A. Pathak^{178,k}, T. Pauly³⁵, B. Pearson¹¹³, M. Pedersen¹³⁰, L. Pedraza Diaz¹¹⁷,
 S. Pedraza Lopez¹⁷¹, R. Pedro^{136a,136b}, S.V. Peleganchuk^{120b,120a}, O. Penc¹³⁷, C. Peng^{15d}, H. Peng^{58a},
 B.S. Peralva^{78a}, M.M. Perego¹⁴², A.P. Pereira Peixoto^{136a}, D.V. Perepelitsa²⁹, F. Peri¹⁹, L. Perini^{66a,66b},
 H. Pernegger³⁵, S. Perrella^{67a,67b}, V.D. Peshekhonov^{77,*}, K. Peters⁴⁴, R.F.Y. Peters⁹⁸, B.A. Petersen³⁵,
 T.C. Petersen³⁹, E. Petit⁵⁶, A. Petridis¹, C. Petridou¹⁵⁹, P. Petroff¹²⁸, E. Petrolo^{70a}, M. Petrov¹³¹,
 F. Petrucci^{72a,72b}, M. Pettee¹⁸⁰, N.E. Pettersson¹⁰⁰, A. Peyaud¹⁴², R. Pezoa^{144b}, T. Pham¹⁰²,
 F.H. Phillips¹⁰⁴, P.W. Phillips¹⁴¹, G. Piacquadio¹⁵², E. Pianori¹⁸, A. Picazio¹⁰⁰, M.A. Pickering¹³¹,
 R. Piegai³⁰, J.E. Pilcher³⁶, A.D. Pilkington⁹⁸, M. Pinamonti^{71a,71b}, J.L. Pinfold³, M. Pitt¹⁷⁷,
 M-A. Pleier²⁹, V. Pleskot¹³⁹, E. Plotnikova⁷⁷, D. Pluth⁷⁶, P. Podberezko^{120b,120a}, R. Poettgen⁹⁴,

R. Poggi⁵², L. Poggioli¹²⁸, I. Pogrebnyak¹⁰⁴, D. Pohl²⁴, I. Pokharel⁵¹, G. Polesello^{68a}, A. Poley⁴⁴,
 A. Policicchio^{40b,40a}, R. Polifka³⁵, A. Polini^{23b}, C.S. Pollard⁴⁴, V. Polychronakos²⁹, D. Ponomarenko¹¹⁰,
 L. Pontecorvo^{70a}, G.A. Popeneciu^{27d}, D.M. Portillo Quintero¹³², S. Pospisil¹³⁸, K. Potamianos⁴⁴,
 I.N. Potrap⁷⁷, C.J. Potter³¹, H. Potti¹¹, T. Poulsen⁹⁴, J. Poveda³⁵, T.D. Powell¹⁴⁶,
 M.E. Pozo Astigarraga³⁵, P. Pralavorio⁹⁹, S. Prell⁷⁶, D. Price⁹⁸, M. Primavera^{65a}, S. Prince¹⁰¹,
 N. Proklova¹¹⁰, K. Prokofiev^{61c}, F. Prokoshin^{144b}, S. Protopopescu²⁹, J. Proudfoot⁶, M. Przybycien^{81a},
 A. Puri¹⁷⁰, P. Puzo¹²⁸, J. Qian¹⁰³, Y. Qin⁹⁸, A. Quadri⁵¹, M. Queitsch-Maitland⁴⁴, A. Qureshi¹,
 P. Rados¹⁰², F. Ragusa^{66a,66b}, G. Rahal⁹⁵, J.A. Raine⁹⁸, S. Rajagopalan²⁹, A. Ramirez Morales⁹⁰,
 T. Rashid¹²⁸, S. Raspopov⁵, M.G. Ratti^{66a,66b}, D.M. Rauch⁴⁴, F. Rauscher¹¹², S. Rave⁹⁷, B. Ravina¹⁴⁶,
 I. Ravinovich¹⁷⁷, J.H. Rawling⁹⁸, M. Raymond³⁵, A.L. Read¹³⁰, N.P. Readoff⁵⁶, M. Reale^{65a,65b},
 D.M. Rebuzzi^{68a,68b}, A. Redelbach¹⁷⁴, G. Redlinger²⁹, R. Reece¹⁴³, R.G. Reed^{32c}, K. Reeves⁴²,
 L. Rehnisch¹⁹, J. Reichert¹³³, A. Reiss⁹⁷, C. Rembser³⁵, H. Ren^{15d}, M. Rescigno^{70a}, S. Resconi^{66a},
 E.D. Ressegue¹³³, S. Rettie¹⁷², E. Reynolds²¹, O.L. Rezanova^{120b,120a}, P. Reznicek¹³⁹, R. Richter¹¹³,
 S. Richter⁹², E. Richter-Was^{81b}, O. Ricken²⁴, M. Ridel¹³², P. Rieck¹¹³, C.J. Riegel¹⁷⁹, O. Rifki⁴⁴,
 M. Rijssenbeek¹⁵², A. Rimoldi^{68a,68b}, M. Rimoldi²⁰, L. Rinaldi^{23b}, G. Ripellino¹⁵¹, B. Ristic⁸⁷,
 E. Ritsch³⁵, I. Riu¹⁴, J.C. Rivera Vergara^{144a}, F. Rizatdinova¹²⁵, E. Rizvi⁹⁰, C. Rizzi¹⁴, R.T. Roberts⁹⁸,
 S.H. Robertson^{101,ad}, A. Robichaud-Veronneau¹⁰¹, D. Robinson³¹, J.E.M. Robinson⁴⁴, A. Robson⁵⁵,
 E. Rocco⁹⁷, C. Roda^{69a,69b}, Y. Rodina⁹⁹, S. Rodriguez Bosca¹⁷¹, A. Rodriguez Perez¹⁴,
 D. Rodriguez Rodriguez¹⁷¹, A.M. Rodríguez Vera^{165b}, S. Roe³⁵, C.S. Rogan⁵⁷, O. Røhne¹³⁰,
 R. Röhrlig¹¹³, C.P.A. Roland⁶³, J. Roloff⁵⁷, A. Romaniouk¹¹⁰, M. Romano^{23b,23a}, N. Rompotis⁸⁸,
 M. Ronzani¹²¹, L. Roos¹³², S. Rosati^{70a}, K. Rosbach⁵⁰, P. Rose¹⁴³, N-A. Rosien⁵¹, E. Rossi^{67a,67b},
 L.P. Rossi^{53b}, L. Rossini^{66a,66b}, J.H.N. Rosten³¹, R. Rosten¹⁴, M. Rotaru^{27b}, J. Rothberg¹⁴⁵,
 D. Rousseau¹²⁸, D. Roy^{32c}, A. Rozanov⁹⁹, Y. Rozen¹⁵⁷, X. Ruan^{32c}, F. Rubbo¹⁵⁰, F. Rühr⁵⁰,
 A. Ruiz-Martinez³³, Z. Rurikova⁵⁰, N.A. Rusakovich⁷⁷, H.L. Russell¹⁰¹, J.P. Rutherford⁷,
 N. Ruthmann³⁵, E.M. Rüttinger^{44,1}, Y.F. Ryabov¹³⁴, M. Rybar¹⁷⁰, G. Rybkin¹²⁸, S. Ryu⁶, A. Ryzhov¹⁴⁰,
 G.F. Rzechorz⁵¹, P. Sabatini⁵¹, G. Sabato¹¹⁸, S. Sacerdoti¹²⁸, H.F-W. Sadrozinski¹⁴³, R. Sadykov⁷⁷,
 F. Safai Tehrani^{70a}, P. Saha¹¹⁹, M. Sahinsoy^{59a}, A. Sahu¹⁷⁹, M. Saimpert⁴⁴, M. Saito¹⁶⁰, T. Saito¹⁶⁰,
 H. Sakamoto¹⁶⁰, A. Sakharov^{121,aj}, D. Salamani⁵², G. Salamanna^{72a,72b}, J.E. Salazar Loyola^{144b},
 D. Salek¹¹⁸, P.H. Sales De Bruin¹⁶⁹, D. Salihagic¹¹³, A. Salnikov¹⁵⁰, J. Salt¹⁷¹, D. Salvatore^{40b,40a},
 F. Salvatore¹⁵³, A. Salvucci^{61a,61b,61c}, A. Salzburger³⁵, D. Sammel⁵⁰, D. Sampsonidis¹⁵⁹,
 D. Sampsonidou¹⁵⁹, J. Sánchez¹⁷¹, A. Sanchez Pineda^{64a,64c}, H. Sandaker¹³⁰, C.O. Sander⁴⁴,
 M. Sandhoff¹⁷⁹, C. Sandoval²², D.P.C. Sankey¹⁴¹, M. Sannino^{53b,53a}, Y. Sano¹¹⁵, A. Sansoni⁴⁹,
 C. Santoni³⁷, H. Santos^{136a}, I. Santoyo Castillo¹⁵³, A. Sapronov⁷⁷, J.G. Saraiva^{136a,136d}, O. Sasaki⁷⁹,
 K. Sato¹⁶⁶, E. Sauvan⁵, P. Savard^{164,as}, N. Savic¹¹³, R. Sawada¹⁶⁰, C. Sawyer¹⁴¹, L. Sawyer^{93,ai},
 C. Sbarra^{23b}, A. Sbrizzi^{23b,23a}, T. Scanlon⁹², J. Schaarschmidt¹⁴⁵, P. Schacht¹¹³, B.M. Schachtner¹¹²,
 D. Schaefer³⁶, L. Schaefer¹³³, J. Schaeffer⁹⁷, S. Schaepe³⁵, U. Schäfer⁹⁷, A.C. Schaffer¹²⁸, D. Schaile¹¹²,
 R.D. Schamberger¹⁵², N. Scharmberg⁹⁸, V.A. Schegelsky¹³⁴, D. Scheirich¹³⁹, F. Schenck¹⁹,
 M. Schernau¹⁶⁸, C. Schiavi^{53b,53a}, S. Schier¹⁴³, L.K. Schildgen²⁴, Z.M. Schillaci²⁶, E.J. Schioppa³⁵,
 M. Schioppa^{40b,40a}, K.E. Schleicher⁵⁰, S. Schlenker³⁵, K.R. Schmidt-Sommerfeld¹¹³, K. Schmieden³⁵,
 C. Schmitt⁹⁷, S. Schmitt⁴⁴, S. Schmitz⁹⁷, U. Schnoor⁵⁰, L. Schoeffel¹⁴², A. Schoening^{59b}, E. Schopf²⁴,
 M. Schott⁹⁷, J.F.P. Schouwenberg¹¹⁷, J. Schovancova³⁵, S. Schramm⁵², A. Schulte⁹⁷,
 H-C. Schultz-Coulon^{59a}, M. Schumacher⁵⁰, B.A. Schumm¹⁴³, Ph. Schune¹⁴², A. Schwartzman¹⁵⁰,
 T.A. Schwarz¹⁰³, H. Schweiger⁹⁸, Ph. Schwemling¹⁴², R. Schwienhorst¹⁰⁴, A. Sciandra²⁴, G. Sciolla²⁶,
 M. Scornajenghi^{40b,40a}, F. Scuri^{69a}, F. Scutti¹⁰², L.M. Scyboz¹¹³, J. Searcy¹⁰³, C.D. Sebastiani^{70a,70b},
 P. Seema²⁴, S.C. Seidel¹¹⁶, A. Seiden¹⁴³, T. Seiss³⁶, J.M. Seixas^{78b}, G. Sekhniaidze^{67a}, K. Sekhon¹⁰³,
 S.J. Sekula⁴¹, N. Semprini-Cesari^{23b,23a}, S. Sen⁴⁷, S. Senkin³⁷, C. Serfon¹³⁰, L. Serin¹²⁸, L. Serkin^{64a,64b},
 M. Sessa^{72a,72b}, H. Severini¹²⁴, F. Sforza¹⁶⁷, A. Sfyrla⁵², E. Shabalina⁵¹, J.D. Shahinian¹⁴³,

N.W. Shaikh^{43a,43b}, L.Y. Shan^{15a}, R. Shang¹⁷⁰, J.T. Shank²⁵, M. Shapiro¹⁸, A.S. Sharma¹, A. Sharma¹³¹, P.B. Shatalov¹⁰⁹, K. Shaw¹⁵³, S.M. Shaw⁹⁸, A. Shcherbakova¹³⁴, Y. Shen¹²⁴, N. Sherafati³³, A.D. Sherman²⁵, P. Sherwood⁹², L. Shi^{155,ao}, S. Shimizu⁸⁰, C.O. Shimmin¹⁸⁰, M. Shimojima¹¹⁴, I.P.J. Shipsey¹³¹, S. Shirabe⁸⁵, M. Shiyakova⁷⁷, J. Shlomi¹⁷⁷, A. Shmeleva¹⁰⁸, D. Shoaleh Saadi¹⁰⁷, M.J. Shochet³⁶, S. Shojaii¹⁰², D.R. Shope¹²⁴, S. Shrestha¹²², E. Shulga¹¹⁰, P. Sicho¹³⁷, A.M. Sickles¹⁷⁰, P.E. Sidebo¹⁵¹, E. Sideras Haddad^{32c}, O. Sidiropoulou¹⁷⁴, A. Sidoti^{23b,23a}, F. Siegert⁴⁶, Dj. Sijacki¹⁶, J. Silva^{136a}, M. Silva Jr.¹⁷⁸, M.V. Silva Oliveira^{78a}, S.B. Silverstein^{43a}, L. Simic⁷⁷, S. Simion¹²⁸, E. Simioni⁹⁷, M. Simon⁹⁷, P. Sinervo¹⁶⁴, N.B. Sinev¹²⁷, M. Sioli^{23b,23a}, G. Siragusa¹⁷⁴, I. Siral¹⁰³, S.Yu. Sivoklokov¹¹¹, J. Sjölin^{43a,43b}, M.B. Skinner⁸⁷, P. Skubic¹²⁴, M. Slater²¹, T. Slavicek¹³⁸, M. Slawinska⁸², K. Sliwa¹⁶⁷, R. Slovak¹³⁹, V. Smakhtin¹⁷⁷, B.H. Smart⁵, J. Smiesko^{28a}, N. Smirnov¹¹⁰, S.Yu. Smirnov¹¹⁰, Y. Smirnov¹¹⁰, L.N. Smirnova¹¹¹, O. Smirnova⁹⁴, J.W. Smith⁵¹, M.N.K. Smith³⁸, R.W. Smith³⁸, M. Smizanska⁸⁷, K. Smolek¹³⁸, A.A. Snesarev¹⁰⁸, I.M. Snyder¹²⁷, S. Snyder²⁹, R. Sobie^{173,ad}, A.M. Soffa¹⁶⁸, A. Soffer¹⁵⁸, A. Søgaard⁴⁸, D.A. Soh¹⁵⁵, G. Sokhrannyi⁸⁹, C.A. Solans Sanchez³⁵, M. Solar¹³⁸, E.Yu. Soldatov¹¹⁰, U. Soldevila¹⁷¹, A.A. Solodkov¹⁴⁰, A. Soloshenko⁷⁷, O.V. Solovyanov¹⁴⁰, V. Solovyev¹³⁴, P. Sommer¹⁴⁶, H. Son¹⁶⁷, W. Song¹⁴¹, A. Sopczak¹³⁸, F. Sopkova^{28b}, D. Sosa^{59b}, C.L. Sotropoulou^{69a,69b}, S. Sottocornola^{68a,68b}, R. Soualah^{64a,64c,i}, A.M. Soukharev^{120b,120a}, D. South⁴⁴, B.C. Sowden⁹¹, S. Spagnolo^{65a,65b}, M. Spalla¹¹³, M. Spangenberg¹⁷⁵, F. Spanò⁹¹, D. Sperlich¹⁹, F. Spettel¹¹³, T.M. Spieker^{59a}, R. Spighi^{23b}, G. Spigo³⁵, L.A. Spiller¹⁰², D.P. Spiteri⁵⁵, M. Spousta¹³⁹, A. Stabile^{66a,66b}, R. Stamen^{59a}, S. Stamm¹⁹, E. Stancka⁸², R.W. Stanek⁶, C. Stanescu^{72a}, B. Stanislaus¹³¹, M.M. Stanitzki⁴⁴, B.S. Stapf¹¹⁸, S. Stapnes¹³⁰, E.A. Starchenko¹⁴⁰, G.H. Stark³⁶, J. Stark⁵⁶, S.H Stark³⁹, P. Staroba¹³⁷, P. Starovoitov^{59a}, S. Stärz³⁵, R. Staszewski⁸², M. Stegler⁴⁴, P. Steinberg²⁹, B. Stelzer¹⁴⁹, H.J. Stelzer³⁵, O. Stelzer-Chilton^{165a}, H. Stenzel⁵⁴, T.J. Stevenson⁹⁰, G.A. Stewart⁵⁵, M.C. Stockton¹²⁷, G. Stoica^{27b}, P. Stolte⁵¹, S. Stonjek¹¹³, A. Straessner⁴⁶, J. Strandberg¹⁵¹, S. Strandberg^{43a,43b}, M. Strauss¹²⁴, P. Strizenec^{28b}, R. Ströhmer¹⁷⁴, D.M. Strom¹²⁷, R. Stroynowski⁴¹, A. Strubig⁴⁸, S.A. Stucci²⁹, B. Stugu¹⁷, J. Stupak¹²⁴, N.A. Styles⁴⁴, D. Su¹⁵⁰, J. Su¹³⁵, S. Suchek^{59a}, Y. Sugaya¹²⁹, M. Suk¹³⁸, V.V. Sulin¹⁰⁸, D.M.S. Sultan⁵², S. Sultansoy^{4c}, T. Sumida⁸³, S. Sun¹⁰³, X. Sun³, K. Suruliz¹⁵³, C.J.E. Suster¹⁵⁴, M.R. Sutton¹⁵³, S. Suzuki⁷⁹, M. Svatos¹³⁷, M. Swiatlowski³⁶, S.P. Swift², A. Sydorenko⁹⁷, I. Sykora^{28a}, T. Sykora¹³⁹, D. Ta⁹⁷, K. Tackmann^{44,aa}, J. Taenzer¹⁵⁸, A. Taffard¹⁶⁸, R. Tafirout^{165a}, E. Tahirovic⁹⁰, N. Taiblum¹⁵⁸, H. Takai²⁹, R. Takashima⁸⁴, E.H. Takasugi¹¹³, K. Takeda⁸⁰, T. Takeshita¹⁴⁷, Y. Takubo⁷⁹, M. Talby⁹⁹, A.A. Talyshev^{120b,120a}, J. Tanaka¹⁶⁰, M. Tanaka¹⁶², R. Tanaka¹²⁸, R. Tanioka⁸⁰, B.B. Tannenwald¹²², S. Tapia Araya^{144b}, S. Tapprogge⁹⁷, A. Tarek Abouelfadl Mohamed¹³², S. Tarem¹⁵⁷, G. Tarna^{27b,e}, G.F. Tartarelli^{66a}, P. Tas¹³⁹, M. Tasevsky¹³⁷, T. Tashiro⁸³, E. Tassi^{40b,40a}, A. Tavares Delgado^{136a,136b}, Y. Tayalati^{34e}, A.C. Taylor¹¹⁶, A.J. Taylor⁴⁸, G.N. Taylor¹⁰², P.T.E. Taylor¹⁰², W. Taylor^{165b}, A.S. Tee⁸⁷, P. Teixeira-Dias⁹¹, H. Ten Kate³⁵, P.K. Teng¹⁵⁵, J.J. Teoh¹²⁹, F. Tepel¹⁷⁹, S. Terada⁷⁹, K. Terashi¹⁶⁰, J. Terron⁹⁶, S. Terzo¹⁴, M. Testa⁴⁹, R.J. Teuscher^{164,ad}, S.J. Thais¹⁸⁰, T. Theveneaux-Pelzer⁴⁴, F. Thiele³⁹, J.P. Thomas²¹, A.S. Thompson⁵⁵, P.D. Thompson²¹, L.A. Thomsen¹⁸⁰, E. Thomson¹³³, Y. Tian³⁸, R.E. Ticse Torres⁵¹, V.O. Tikhomirov^{108,al}, Yu.A. Tikhonov^{120b,120a}, S. Timoshenko¹¹⁰, P. Tipton¹⁸⁰, S. Tisserant⁹⁹, K. Todome¹⁶², S. Todorova-Nova⁵, S. Todt⁴⁶, J. Tojo⁸⁵, S. Tokár^{28a}, K. Tokushuku⁷⁹, E. Tolley¹²², K.G. Tomiwa^{32c}, M. Tomoto¹¹⁵, L. Tompkins¹⁵⁰, K. Toms¹¹⁶, B. Tong⁵⁷, P. Tornambe⁵⁰, E. Torrence¹²⁷, H. Torres⁴⁶, E. Torró Pastor¹⁴⁵, C. Toscirci¹³¹, J. Toth^{99,ac}, F. Touchard⁹⁹, D.R. Tovey¹⁴⁶, C.J. Treado¹²¹, T. Trefzger¹⁷⁴, F. Tresoldi¹⁵³, A. Tricoli²⁹, I.M. Trigger^{165a}, S. Trincaz-Duvoid¹³², M.F. Tripiana¹⁴, W. Trischuk¹⁶⁴, B. Trocmé⁵⁶, A. Trofymov¹²⁸, C. Troncon^{66a}, M. Trovatelli¹⁷³, F. Trovato¹⁵³, L. Truong^{32b}, M. Trzebinski⁸², A. Trzupek⁸², F. Tsai⁴⁴, J.C.-L. Tseng¹³¹, P.V. Tsiareshka¹⁰⁵, N. Tsirintanis⁹, V. Tsiskaridze¹⁵², E.G. Tskhadadze^{156a}, I.I. Tsukerman¹⁰⁹, V. Tsulaia¹⁸, S. Tsuno⁷⁹, D. Tsybychev¹⁵², Y. Tu^{61b}, A. Tudorache^{27b}, V. Tudorache^{27b}, T.T. Tulbure^{27a}, A.N. Tuna⁵⁷, S. Turchikhin⁷⁷, D. Turgeman¹⁷⁷, I. Turk Cakir^{4b,u}, R. Turra^{66a}, P.M. Tuts³⁸, E. Tzovara⁹⁷,

G. Ucchielli^{23b,23a}, I. Ueda⁷⁹, M. Ughetto^{43a,43b}, F. Ukegawa¹⁶⁶, G. Unal³⁵, A. Undrus²⁹, G. Unel¹⁶⁸,
 F.C. Ungaro¹⁰², Y. Unno⁷⁹, K. Uno¹⁶⁰, J. Urban^{28b}, P. Urquijo¹⁰², P. Urrejola⁹⁷, G. Usai⁸, J. Usui⁷⁹,
 L. Vacavant⁹⁹, V. Vacek¹³⁸, B. Vachon¹⁰¹, K.O.H. Vadla¹³⁰, A. Vaidya⁹², C. Valderanis¹¹²,
 E. Valdes Santurio^{43a,43b}, M. Valente⁵², S. Valentinetto^{23b,23a}, A. Valero¹⁷¹, L. Valéry⁴⁴, R.A. Vallance²¹,
 A. Vallier⁵, J.A. Valls Ferrer¹⁷¹, T.R. Van Daalen¹⁴, W. Van Den Wollenberg¹¹⁸, H. Van der Graaf¹¹⁸,
 P. Van Gemmeren⁶, J. Van Nieuwkoop¹⁴⁹, I. Van Vulpen¹¹⁸, M.C. van Woerden¹¹⁸, M. Vanadia^{71a,71b},
 W. Vandelli³⁵, A. Vaniachine¹⁶³, P. Vankov¹¹⁸, R. Vari^{70a}, E.W. Varnes⁷, C. Varni^{53b,53a}, T. Varol⁴¹,
 D. Varouchas¹²⁸, K.E. Varvell¹⁵⁴, G.A. Vasquez^{144b}, J.G. Vasquez¹⁸⁰, F. Vazeille³⁷,
 D. Vazquez Furelos¹⁴, T. Vazquez Schroeder¹⁰¹, J. Veatch⁵¹, V. Vecchio^{72a,72b}, L.M. Veloce¹⁶⁴,
 F. Veloso^{136a,136c}, S. Veneziano^{70a}, A. Ventura^{65a,65b}, M. Venturi¹⁷³, N. Venturi³⁵, V. Vercesi^{68a},
 M. Verducci^{72a,72b}, C.M. Vergel Infante⁷⁶, W. Verkerke¹¹⁸, A.T. Vermeulen¹¹⁸, J.C. Vermeulen¹¹⁸,
 M.C. Vetterli^{149,as}, N. Viaux Maira^{144b}, O. Viazlo⁹⁴, I. Vichou^{170,*}, T. Vickey¹⁴⁶, O.E. Vickey Boeriu¹⁴⁶,
 G.H.A. Viehhauser¹³¹, S. Viel¹⁸, L. Vigani¹³¹, M. Villa^{23b,23a}, M. Villaplana Perez^{66a,66b}, E. Vilucchi⁴⁹,
 M.G. Vincter³³, V.B. Vinogradov⁷⁷, A. Vishwakarma⁴⁴, C. Vittori^{23b,23a}, I. Vivarelli¹⁵³, S. Vlachos¹⁰,
 M. Vogel¹⁷⁹, P. Vokac¹³⁸, G. Volpi¹⁴, S.E. Von Buddenbrock^{32c}, E. Von Toerne²⁴, V. Vorobel¹³⁹,
 K. Vorobev¹¹⁰, M. Vos¹⁷¹, J.H. Vossebeld⁸⁸, N. Vranjes¹⁶, M. Vranjes Milosavljevic¹⁶, V. Vrba¹³⁸,
 M. Vreeswijk¹¹⁸, T. Šfiligoj⁸⁹, R. Vuillermet³⁵, I. Vukotic³⁶, T. Ženiš^{28a}, L. Živković¹⁶, P. Wagner²⁴,
 W. Wagner¹⁷⁹, J. Wagner-Kuhr¹¹², H. Wahlberg⁸⁶, S. Wahrmund⁴⁶, K. Wakamiya⁸⁰, V.M. Walbrecht¹¹³,
 J. Walder⁸⁷, R. Walker¹¹², W. Walkowiak¹⁴⁸, V. Wallangen^{43a,43b}, A.M. Wang⁵⁷, C. Wang^{58b,e},
 F. Wang¹⁷⁸, H. Wang¹⁸, H. Wang³, J. Wang¹⁵⁴, J. Wang^{59b}, P. Wang⁴¹, Q. Wang¹²⁴, R.-J. Wang¹³²,
 R. Wang^{58a}, R. Wang⁶, S.M. Wang¹⁵⁵, W.T. Wang^{58a}, W. Wang^{155,p}, W.X. Wang^{58a,ae}, Y. Wang^{58a},
 Z. Wang^{58c}, C. Wanotayaroj⁴⁴, A. Warburton¹⁰¹, C.P. Ward³¹, D.R. Wardrope⁹², A. Washbrook⁴⁸,
 P.M. Watkins²¹, A.T. Watson²¹, M.F. Watson²¹, G. Watts¹⁴⁵, S. Watts⁹⁸, B.M. Waugh⁹², A.F. Webb¹¹,
 S. Webb⁹⁷, C. Weber¹⁸⁰, M.S. Weber²⁰, S.A. Weber³³, S.M. Weber^{59a}, J.S. Webster⁶, A.R. Weidberg¹³¹,
 B. Weinert⁶³, J. Weingarten⁵¹, M. Weirich⁹⁷, C. Weiser⁵⁰, P.S. Wells³⁵, T. Wenaus²⁹, T. Wengler³⁵,
 S. Wenig³⁵, N. Wermes²⁴, M.D. Werner⁷⁶, P. Werner³⁵, M. Wessels^{59a}, T.D. Weston²⁰, K. Whalen¹²⁷,
 N.L. Whallon¹⁴⁵, A.M. Wharton⁸⁷, A.S. White¹⁰³, A. White⁸, M.J. White¹, R. White^{144b},
 D. Whiteson¹⁶⁸, B.W. Whitmore⁸⁷, F.J. Wicksens¹⁴¹, W. Wiedenmann¹⁷⁸, M. Wielers¹⁴¹,
 C. Wiglesworth³⁹, L.A.M. Wiik-Fuchs⁵⁰, A. Wildauer¹¹³, F. Wilk⁹⁸, H.G. Wilkens³⁵, L.J. Wilkins⁹¹,
 H.H. Williams¹³³, S. Williams³¹, C. Willis¹⁰⁴, S. Willocq¹⁰⁰, J.A. Wilson²¹, I. Wingerter-Seez⁵,
 E. Winkels¹⁵³, F. Winklmeier¹²⁷, O.J. Winston¹⁵³, B.T. Winter²⁴, M. Wittgen¹⁵⁰, M. Wobisch⁹³,
 A. Wolf⁹⁷, T.M.H. Wolf¹¹⁸, R. Wolff⁹⁹, M.W. Wolter⁸², H. Wolters^{136a,136c}, V.W.S. Wong¹⁷²,
 N.L. Woods¹⁴³, S.D. Worm²¹, B.K. Wosiek⁸², K.W. Woźniak⁸², K. Wraight⁵⁵, M. Wu³⁶, S.L. Wu¹⁷⁸,
 X. Wu⁵², Y. Wu^{58a}, T.R. Wyatt⁹⁸, B.M. Wynne⁴⁸, S. Xella³⁹, Z. Xi¹⁰³, L. Xia¹⁷⁵, D. Xu^{15a}, H. Xu^{58a},
 L. Xu²⁹, T. Xu¹⁴², W. Xu¹⁰³, B. Yabsley¹⁵⁴, S. Yacoob^{32a}, K. Yajima¹²⁹, D.P. Yallup⁹², D. Yamaguchi¹⁶²,
 Y. Yamaguchi¹⁶², A. Yamamoto⁷⁹, T. Yamanaka¹⁶⁰, F. Yamane⁸⁰, M. Yamatani¹⁶⁰, T. Yamazaki¹⁶⁰,
 Y. Yamazaki⁸⁰, Z. Yan²⁵, H.J. Yang^{58c,58d}, H.T. Yang¹⁸, S. Yang⁷⁵, Y. Yang¹⁶⁰, Z. Yang¹⁷, W-M. Yao¹⁸,
 Y.C. Yap⁴⁴, Y. Yasu⁷⁹, E. Yatsenko^{58c,58d}, J. Ye⁴¹, S. Ye²⁹, I. Yeletskikh⁷⁷, E. Yigitbasi²⁵, E. Yildirim⁹⁷,
 K. Yorita¹⁷⁶, K. Yoshihara¹³³, C.J.S. Young³⁵, C. Young¹⁵⁰, J. Yu⁸, J. Yu⁷⁶, X. Yue^{59a}, S.P.Y. Yuen²⁴,
 I. Yusuff^{31,a}, B. Zabinski⁸², G. Zacharis¹⁰, E. Zaffaroni⁵², R. Zaidan¹⁴, A.M. Zaitsev^{140,ak},
 N. Zakharchuk⁴⁴, J. Zalieckas¹⁷, S. Zambito⁵⁷, D. Zanzi³⁵, D.R. Zaripovas⁵⁵, S.V. Zeißner⁴⁵,
 C. Zeitnitz¹⁷⁹, G. Zemaityte¹³¹, J.C. Zeng¹⁷⁰, Q. Zeng¹⁵⁰, O. Zenin¹⁴⁰, D. Zerwas¹²⁸, M. Zgubič¹³¹,
 D.F. Zhang^{58b}, D. Zhang¹⁰³, F. Zhang¹⁷⁸, G. Zhang^{58a,ae}, H. Zhang^{15c}, J. Zhang⁶, L. Zhang⁵⁰,
 L. Zhang^{58a}, M. Zhang¹⁷⁰, P. Zhang^{15c}, R. Zhang^{58a,e}, R. Zhang²⁴, X. Zhang^{58b}, Y. Zhang^{15d},
 Z. Zhang¹²⁸, X. Zhao⁴¹, Y. Zhao^{58b,128,ah}, Z. Zhao^{58a}, A. Zhemchugov⁷⁷, B. Zhou¹⁰³, C. Zhou¹⁷⁸,
 L. Zhou⁴¹, M.S. Zhou^{15d}, M. Zhou¹⁵², N. Zhou^{58c}, Y. Zhou⁷, C.G. Zhu^{58b}, H.L. Zhu^{58a}, H. Zhu^{15a},
 J. Zhu¹⁰³, Y. Zhu^{58a}, X. Zhuang^{15a}, K. Zhukov¹⁰⁸, V. Zhulanov^{120b,120a}, A. Zibell¹⁷⁴, D. Ziernska⁶³,

N.I. Zimine⁷⁷, S. Zimmermann⁵⁰, Z. Zinonos¹¹³, M. Zinser⁹⁷, M. Ziolkowski¹⁴⁸, G. Zobernig¹⁷⁸, A. Zoccoli^{23b,23a}, K. Zoch⁵¹, T.G. Zorbas¹⁴⁶, R. Zou³⁶, M. Zur Nedden¹⁹, L. Zwalski³⁵.

¹Department of Physics, University of Adelaide, Adelaide; Australia.

²Physics Department, SUNY Albany, Albany NY; United States of America.

³Department of Physics, University of Alberta, Edmonton AB; Canada.

^{4(a)}Department of Physics, Ankara University, Ankara;^(b)Istanbul Aydin University, Istanbul;^(c)Division of Physics, TOBB University of Economics and Technology, Ankara; Turkey.

⁵LAPP, Université Grenoble Alpes, Université Savoie Mont Blanc, CNRS/IN2P3, Annecy; France.

⁶High Energy Physics Division, Argonne National Laboratory, Argonne IL; United States of America.

⁷Department of Physics, University of Arizona, Tucson AZ; United States of America.

⁸Department of Physics, University of Texas at Arlington, Arlington TX; United States of America.

⁹Physics Department, National and Kapodistrian University of Athens, Athens; Greece.

¹⁰Physics Department, National Technical University of Athens, Zografou; Greece.

¹¹Department of Physics, University of Texas at Austin, Austin TX; United States of America.

^{12(a)}Bahcesehir University, Faculty of Engineering and Natural Sciences, Istanbul;^(b)Istanbul Bilgi University, Faculty of Engineering and Natural Sciences, Istanbul;^(c)Department of Physics, Bogazici University, Istanbul;^(d)Department of Physics Engineering, Gaziantep University, Gaziantep; Turkey.

¹³Institute of Physics, Azerbaijan Academy of Sciences, Baku; Azerbaijan.

¹⁴Institut de Física d'Altes Energies (IFAE), Barcelona Institute of Science and Technology, Barcelona; Spain.

^{15(a)}Institute of High Energy Physics, Chinese Academy of Sciences, Beijing;^(b)Physics Department, Tsinghua University, Beijing;^(c)Department of Physics, Nanjing University, Nanjing;^(d)University of Chinese Academy of Science (UCAS), Beijing; China.

¹⁶Institute of Physics, University of Belgrade, Belgrade; Serbia.

¹⁷Department for Physics and Technology, University of Bergen, Bergen; Norway.

¹⁸Physics Division, Lawrence Berkeley National Laboratory and University of California, Berkeley CA; United States of America.

¹⁹Institut für Physik, Humboldt Universität zu Berlin, Berlin; Germany.

²⁰Albert Einstein Center for Fundamental Physics and Laboratory for High Energy Physics, University of Bern, Bern; Switzerland.

²¹School of Physics and Astronomy, University of Birmingham, Birmingham; United Kingdom.

²²Centro de Investigaciones, Universidad Antonio Nariño, Bogota; Colombia.

^{23(a)}Dipartimento di Fisica e Astronomia, Università di Bologna, Bologna;^(b)INFN Sezione di Bologna; Italy.

²⁴Physikalischs Institut, Universität Bonn, Bonn; Germany.

²⁵Department of Physics, Boston University, Boston MA; United States of America.

²⁶Department of Physics, Brandeis University, Waltham MA; United States of America.

^{27(a)}Transilvania University of Brasov, Brasov;^(b)Horia Hulubei National Institute of Physics and Nuclear Engineering, Bucharest;^(c)Department of Physics, Alexandru Ioan Cuza University of Iasi, Iasi;^(d)National Institute for Research and Development of Isotopic and Molecular Technologies, Physics Department, Cluj-Napoca;^(e)University Politehnica Bucharest, Bucharest;^(f)West University in Timisoara, Timisoara; Romania.

^{28(a)}Faculty of Mathematics, Physics and Informatics, Comenius University, Bratislava;^(b)Department of Subnuclear Physics, Institute of Experimental Physics of the Slovak Academy of Sciences, Kosice; Slovak Republic.

²⁹Physics Department, Brookhaven National Laboratory, Upton NY; United States of America.

- ³⁰Departamento de Física, Universidad de Buenos Aires, Buenos Aires; Argentina.
- ³¹Cavendish Laboratory, University of Cambridge, Cambridge; United Kingdom.
- ^{32(a)}Department of Physics, University of Cape Town, Cape Town;^(b)Department of Mechanical Engineering Science, University of Johannesburg, Johannesburg;^(c)School of Physics, University of the Witwatersrand, Johannesburg; South Africa.
- ³³Department of Physics, Carleton University, Ottawa ON; Canada.
- ^{34(a)}Faculté des Sciences Ain Chock, Réseau Universitaire de Physique des Hautes Energies - Université Hassan II, Casablanca;^(b)Centre National de l'Energie des Sciences Techniques Nucleaires (CNESTEN), Rabat;^(c)Faculté des Sciences Semlalia, Université Cadi Ayyad, LPHEA-Marrakech;^(d)Faculté des Sciences, Université Mohamed Premier and LPTPM, Oujda;^(e)Faculté des sciences, Université Mohammed V, Rabat; Morocco.
- ³⁵CERN, Geneva; Switzerland.
- ³⁶Enrico Fermi Institute, University of Chicago, Chicago IL; United States of America.
- ³⁷LPC, Université Clermont Auvergne, CNRS/IN2P3, Clermont-Ferrand; France.
- ³⁸Nevis Laboratory, Columbia University, Irvington NY; United States of America.
- ³⁹Niels Bohr Institute, University of Copenhagen, Copenhagen; Denmark.
- ^{40(a)}Dipartimento di Fisica, Università della Calabria, Rende;^(b)INFN Gruppo Collegato di Cosenza, Laboratori Nazionali di Frascati; Italy.
- ⁴¹Physics Department, Southern Methodist University, Dallas TX; United States of America.
- ⁴²Physics Department, University of Texas at Dallas, Richardson TX; United States of America.
- ^{43(a)}Department of Physics, Stockholm University;^(b)Oskar Klein Centre, Stockholm; Sweden.
- ⁴⁴Deutsches Elektronen-Synchrotron DESY, Hamburg and Zeuthen; Germany.
- ⁴⁵Lehrstuhl für Experimentelle Physik IV, Technische Universität Dortmund, Dortmund; Germany.
- ⁴⁶Institut für Kern- und Teilchenphysik, Technische Universität Dresden, Dresden; Germany.
- ⁴⁷Department of Physics, Duke University, Durham NC; United States of America.
- ⁴⁸SUPA - School of Physics and Astronomy, University of Edinburgh, Edinburgh; United Kingdom.
- ⁴⁹INFN e Laboratori Nazionali di Frascati, Frascati; Italy.
- ⁵⁰Physikalisch Institut, Albert-Ludwigs-Universität Freiburg, Freiburg; Germany.
- ⁵¹II. Physikalisch Institut, Georg-August-Universität Göttingen, Göttingen; Germany.
- ⁵²Département de Physique Nucléaire et Corpusculaire, Université de Genève, Genève; Switzerland.
- ^{53(a)}Dipartimento di Fisica, Università di Genova, Genova;^(b)INFN Sezione di Genova; Italy.
- ⁵⁴II. Physikalisch Institut, Justus-Liebig-Universität Giessen, Giessen; Germany.
- ⁵⁵SUPA - School of Physics and Astronomy, University of Glasgow, Glasgow; United Kingdom.
- ⁵⁶LPSC, Université Grenoble Alpes, CNRS/IN2P3, Grenoble INP, Grenoble; France.
- ⁵⁷Laboratory for Particle Physics and Cosmology, Harvard University, Cambridge MA; United States of America.
- ^{58(a)}Department of Modern Physics and State Key Laboratory of Particle Detection and Electronics, University of Science and Technology of China, Hefei;^(b)Institute of Frontier and Interdisciplinary Science and Key Laboratory of Particle Physics and Particle Irradiation (MOE), Shandong University, Qingdao;^(c)School of Physics and Astronomy, Shanghai Jiao Tong University, KLPPAC-MoE, SKLPPC, Shanghai;^(d)Tsung-Dao Lee Institute, Shanghai; China.
- ^{59(a)}Kirchhoff-Institut für Physik, Ruprecht-Karls-Universität Heidelberg, Heidelberg;^(b)Physikalisches Institut, Ruprecht-Karls-Universität Heidelberg, Heidelberg; Germany.
- ⁶⁰Faculty of Applied Information Science, Hiroshima Institute of Technology, Hiroshima; Japan.
- ^{61(a)}Department of Physics, Chinese University of Hong Kong, Shatin, N.T., Hong Kong;^(b)Department of Physics, University of Hong Kong, Hong Kong;^(c)Department of Physics and Institute for Advanced Study, Hong Kong University of Science and Technology, Clear Water Bay, Kowloon, Hong Kong;

China.

⁶²Department of Physics, National Tsing Hua University, Hsinchu; Taiwan.

⁶³Department of Physics, Indiana University, Bloomington IN; United States of America.

^{64(a)}INFN Gruppo Collegato di Udine, Sezione di Trieste, Udine;^(b)ICTP, Trieste;^(c)Dipartimento di Chimica, Fisica e Ambiente, Università di Udine, Udine; Italy.

^{65(a)}INFN Sezione di Lecce;^(b)Dipartimento di Matematica e Fisica, Università del Salento, Lecce; Italy.

^{66(a)}INFN Sezione di Milano;^(b)Dipartimento di Fisica, Università di Milano, Milano; Italy.

^{67(a)}INFN Sezione di Napoli;^(b)Dipartimento di Fisica, Università di Napoli, Napoli; Italy.

^{68(a)}INFN Sezione di Pavia;^(b)Dipartimento di Fisica, Università di Pavia, Pavia; Italy.

^{69(a)}INFN Sezione di Pisa;^(b)Dipartimento di Fisica E. Fermi, Università di Pisa, Pisa; Italy.

^{70(a)}INFN Sezione di Roma;^(b)Dipartimento di Fisica, Sapienza Università di Roma, Roma; Italy.

^{71(a)}INFN Sezione di Roma Tor Vergata;^(b)Dipartimento di Fisica, Università di Roma Tor Vergata, Roma; Italy.

^{72(a)}INFN Sezione di Roma Tre;^(b)Dipartimento di Matematica e Fisica, Università Roma Tre, Roma; Italy.

^{73(a)}INFN-TIFPA;^(b)Università degli Studi di Trento, Trento; Italy.

⁷⁴Institut für Astro- und Teilchenphysik, Leopold-Franzens-Universität, Innsbruck; Austria.

⁷⁵University of Iowa, Iowa City IA; United States of America.

⁷⁶Department of Physics and Astronomy, Iowa State University, Ames IA; United States of America.

⁷⁷Joint Institute for Nuclear Research, Dubna; Russia.

^{78(a)}Departamento de Engenharia Elétrica, Universidade Federal de Juiz de Fora (UFJF), Juiz de Fora;^(b)Universidade Federal do Rio De Janeiro COPPE/EE/IF, Rio de Janeiro;^(c)Universidade Federal de São João del Rei (UFSJ), São João del Rei;^(d)Instituto de Física, Universidade de São Paulo, São Paulo; Brazil.

⁷⁹KEK, High Energy Accelerator Research Organization, Tsukuba; Japan.

⁸⁰Graduate School of Science, Kobe University, Kobe; Japan.

^{81(a)}AGH University of Science and Technology, Faculty of Physics and Applied Computer Science, Krakow;^(b)Marian Smoluchowski Institute of Physics, Jagiellonian University, Krakow; Poland.

⁸²Institute of Nuclear Physics Polish Academy of Sciences, Krakow; Poland.

⁸³Faculty of Science, Kyoto University, Kyoto; Japan.

⁸⁴Kyoto University of Education, Kyoto; Japan.

⁸⁵Research Center for Advanced Particle Physics and Department of Physics, Kyushu University, Fukuoka ; Japan.

⁸⁶Instituto de Física La Plata, Universidad Nacional de La Plata and CONICET, La Plata; Argentina.

⁸⁷Physics Department, Lancaster University, Lancaster; United Kingdom.

⁸⁸Oliver Lodge Laboratory, University of Liverpool, Liverpool; United Kingdom.

⁸⁹Department of Experimental Particle Physics, Jožef Stefan Institute and Department of Physics, University of Ljubljana, Ljubljana; Slovenia.

⁹⁰School of Physics and Astronomy, Queen Mary University of London, London; United Kingdom.

⁹¹Department of Physics, Royal Holloway University of London, Egham; United Kingdom.

⁹²Department of Physics and Astronomy, University College London, London; United Kingdom.

⁹³Louisiana Tech University, Ruston LA; United States of America.

⁹⁴Fysiska institutionen, Lunds universitet, Lund; Sweden.

⁹⁵Centre de Calcul de l’Institut National de Physique Nucléaire et de Physique des Particules (IN2P3), Villeurbanne; France.

⁹⁶Departamento de Física Teorica C-15 and CIAFF, Universidad Autónoma de Madrid, Madrid; Spain.

⁹⁷Institut für Physik, Universität Mainz, Mainz; Germany.

- ⁹⁸School of Physics and Astronomy, University of Manchester, Manchester; United Kingdom.
- ⁹⁹CPPM, Aix-Marseille Université, CNRS/IN2P3, Marseille; France.
- ¹⁰⁰Department of Physics, University of Massachusetts, Amherst MA; United States of America.
- ¹⁰¹Department of Physics, McGill University, Montreal QC; Canada.
- ¹⁰²School of Physics, University of Melbourne, Victoria; Australia.
- ¹⁰³Department of Physics, University of Michigan, Ann Arbor MI; United States of America.
- ¹⁰⁴Department of Physics and Astronomy, Michigan State University, East Lansing MI; United States of America.
- ¹⁰⁵B.I. Stepanov Institute of Physics, National Academy of Sciences of Belarus, Minsk; Belarus.
- ¹⁰⁶Research Institute for Nuclear Problems of Byelorussian State University, Minsk; Belarus.
- ¹⁰⁷Group of Particle Physics, University of Montreal, Montreal QC; Canada.
- ¹⁰⁸P.N. Lebedev Physical Institute of the Russian Academy of Sciences, Moscow; Russia.
- ¹⁰⁹Institute for Theoretical and Experimental Physics (ITEP), Moscow; Russia.
- ¹¹⁰National Research Nuclear University MEPhI, Moscow; Russia.
- ¹¹¹D.V. Skobeltsyn Institute of Nuclear Physics, M.V. Lomonosov Moscow State University, Moscow; Russia.
- ¹¹²Fakultät für Physik, Ludwig-Maximilians-Universität München, München; Germany.
- ¹¹³Max-Planck-Institut für Physik (Werner-Heisenberg-Institut), München; Germany.
- ¹¹⁴Nagasaki Institute of Applied Science, Nagasaki; Japan.
- ¹¹⁵Graduate School of Science and Kobayashi-Maskawa Institute, Nagoya University, Nagoya; Japan.
- ¹¹⁶Department of Physics and Astronomy, University of New Mexico, Albuquerque NM; United States of America.
- ¹¹⁷Institute for Mathematics, Astrophysics and Particle Physics, Radboud University Nijmegen/Nikhef, Nijmegen; Netherlands.
- ¹¹⁸Nikhef National Institute for Subatomic Physics and University of Amsterdam, Amsterdam; Netherlands.
- ¹¹⁹Department of Physics, Northern Illinois University, DeKalb IL; United States of America.
- ^{120^(a)}Budker Institute of Nuclear Physics, SB RAS, Novosibirsk;^(b)Novosibirsk State University Novosibirsk; Russia.
- ¹²¹Department of Physics, New York University, New York NY; United States of America.
- ¹²²Ohio State University, Columbus OH; United States of America.
- ¹²³Faculty of Science, Okayama University, Okayama; Japan.
- ¹²⁴Homer L. Dodge Department of Physics and Astronomy, University of Oklahoma, Norman OK; United States of America.
- ¹²⁵Department of Physics, Oklahoma State University, Stillwater OK; United States of America.
- ¹²⁶Palacký University, RCPTM, Joint Laboratory of Optics, Olomouc; Czech Republic.
- ¹²⁷Center for High Energy Physics, University of Oregon, Eugene OR; United States of America.
- ¹²⁸LAL, Université Paris-Sud, CNRS/IN2P3, Université Paris-Saclay, Orsay; France.
- ¹²⁹Graduate School of Science, Osaka University, Osaka; Japan.
- ¹³⁰Department of Physics, University of Oslo, Oslo; Norway.
- ¹³¹Department of Physics, Oxford University, Oxford; United Kingdom.
- ¹³²LPNHE, Sorbonne Université, Paris Diderot Sorbonne Paris Cité, CNRS/IN2P3, Paris; France.
- ¹³³Department of Physics, University of Pennsylvania, Philadelphia PA; United States of America.
- ¹³⁴Konstantinov Nuclear Physics Institute of National Research Centre "Kurchatov Institute", PNPI, St. Petersburg; Russia.
- ¹³⁵Department of Physics and Astronomy, University of Pittsburgh, Pittsburgh PA; United States of America.

- ^{136(a)}Laboratório de Instrumentação e Física Experimental de Partículas - LIP;^(b)Departamento de Física, Faculdade de Ciências, Universidade de Lisboa, Lisboa;^(c)Departamento de Física, Universidade de Coimbra, Coimbra;^(d)Centro de Física Nuclear da Universidade de Lisboa, Lisboa;^(e)Departamento de Física, Universidade do Minho, Braga;^(f)Departamento de Física Teorica y del Cosmos, Universidad de Granada, Granada (Spain);^(g)Dep Física and CEFITEC of Faculdade de Ciências e Tecnologia, Universidade Nova de Lisboa, Caparica; Portugal.
- ¹³⁷Institute of Physics, Academy of Sciences of the Czech Republic, Prague; Czech Republic.
- ¹³⁸Czech Technical University in Prague, Prague; Czech Republic.
- ¹³⁹Charles University, Faculty of Mathematics and Physics, Prague; Czech Republic.
- ¹⁴⁰State Research Center Institute for High Energy Physics, NRC KI, Protvino; Russia.
- ¹⁴¹Particle Physics Department, Rutherford Appleton Laboratory, Didcot; United Kingdom.
- ¹⁴²IRFU, CEA, Université Paris-Saclay, Gif-sur-Yvette; France.
- ¹⁴³Santa Cruz Institute for Particle Physics, University of California Santa Cruz, Santa Cruz CA; United States of America.
- ^{144(a)}Departamento de Física, Pontificia Universidad Católica de Chile, Santiago;^(b)Departamento de Física, Universidad Técnica Federico Santa María, Valparaíso; Chile.
- ¹⁴⁵Department of Physics, University of Washington, Seattle WA; United States of America.
- ¹⁴⁶Department of Physics and Astronomy, University of Sheffield, Sheffield; United Kingdom.
- ¹⁴⁷Department of Physics, Shinshu University, Nagano; Japan.
- ¹⁴⁸Department Physik, Universität Siegen, Siegen; Germany.
- ¹⁴⁹Department of Physics, Simon Fraser University, Burnaby BC; Canada.
- ¹⁵⁰SLAC National Accelerator Laboratory, Stanford CA; United States of America.
- ¹⁵¹Physics Department, Royal Institute of Technology, Stockholm; Sweden.
- ¹⁵²Departments of Physics and Astronomy, Stony Brook University, Stony Brook NY; United States of America.
- ¹⁵³Department of Physics and Astronomy, University of Sussex, Brighton; United Kingdom.
- ¹⁵⁴School of Physics, University of Sydney, Sydney; Australia.
- ¹⁵⁵Institute of Physics, Academia Sinica, Taipei; Taiwan.
- ^{156(a)}E. Andronikashvili Institute of Physics, Iv. Javakhishvili Tbilisi State University, Tbilisi;^(b)High Energy Physics Institute, Tbilisi State University, Tbilisi; Georgia.
- ¹⁵⁷Department of Physics, Technion, Israel Institute of Technology, Haifa; Israel.
- ¹⁵⁸Raymond and Beverly Sackler School of Physics and Astronomy, Tel Aviv University, Tel Aviv; Israel.
- ¹⁵⁹Department of Physics, Aristotle University of Thessaloniki, Thessaloniki; Greece.
- ¹⁶⁰International Center for Elementary Particle Physics and Department of Physics, University of Tokyo, Tokyo; Japan.
- ¹⁶¹Graduate School of Science and Technology, Tokyo Metropolitan University, Tokyo; Japan.
- ¹⁶²Department of Physics, Tokyo Institute of Technology, Tokyo; Japan.
- ¹⁶³Tomsk State University, Tomsk; Russia.
- ¹⁶⁴Department of Physics, University of Toronto, Toronto ON; Canada.
- ^{165(a)}TRIUMF, Vancouver BC;^(b)Department of Physics and Astronomy, York University, Toronto ON; Canada.
- ¹⁶⁶Division of Physics and Tomonaga Center for the History of the Universe, Faculty of Pure and Applied Sciences, University of Tsukuba, Tsukuba; Japan.
- ¹⁶⁷Department of Physics and Astronomy, Tufts University, Medford MA; United States of America.
- ¹⁶⁸Department of Physics and Astronomy, University of California Irvine, Irvine CA; United States of America.
- ¹⁶⁹Department of Physics and Astronomy, University of Uppsala, Uppsala; Sweden.

- ¹⁷⁰Department of Physics, University of Illinois, Urbana IL; United States of America.
- ¹⁷¹Instituto de Física Corpuscular (IFIC), Centro Mixto Universidad de Valencia - CSIC, Valencia; Spain.
- ¹⁷²Department of Physics, University of British Columbia, Vancouver BC; Canada.
- ¹⁷³Department of Physics and Astronomy, University of Victoria, Victoria BC; Canada.
- ¹⁷⁴Fakultät für Physik und Astronomie, Julius-Maximilians-Universität Würzburg, Würzburg; Germany.
- ¹⁷⁵Department of Physics, University of Warwick, Coventry; United Kingdom.
- ¹⁷⁶Waseda University, Tokyo; Japan.
- ¹⁷⁷Department of Particle Physics, Weizmann Institute of Science, Rehovot; Israel.
- ¹⁷⁸Department of Physics, University of Wisconsin, Madison WI; United States of America.
- ¹⁷⁹Fakultät für Mathematik und Naturwissenschaften, Fachgruppe Physik, Bergische Universität Wuppertal, Wuppertal; Germany.
- ¹⁸⁰Department of Physics, Yale University, New Haven CT; United States of America.
- ¹⁸¹Yerevan Physics Institute, Yerevan; Armenia.
- ^a Also at Department of Physics, University of Malaya, Kuala Lumpur; Malaysia.
- ^b Also at Borough of Manhattan Community College, City University of New York, NY; United States of America.
- ^c Also at Centre for High Performance Computing, CSIR Campus, Rosebank, Cape Town; South Africa.
- ^d Also at CERN, Geneva; Switzerland.
- ^e Also at CPPM, Aix-Marseille Université, CNRS/IN2P3, Marseille; France.
- ^f Also at Département de Physique Nucléaire et Corpusculaire, Université de Genève, Genève; Switzerland.
- ^g Also at Departament de Fisica de la Universitat Autònoma de Barcelona, Barcelona; Spain.
- ^h Also at Departamento de Física Teórica y del Cosmos, Universidad de Granada, Granada (Spain); Spain.
- ⁱ Also at Department of Applied Physics and Astronomy, University of Sharjah, Sharjah; United Arab Emirates.
- ^j Also at Department of Financial and Management Engineering, University of the Aegean, Chios; Greece.
- ^k Also at Department of Physics and Astronomy, University of Louisville, Louisville, KY; United States of America.
- ^l Also at Department of Physics and Astronomy, University of Sheffield, Sheffield; United Kingdom.
- ^m Also at Department of Physics, California State University, Fresno CA; United States of America.
- ⁿ Also at Department of Physics, California State University, Sacramento CA; United States of America.
- ^o Also at Department of Physics, King's College London, London; United Kingdom.
- ^p Also at Department of Physics, Nanjing University, Nanjing; China.
- ^q Also at Department of Physics, St. Petersburg State Polytechnical University, St. Petersburg; Russia.
- ^r Also at Department of Physics, University of Fribourg, Fribourg; Switzerland.
- ^s Also at Department of Physics, University of Michigan, Ann Arbor MI; United States of America.
- ^t Also at Dipartimento di Fisica E. Fermi, Università di Pisa, Pisa; Italy.
- ^u Also at Giresun University, Faculty of Engineering, Giresun; Turkey.
- ^v Also at Graduate School of Science, Osaka University, Osaka; Japan.
- ^w Also at Hellenic Open University, Patras; Greece.
- ^x Also at Horia Hulubei National Institute of Physics and Nuclear Engineering, Bucharest; Romania.
- ^y Also at II. Physikalisches Institut, Georg-August-Universität Göttingen, Göttingen; Germany.
- ^z Also at Institució Catalana de Recerca i Estudis Avançats, ICREA, Barcelona; Spain.
- ^{aa} Also at Institut für Experimentalphysik, Universität Hamburg, Hamburg; Germany.
- ^{ab} Also at Institute for Mathematics, Astrophysics and Particle Physics, Radboud University

Nijmegen/Nikhef, Nijmegen; Netherlands.

ac Also at Institute for Particle and Nuclear Physics, Wigner Research Centre for Physics, Budapest; Hungary.

ad Also at Institute of Particle Physics (IPP); Canada.

ae Also at Institute of Physics, Academia Sinica, Taipei; Taiwan.

af Also at Institute of Physics, Azerbaijan Academy of Sciences, Baku; Azerbaijan.

ag Also at Institute of Theoretical Physics, Ilia State University, Tbilisi; Georgia.

ah Also at LAL, Université Paris-Sud, CNRS/IN2P3, Université Paris-Saclay, Orsay; France.

ai Also at Louisiana Tech University, Ruston LA; United States of America.

aj Also at Manhattan College, New York NY; United States of America.

ak Also at Moscow Institute of Physics and Technology State University, Dolgoprudny; Russia.

al Also at National Research Nuclear University MEPhI, Moscow; Russia.

am Also at Near East University, Nicosia, North Cyprus, Mersin; Turkey.

an Also at Physikalisches Institut, Albert-Ludwigs-Universität Freiburg, Freiburg; Germany.

ao Also at School of Physics, Sun Yat-sen University, Guangzhou; China.

ap Also at The City College of New York, New York NY; United States of America.

aq Also at The Collaborative Innovation Center of Quantum Matter (CICQM), Beijing; China.

ar Also at Tomsk State University, Tomsk, and Moscow Institute of Physics and Technology State University, Dolgoprudny; Russia.

as Also at TRIUMF, Vancouver BC; Canada.

at Also at Universita di Napoli Parthenope, Napoli; Italy.

* Deceased